AN INVESTIGATION OF SOIL MOISTURE ASSOCIATED WITH EPHEMERAL STREAMS, WRIGHT VALLEY, ANTARCTICA

A thesis

submitted in fulfilment

of the requirements for the degree

of

Master of Science in Earth Science

at

The University of Waikato

by

Fiona Louise Shanhun

THE UNIVERSITY OF
WAIKATO
Te Whare Wānanga o Waikato

2005

Abstract

Ephemeral streams in Wright Valley, Antarctica, are fed by glacial melt and flow for between four and ten weeks annually. Hyporheic zones develop concomitantly with ephemeral stream channels. These zones are areas of saturated or moistened soil, depending on their proximity to the stream. The hyporheic zones are laterally extensive, and may represent a greater proportion of total meltwater than surface water in the stream channel, thus exacerbating the risk of accidental contamination of streams. The hydrological system in Wright Valley is closed, with streams flowing inland to Lake Vanda via the Onyx River.

This study aimed to quantify the extent to which liquid moisture was present in soils associated with Goodspeed Stream, in order to better predict the vulnerability of stream margins to impacts of human activities. Soil samples were collected from transects across the Goodspeed lower alluvial fan and analysed for gravimetric moisture content, electrical conductivity, and particle size distribution. A pedotransfer function was used to estimate soil moisture potential in order to show the direction of water movement across the lower alluvial fan. Climate data including air temperature, soil temperature, and total solar radiation were measured; stream flow in Goodspeed Stream was estimated.

The Goodspeed Stream near-stream and extended hyporheic zones were identified. Distal components of the hyporheic zone were also identified at distances of up to 74 m from Goodspeed Stream.

Soil gravimetric moisture content increased with soil depth and proximity to Goodspeed Stream. Distal components of the hyporheic zone observed at distances of 21, 59 and 74 m from Goodspeed Stream had relatively high gravimetric moisture contents (up to 7%; θ_g in visibly dry soils was 0.6%). The distal hyporheic zones have the potential to develop into flowing stream channels during periods of increased melt.

Soil electrical conductivity ranged from 34 – 10520 μS/cm. Salts precipitated at the soil surface were concentrated at the western-most edge of the extended hyporheic zone and on raised bar features across the fan, highlighting zones of movement and evaporation of soil moisture. The particle size distribution of the <2 mm fraction was relatively uniform across the fan, being dominated by medium sand (45%).

Soil moisture potential decreased with distance from Goodspeed Stream, indicating that small spills occurring outside the extended hyporheic zone would be driven laterally across the fan, away from the stream. Spills within the extended hyporheic may be incorporated into Goodspeed Stream. Large spills anywhere on the Goodspeed lower alluvial fan would migrate downwards to ice cement before flowing down-slope under gravity towards the Onyx River.

Areas vulnerable to accidental spills and physical disturbance were highlighted on oblique photographs. Three vulnerability zones were identified based predominantly on the observed extent and movement of soil moisture. Zone 1 designates stream channels or surface waters and near-stream hyporheic zones, Zone 2 encompasses extended hyporheic zones, while Zone 3 applies to soils of alluvial fans, including distal hyporheic zones. Recommendations were made as to the types of activities permissible in each of the three zones.

Acknowledgements

I gratefully acknowledge the opportunity provided to me by my supervisor, Megan Balks, enabling me to do research in such a fantastic and inspiring landscape. Thanks also to Megan for her enthusiasm, help and company in the field, and for encouragement with my writing and analyses. Thanks also to my second supervisor, Dave Campbell, for providing effective feedback and support.

Thanks to Jackie Aislabie for incorporating this study into her FRST funded research programme (Contract number C09X0307), Antarctica New Zealand for logistic support, and the University, the Broad Memorial Fund, and the Waikato Branch of the New Zealand Federation of Graduate Women for financial support.

I also appreciate the assistance of the K123 field team – Malcolm McLeod for his advice and entertainment, Jim Bockheim for sharing his invaluable knowledge of soils of the Wright Valley, and Allan Hewitt for his help with field work and useful discussions regarding sampling strategy. Thanks to Ron Paetzold for providing the Bull Pass climate station data.

Thank you to Craig Burgess for his technical support with field equipment, Tarnia Hodges for helping with my laboratory queries, and Penny Cooke for offering practical advice regarding particle size analyses.

Special thanks to my fellow dungeon dwellers for their assistance with procrastination and for their like-minded senses of humour: Erica Hofstee, Stacey O'Driscoll, Christian Fritz, and honourary inhabitant, Tracey Bear. Thanks also to Debra Stokes for surviving rock climbing beneath me, and to my flatmates Nicky Buchanan and Kerry Wilson for much fun and hilarity. Thanks to all my other friends for their support – you have all helped me in some way. Thanks also to my in-town flatmates Tracey, Debs and Christian for sharing your house with me, and for being fun to be with.

Finally, to my Mum, Dad, David, Charlie and Peter, thank you so much for your love, support, encouragement and advice.

Table of Contents

List of Figures

List of Tables

Chapter 1
General Introduction

Chapter 1 General Introduction

1.1 Background

Antarctica, although almost completely covered in ice, has a distinct paucity of liquid water. Consequently, the continent affords one of the most inhospitable environments for life on Earth. The McMurdo Dry Valleys (Figure 1.1) constitute one of the largest (~ 4000 km^2) ice-free areas in Antarctica (Bockheim, 2002), and are therefore one of the most biologically active non-coastal terrestrial areas in Antarctica. However, the ice-free areas attract scientists, and, increasingly, tourists from around the world, whose presence acts to increase the risk of disturbance to the pristine environment (Waterhouse, 2001).

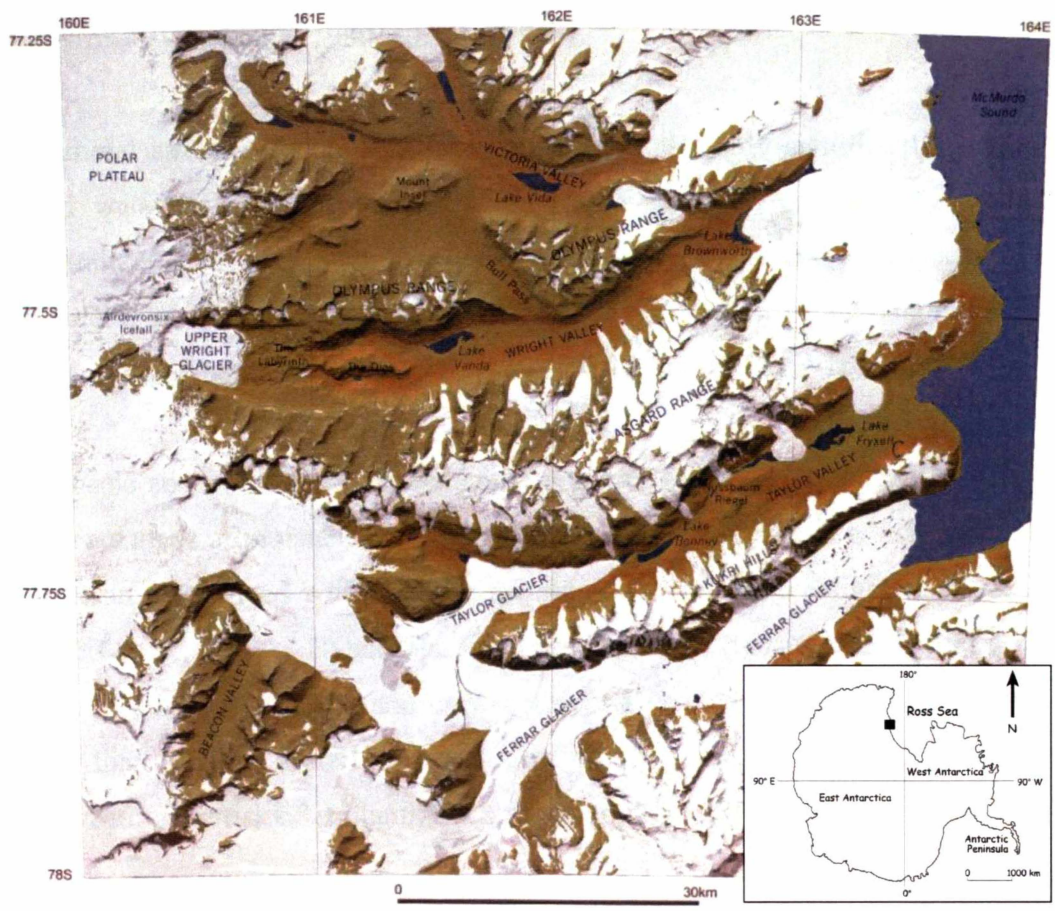

Figure 1.1. Location of the McMurdo Dry Valleys. (Adapted from Potton and Green, 2003)

The McMurdo Dry Valleys are designated as an Antarctic Specially Managed Area (ASMA) under the Protocol on Environmental Protection to the Antarctic Treaty (Antarctica New Zealand, 2004). This legislation means that the Area must be managed in order to ensure that its scientific, wilderness, ecological and aesthetic values are protected.

1.1.1 Characteristics of the McMurdo Dry Valleys

The McMurdo Dry Valleys are the coldest and driest deserts in the world (McKnight et al., 1999). Wright Valley (77°30' S, 161°00 - 163°00' E) is one of the McMurdo Dry Valleys. The present climate within Wright Valley is characterised by extremely low temperatures (mean annual temperature –20° C) and precipitation (mean annual precipitation <100 mm) (Keys, 1980); snowfall generally sublimates before melt can occur (Nichols, 1966; Fenwick and Anderton, 1975; Chinn, 1980; Chinn, 1981b).

Ephemeral streams, fed by glacial melt, provide the only significant source of liquid water to hydrological and biological systems within the Dry Valleys (Fountain et al., 1998). Such streams flow for between four and ten weeks during the austral summer (Lyons et al., 1997b; McKnight et al., 1999; Treonis et al., 1999), and are markedly influenced by diurnal variation in solar radiation.

Hyporheic zones develop concomitantly with ephemeral stream channels. These zones are areas of moistened soil adjacent to stream channels, in which water and solutes are exchanged with water in the stream channel (McKnight et al., 1999; Gooseff et al., 2003). Hyporheic zones are laterally extensive (McKnight et al., 1999; Treonis et al., 1999), and may represent a greater proportion of total melt-water than surface water in the stream itself (Conovitz et al., 1998), thus exacerbating the risk of contamination of waterways.

Soils formed under the cold, arid climatic conditions prevalent within the Dry Valleys depict evidence of climate having the dominant influence on soil genesis. The effects of the arid climate are primarily manifest as accumulations of soluble

salts within soils (Claridge and Campbell, 1977; Bockheim, 1979), though the limited rate at which chemical weathering proceeds means that soils are typically gravelly (Bockheim, 1980), and weakly oxidised.

1.2 Existing research

Antarctic research group K123, a FRST-funded, Landcare Research programme entitled "Environmental Protection of Antarctic Soils", focuses on mitigation of human impacts on Antarctic ice-free ecosystems, as well as mapping and characterising the soil resource. As part of K123's programme, this study further contributes to an understanding of ecosystem processes, namely those associated with the hyporheic and stream-soil transition zones. An improved understanding of the processes operating within hyporheic zones, and measurement of the extent to which liquid water is present in soils of the associated alluvial fans will ultimately enhance management decisions regarding access to stream margins.

1.3 Objectives

This study aimed to assess the vulnerability of streams, hyporheic zones and associated fans to impacts from human activities in Wright Valley, Antarctica. Specific objectives were to:

- monitor stream flow in Goodspeed Stream;
- monitor key climate parameters to provide the basis for interpretation of variations in stream flow;
- determine the lateral and vertical extent of the Goodspeed Stream hyporheic zone;
- determine the extent and distribution of soil moisture within the Goodspeed Stream hyporheic zone and in soils of the Goodspeed lower alluvial fan during the period of maximum melt (January);

- investigate the relationship between soil moisture content and salt concentration within the fan area;

- interpret soil moisture data with respect to potential vulnerability to, and potential fate of, contaminant spills;

- extrapolate the findings to other streams in Wright Valley, based on geomorphic interpretation.

1.4 Relevance

Further characterisation of hyporheic zones and soils of alluvial fans is important in understanding the relatively dynamic nature of Antarctic ice-free areas. Evaluation of the vulnerability of soils associated with streams to human activities in Antarctica is, to the best of my knowledge, the first study addressing this issue. Climate and soil data obtained from this study will also contribute baseline information pertinent to on-going research in the Dry Valleys.

Chapter 2
Literature Review

Chapter 2 Literature Review

2.1 Introduction

Antarctica is almost directly centred on the South Pole of Earth's axis, and is isolated from other land masses by the Southern Ocean (Benninghoff, 1987). It is a continent of extremes; cold temperatures and high winds prevail for much of the year. Ninety-eight percent of the surface is mantled by 2000 m or more of glacial ice, flowing towards coastal outlets to the sea (Benninghoff, 1987). Despite the vast quantity of water stored in ice sheets, glaciers, and frozen ground within Antarctica (Keys, 1980; Kennedy, 1993), the cold temperatures dictate a scarce availability of liquid water, rendering the continent almost inhospitable to life.

This chapter describes the environment of the McMurdo Dry Valleys, detailing the present climate and geomorphology. The characteristics of Antarctic streams are discussed, with particular emphasis on the variability of stream flow. Properties of soils in the Dry Valleys are reviewed, and human impacts on the McMurdo Dry Valley ecosystem are outlined.

2.2 McMurdo Dry Valleys

The McMurdo Dry Valleys are located on the western edge of the Ross Sea (76°30' – 78°30' S, 160 – 164° E), and are the largest (~ 4000 km^2) ice-free area in Antarctica (Fountain et al., 1999; Doran et al., 2002). The Dry Valleys were first discovered by Scott's 1903 expedition, and have become one of the most intensively studied areas in Antarctica (Keys, 1980; Doran et al., 2002).

The McMurdo Dry Valleys are predominantly comprised of three large valleys: Taylor Valley, Wright Valley, and the Victoria Valley system. They extend from the crest of the Transantarctic Mountains to the ocean (McMurdo Sound), being about 80-100 km in length, and 5-10 km in width (Prentice et al., 1998). Relief ranges from sea level to over 2000 m in a horizontal distance of only a few kilometres (Fountain et al., 1999; Doran et al., 2002; Nylen et al., 2004). The

landscape of the Dry Valleys consists of an array of cold-based alpine glaciers, ephemeral streams, perennially ice-covered lakes, and extensive areas of soils and exposed bedrock (Fountain et al., 1999; Doran et al., 2002).

The ice-free nature of the valleys results from the Transantarctic Mountains blocking much of the flow of the East Antarctic Ice Sheet toward McMurdo Sound (Bull, 1966; Nichols, 1966; Clow et al., 1988). Furthermore, in the valley floor, ablation of snow and ice exceeds accumulation throughout the year (Clow et al., 1988; Fountain et al., 1999), and the annual net-radiation balance is positive (Bull, 1966).

2.2.1 Climate

The McMurdo Dry Valleys are considered a cold desert environment, being characterised by a paucity of liquid water and extreme cold conditions (Fountain et al., 1999). The austral summer is characterised by continuous daylight, near-freezing temperatures, and the presence of meltwater flow (Fountain et al., 1999), with climate being predominantly controlled by solar radiation (Clow et al., 1988). In contrast, the winter months provide almost continuous darkness, liquid water is absent (Fountain et al., 1999), and temperatures are controlled by the wind (Clow et al., 1988).

Despite climatic conditions being generally unfavourable for life, biological communities are found in the lakes, streams, and soils (Wynn-Williams, 1990; Fountain et al., 1999). Such communities are adapted for survival in conditions including freeze-thaw cycles, high winds, prolonged low temperatures, hypersalinity, and exposure during summer to high intensities of solar radiation (Wynn-Williams, 1990; Vincent et al., 1993; Fountain et al., 1999), though resistance to extreme dessication is arguably the most important factor influencing the distribution of biological communities in Antarctica (Wynn-Williams, 1990; Kennedy, 1993).

The McMurdo Dry Valleys are highly climate-sensitive environments (Fountain et al., 1999), with small climatic changes potentially leading to extreme variations

in the local hydrologic regime (Lyons et al., 1997a; Fountain et al., 1999). Increases in the number of degree days above 0 °C result in increased stream flow and lake levels; conversely, fewer degree days above freezing decreases the availability of liquid moisture (Clow et al., 1988; Lyons et al., 1997a). Changes in hydrology are likely to have a substantial impact on the biological communities within the valleys, as the existence of biota is primarily dependent on the availability of liquid water (Kennedy, 1993).

2.2.1.1 Temperature and solar radiation

The mean annual temperature in Wright Valley ranges from –17 to –20 °C (Thompson et al., 1971b; Keys, 1980; Clow et al., 1988), although mean annual temperature decreases inland as surface elevation increases (Keys, 1980). Mean annual solar radiation flux density in the Dry Valleys ranges from 73 – 117 Wm^{-2} (Doran et al., 2002); maximum solar radiation is received at the summer solstice, while sunlight is absent between the months of April and August (Nylen et al., 2004).

A strong east to west gradient in summer temperature exists within the valleys; temperatures increase with distance inland (Bull, 1966). The east to west temperature gradient is correlated with the occurrence of coastal winds, with easterly sea breezes accounting for the majority of the cooling effect observed toward the coast (Doran et al., 2002). However, it is not the spatial variation in the frequency of easterly winds inland that explains the temperature increase up-valley, but more a result of their warming as they progress inland, presumably due to the movement of the cold coastal air mass over the relatively warmer dark valley surfaces (Doran et al., 2002).

2.2.1.2 Precipitation

Mean annual precipitation is estimated to be <100 mm water equivalent, with most occurring as snow (Keys, 1980; Doran et al., 2002), although rain does occasionally occur (Keys, 1980; Bromley, 1985). Snow patches are generally

rapidly sublimed, and hence lost as a source of moisture to soils or streams (Nichols, 1966; Fenwick and Anderton, 1975; Chinn, 1980; Chinn, 1981b), though when air temperatures are greater than 0 °C, melting may be intense (Keys, 1980).

The low levels of precipitation received in the McMurdo Dry Valleys are derived from low-pressure systems passing over the Ross Sea. Low-pressure systems bring moist air to the valleys, with moisture precipitating out as the air mass is forced to rise over the Transantarctic Mountains (Bromley, 1985). Thus a marked precipitation gradient exists, decreasing from east to west as the distance from the ocean increases (Bull, 1966; Keys, 1980). Precipitation is generally greater at higher elevations, especially in summer (Keys, 1980). The frequency at which precipitation events occur also decreases as distance from the coast towards the polar plateau increases (Genthon et al., 1998).

2.2.1.3 Wind

The wind regime of the Dry Valleys is dominated by easterly and westerly winds, and has a substantial influence on air temperatures. Wind direction is almost completely controlled by and is generally parallel to valley orientation, blowing either down-valley from the polar plateau (westerlies), or up-valley from the ocean (easterlies) (Bull, 1966; Keys, 1980; Nylen et al., 2004).

In summer, the most frequent wind direction in the valley floors is up-valley winds (easterly sea breezes) (Thompson et al., 1971b; Keys, 1980; Nylen et al., 2004). Easterly sea breezes are generated as a result of differential heating of the valley floors and the ice-covered ocean, and in the case of Wright Valley, the Wilson Piedmont and Wright Lower Glaciers driving flow up-valley. These winds typically intensify during the day, becoming strongest in the afternoons and evenings when ground temperatures are warmest (Keys, 1980; Clow et al., 1988; Nylen et al., 2004). The easterly winds also warm as they progress up-valley; Doran et al. (2002) show that a strong linear relationship exists between potential temperature and distance from the coast, with air temperatures increasing by 0.09 °C per kilometre inland.

Mean annual wind speed increases with proximity to the polar plateau (Doran et al., 2002), while mean summer wind speed increases at a rate of 0.04 m s^{-1} per km inland (Doran et al., 2002). Furthermore, the ratio of easterly to westerly wind frequency decreases from ~7 near the coast to ~2, 50 km inland (Doran et al., 2002).

Wright Valley has a bimodal wind regime, with strong warm katabatic winds (westerlies) coming from the plateau, and lighter sea breezes (easterlies) coming from McMurdo Sound (Doran et al., 2002). The mean annual wind speed recorded at Lake Vanda is 4.9 m s^{-1} (Keys, 1980).

Katabatic winds

Westerly winds in the McMurdo Dry Valleys, commonly referred to as katabatic winds, are generally föhn winds where the air is warmed adiabatically as it descends into the valleys (Keys, 1980). Therefore, the westerly winds are warmer than the air they displace, as opposed to being true katabatics which are a gravity flow of cold air, and are colder than the air they displace (Keys, 1980). However, the föhn type winds will continue to be referred to as katabatic winds for consistency with the current literature (e.g. Nylen et al., 2004).

Katabatic winds, sourced from the polar plateau, have a strong influence on the climate of the McMurdo Dry Valleys (Nylen et al., 2004). The onset and cessation of katabatic winds is generally abrupt, though elevated air temperatures remain for days after the winds cease (Nylen et al., 2004). The frequency of katabatic winds increases with distance away from the coast towards the polar plateau (Nylen et al., 2004). Winter wind events increase by 14% for every 10 km inland, while summer events increase by only 3% per 10 km (Nylen et al., 2004). The increase in katabatic wind frequency inland is probably a result of the proximity to the katabatic source.

Westerly katabatic winds occur infrequently during summer (Nylen et al., 2004), and are generally limited to the mornings, when solar radiation is minimal (Thompson et al., 1971b; Keys, 1980; Clow et al., 1988). However, katabatic winds exhibit the greatest wind speeds (up to 37 m s^{-1}) (Keys, 1980; Nylen et al., 2004). In winter, katabatic winds occur more frequently (Thompson et al., 1971b), and are stronger than summer katabatics (Nylen et al., 2004).

Adiabatic warming of the katabatic winds, combined with the disruption they cause to temperature inversions (Thompson et al., 1971b; Nylen et al., 2004), acts to increase valley air temperatures and decrease relative humidity (Bull, 1966; Thompson et al., 1971b; Clow et al., 1988). Nylen et al. (2004) estimate that katabatic winds increase average annual temperatures by 0.7 – 2.2 °C, depending on location. Seasonally, katabatic winds increase average winter temperatures by 0.8 – 4.2 °C, and average summer temperatures by 0.1 – 0.4 °C. Katabatic winds decrease relative humidity by –1.8 to –8.5% in winter, and –0.9 to –4.1% in summer, and increase wind speeds by 0.6 – 2.3 ms^{-1} in winter, and 0.2 – 0.8 ms^{-1} in summer (Nylen et al., 2004).

Local glacier drainage

Strong local glacier drainage winds also occur in the valleys (Doran et al., 2002) when the sun is low along the southern horizon, and heating of valley soils is minimal (Nylen et al., 2004). Down-glacier winds operate in much the same way as the katabatics, acting to drain cold air accumulated in basins above the alpine glaciers.

2.2.2 Influence of climate on geomorphology

Climate is a major factor controlling landform development in the McMurdo Dry Valleys (Marchant and Denton, 1996). The scarcity of liquid water in the Dry Valleys dictates that soil moisture content and relative humidity are fundamental in influencing the spatial distribution of solifluction terraces, gelifluction lobes, polygonal ground, and scree slopes (Marchant and Denton, 1996). Soil moisture

content and relative humidity are both strongly affected by atmospheric temperature and wind direction (Keys, 1980), thus landscape features vary spatially in relation to temperature and wind.

The availability of liquid moisture in soils largely determines the rate at which chemical and physical weathering processes, and hence soil development, occurs (Campbell and Claridge, 1982). Consequently, weathering and soil development act to control rates of downslope movement, fan development, and gullying (Marchant and Denton, 1996).

Marchant and Denton (1996) differentiate three climatic zones within the Dry Valleys on the basis of differences in precipitation, wind direction, relative humidity, temperature, and soil moisture content. Zone 1 is coastal, Zone 2 intermediate, and Zone 3 the far-western areas of the McMurdo Dry Valleys.

The coastal zone extends to about 1000 m elevation near the coast, and covers the inland valley bottoms to about 100 m elevation, having a relatively mild climate that facilitates the development of solifluction terraces, gelifluction lobes, ice wedges, rills, channels, debris flows, levees, and ephemeral ponds, lakes, and streams (Marchant and Denton, 1996). Therefore, as such landscape features require the presence of liquid water, soils developed in the coastal zone are described as subxerous, being moist for some period during the year, and thus having more moisture available for weathering than xerous or ultraxerous soils (Campbell and Claridge, 1982).

Zone 2, the intermediate zone, includes moderate-to-low elevation areas in the central Dry Valleys region and high-elevation areas near the coast (Marchant and Denton, 1996). Zone 2 is characterised by the presence of katabatic winds, which produce relatively cold and very dry conditions. Hence soil moisture and its associated landforms are rare, with ephemeral streams, accounting for less than 5% of the area in Zone 2, flowing for a few weeks each summer (Marchant and Denton, 1996).

The far-western inland areas of the Dry Valleys constitute Zone 3. Zone 3 encompasses all ice-free areas above 800 m elevation along the western edges of the Asgard and Olympus Ranges (Marchant and Denton, 1996). The climate of the inland region is hyper-arid, soils are ultraxerous, and glacial ablation is entirely by sublimation (Marchant and Denton, 1996), hence liquid water rarely, if ever, exists.

Dating of landforms and volcanic ash present within each of the climatic zones indicates that landscape stability increases with distance inland. Features of the coastal zone, such as solifluction terraces, gelifluction lobes, and fans, are younger than 12 000 years old, whereas undisturbed ash samples from within Zone 2 are late Miocene to mid-Pliocene in age (Marchant and Denton, 1996). Ashfalls of mid-Miocene and mid-Pliocene age are found in Zone 3, with their preservation in sand-wedges implying that relatively warm and wet climatic conditions, necessary for their disturbance through freezing and thawing of an active layer or erosion by liquid meltwater, have not occurred in the western Asgard and Olympus Ranges during the last 15.0 Ma (Marchant and Denton, 1996).

2.3 Antarctic streams

Streams in the McMurdo Dry Valleys differ considerably from most streams on Earth (McKnight et al., 1999). Ephemeral streams, flowing for between four and ten weeks during the austral summer (Lyons et al., 1997b; McKnight et al., 1999; Treonis et al., 1999), provide the only significant source of water to hydrological and biological systems within the Dry Valleys (Fountain et al., 1998).

Stream water is sourced from glacial melt (Gooseff et al., 2003; Gooseff et al., 2004), which begins in late November to mid-December, and continues until mid-January to early February (Conovitz et al., 1998). The onset of glacial melt and the concomitant arrival of liquid water enables microbial communities, having lain dormant, in a dessicated state over the winter months, to re-establish themselves (Vincent et al., 1993). Consequently, what appears a relatively

passive system over the winter months is transformed into a myriad of dynamic subsystems.

2.3.1 Stream characteristics

Stream length in the McMurdo Dry Valleys varies from less than 1 km to over 30 km, with the Onyx River in Wright Valley representing the latter. Stream bed width varies from 1 to 30 m (McKnight et al., 1999). The virtual absence of vegetation within the valleys constrains the stability of stream banks; small, sporadic patches of moss have a negligible stabilising effect on steeply sloped banks of poorly sorted sediment (McKnight et al., 1994; Conovitz et al., 1998; McKnight et al., 1999).

Most Antarctic streams flow through unconsolidated alluvium comprised predominantly of sand-sized particles interbedded with gravels, large cobbles and boulders (Conovitz et al., 1998). The unconsolidated nature of the alluvium, combined with the absence of stabilising vegetation, results in large sediment loads during high flows (Conovitz et al., 1998). Similarly, undercutting of the unstable stream banks during high stream flows can result in 1-2 cm deposits of sediment in the lower reaches of the streams (McKnight et al., 1999). However, some streams have diminished sediment transport levels resulting from the presence of a stone pavement within the stream bed. This armoured surface acts to stabilise the stream bed, and is formed by a combination of both fluvial and periglacial processes (Conovitz et al., 1998).

The relatively uniform substrate through which Antarctic streams flow leads to a strong similarity between streams. Dominant features of each stream are controlled by topography and hydrologic and periglacial processes (Fountain et al., 1999). However, the common features of Antarctic streams can be generalised as follows:

- In steep gradient reaches, the active channel ranges from 5 – 20 m in width, with steep stream banks at the angle of repose of the alluvium (at an angle in equilibrium with the alluvial material). Large, poorly sorted rocks

are present in the stream bed, with deposited sediment abundant at the margins of the active channel;

- In moderate gradient reaches, the active channel is composed of rocks wedged together to form an armoured stream bed, with steep stream banks again at an angle in equilibrium with the alluvial material of which they are comprised. Less sediment deposition is evident than in steep gradient reaches;
- In shallow gradient reaches such as second-order streams in the valley bottoms (e.g. the Onyx River), a sandy braided channel is formed as a result of sediment deposition from tributaries. Some channels may also have armoured stream beds. Stream banks are low, and again at the angle of repose of the alluvium (Fountain et al., 1999).

The armoured stream beds found in moderate and shallow gradient Antarctic streams probably develop as a result of long-term freeze and thaw cycles. Saturated alluvium within the stream channel freezes at the end of summer and thaws at the beginning of the following summer; this acts to rotate rocks until the larger side is upward, with clasts then becoming wedged together across the stream bed (Fountain et al., 1999). The fact that armoured stream channels are not commonly found in streams with steeper gradients may be attributed to greater stream flow velocities eroding the finer textured material, thus making larger rocks less prone to the action of freeze-thaw cycles (Fountain et al., 1999).

2.3.2 Hyporheic zones

The development of ephemeral stream channels produces contemporaneous hyporheic zones. Hyporheic zones extend several metres from ephemeral stream channels (Gooseff et al., 2003; Gooseff et al., 2004), and are evident as dark bands of moistened soil that border the streams (Figure 2.1).

Figure 2.1. Dark bands of moistened soil, indicative of the extended hyporheic zone, western branch of Hart Stream, Wright Valley. (Photo: M.R. Balks)

Hyporheic zones are defined by McKnight et al. (1999) as "the area adjacent to and underneath the stream, in which water flows through the stream bed in the downstream direction and exchanges with water in the main channel". Gooseff et al. (2003) elaborate on this definition, differentiating two hyporheic zones based on the time-scale over which exchanges take place. The near-stream hyporheic zone exchanges water and solutes with those in the stream on an hourly timescale, whereas exchanges with the extended hyporheic zone occur over a period of days to weeks or longer (Gooseff et al., 2003).

The rapid rate at which exchanges occur between the stream and the near-stream hyporheic zone is partly due to the high permeability of Antarctic stream beds and hyporheic zone sediments (McKnight et al., 1999), and dictates that the near-stream hyporheic zone is saturated, thus being in direct contact with the stream (Gooseff et al., 2003). Slower exchanges occurring between the stream and extended hyporheic zones, which are not in direct contact with the stream (Gooseff et al., 2003), mean that extended hyporheic zones are moistened, rather than saturated.

The exchange of water between stream channels and hyporheic zones means that any dissolved solutes are also exchanged. Solutes exchanged through the alluvial substrate on the sides and beneath the stream bed may undergo reactions that affect their transport (McKnight et al., 1999); thus solute exchanges and reactions may substantially influence the concentration of salts in soils of the hyporheic zone. Solutes present within extended hyporheic zones may be concentrated as a result of evaporation in summer, and sublimation in winter (Gooseff et al., 2003).

2.3.2.1 Extent of hyporheic zones

The absence of inflows from groundwater, combined with the rapid exchange rates of water between the hyporheic zone and main channel and the shallow ice cement barrier dictates that the hyporheic zones associated with Dry Valley streams are generally laterally extensive (McKnight et al., 1999; Treonis et al., 1999).

The vertical extent of the hyporheic zone is limited by the presence of ice cement, commonly at depths of around 50 cm beneath the ground surface. The depth to ice cement coincides with the lower limit of the active layer, which acts to increase or decrease the vertical limit of the hyporheic zone based on seasonal thawing. Consequently, the vertical extent of the hyporheic zone tends to increase over summer; Gooseff et al. (2003) report a vertical extent of up to 70 cm depth as the active layer thaws.

The combined lateral and vertical extent of the hyporheic zone can produce a lateral cross-section as large as 12 m^2 (Gooseff et al., 2003), thus providing a substantial reservoir of water which persists after glacial melt subsides. There are contrasting opinions as to the fate of such water over the winter season; Conovitz et al. (1998) suggest that water in the hyporheic zone is largely lost to evaporation rather than remaining until the next summer, whereas Gooseff et al. (2003) advocate the persistence of water in the hyporheic zone from one flow season to the next. Such contrasting views must be further investigated, as the fate of water in the hyporheic zone over the winter season has implications for the rate of

exchange of water in extended hyporheic zones, and the accumulation of salts in dry valley soils.

During colder, low-flow years, the amount of water stored in the hyporheic zone may constitute a greater proportion of the total meltwater from the source glacier than that in the stream itself (Conovitz et al., 1998). Such low flows in streams are likely to reflect the volume of water required to wet the hyporheic zone, with less water remaining as surface flow. This is fundamental in terms of its importance pertaining to regional hydrology, as well as human impacts on hydrological systems as moisture may not always be evident at the soil surface.

2.3.3 Stream flow variation

Hydrologic data from both Wright and Taylor Valley highlights tremendous variability in stream flow over daily, seasonal, and interannual time scales (Kennedy, 1993; Vincent et al., 1993; McKnight et al., 1994; House et al., 1995; Lyons et al., 1997b; Conovitz et al., 1998; McKnight et al., 1999).

Such variation is, arguably, predominantly a result of differences in solar intensity on source glaciers, with changes in intensity influenced by the sun angle (solar geometry) and the aspect of the glaciers (McKnight et al., 1994; Conovitz et al., 1998; Fountain et al., 1998). While recognising aspect and exposure to prevailing winds as being important in glacial melt, Chinn (1981b) cites altitude as the dominant factor controlling glacial ablation. However, Clow et al. (1988) suggest that the amount of meltwater sourced from alpine glaciers each summer is highly sensitive to the duration of periods when air temperatures are above 0 °C.

Clow et al.'s (1988) data from the austral summers of 1985/86 and 1986/87 indicate that the conditions required for temperatures to exceed 0 °C are somewhat erratic, giving rise to large interannual variations in meltwater production. Such variation in meltwater production is evident in stream flow data from the Onyx River (e.g. Fenwick and Anderton, 1975; Chinn, 1980; Chinn and Woods, 1984; Chinn and Dickson, 1986).

Nonetheless, temporal variability in stream flow is intimately linked to the rate of glacial melt, irrespective of its relative dependence on solar radiation, air temperature and altitude, which can ultimately provide an indication of both long and short term climatic fluctuations (Conovitz et al., 1998). Therefore, comparisons of measured stream flow rates with those expected under 'ideal' melt conditions can be used to monitor trends in climate change, over both spatial and temporal scales.

2.3.3.1 Factors affecting stream flow variation

Variation in stream flow is influenced by both "source" and "instream" processes (Conovitz et al., 1998). Source processes control the production of meltwater, hence they are primarily driven by climatic conditions such as cloud cover, temperature regime, and solar energy inputs to glacier surfaces and terminal faces (Conovitz et al., 1998). Stream flow is very responsive to changes in temperature and solar radiation, with such conditions rapidly altering the flow rate (Vincent et al., 1993; Conovitz et al., 1998).

Instream processes are thought to influence stream discharge patterns, and are affected by stream morphological characteristics such as gradient, length, bed morphology, and properties of the alluvium (Conovitz et al., 1998; McKnight et al., 1999). Variations in stream morphology affect the volume of water stored in the hyporheic zone, and, accordingly, the volume available to be exchanged with water in the main channel (Figure 2.2). Individual stream morphologies also influence flow velocity and sediment transport (Conovitz et al., 1998). Thus, as stream flow is controlled both climatically and morphologically, it is both highly spatially and temporally variable.

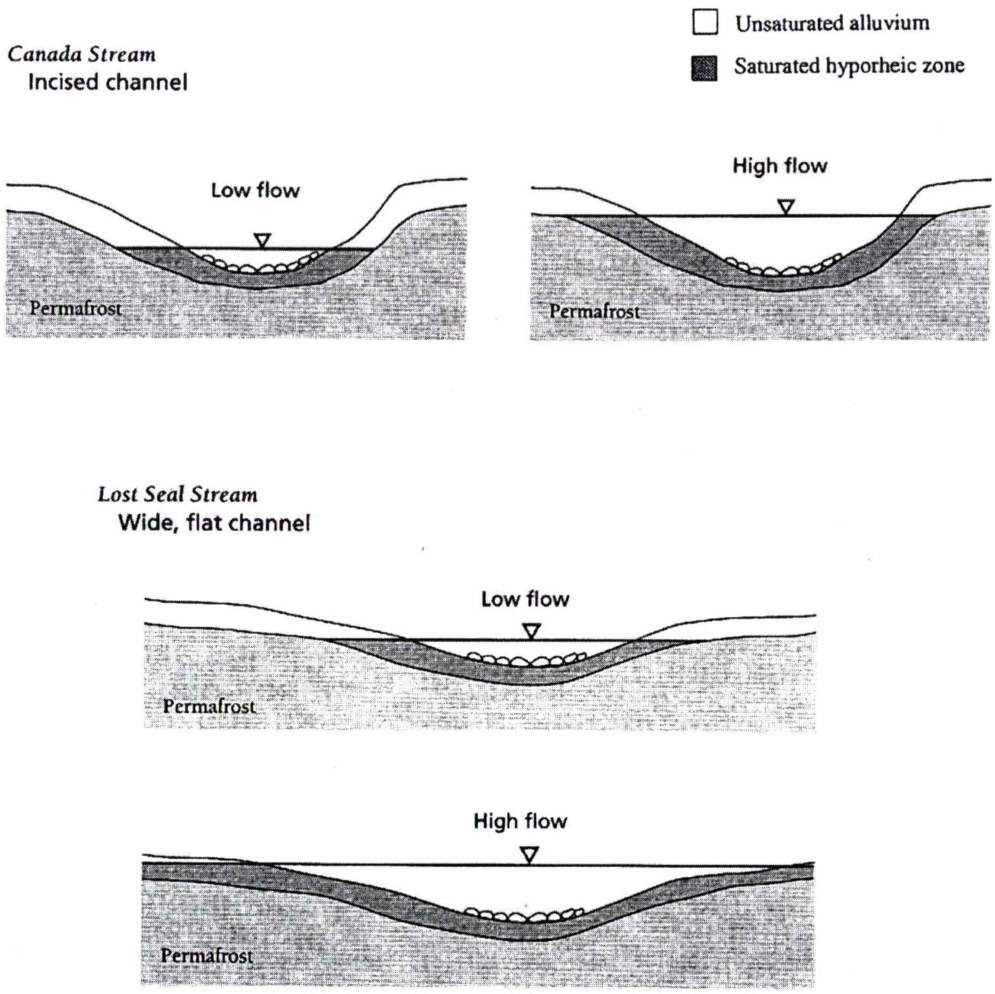

Figure 2.2. Schematic representation of the variation in extent of the hyporheic zone under low and high flow conditions in two morphologically different stream channels in Taylor Valley. (Source: Conovitz et al., 1998)

Solar radiation

The duration of flow is dependent on climatic conditions (McKnight et al., 1999), with solar radiation acting to drive the melt cycle (Vincent et al., 1993; Conovitz et al., 1998; Dana et al., 1998), and thus stream flow. Solar radiation however, is subject to considerable topographic variability, though coastal cloudiness and orographic effects may also influence solar radiation received (Dana et al., 1998). North facing slopes receive more energy than south facing slopes, while differences in solar radiation received also arise from terrain shading effects.

The variable nature of solar radiation received within the Dry Valleys produces strong daily and seasonal variations in glacier melting and stream flow (Vincent et

al., 1993; Conovitz et al., 1998; Dana et al., 1998). Solar radiation received is predominantly a function of changing solar zenith angle and azimuth, and shading by terrain (Dana et al., 1998). The maximum intensity of solar radiation occurs when the solar azimuth is normal to the glacial face (Conovitz et al., 1998). The diurnal and seasonal changes in solar zenith angle acts to influence incident radiation on glacial cliff faces.

Though glacial melt is small, the cliff faces are particularly important sources for stream flow (Lewis et al., 1999). Chinn's (1981b) data from the Wright Lower Glacier suggests that glacial meltwater volumes are more dependent on ice cliff length and orientation that the catchment area of the glacier surface. Cliff faces are the first part of the glacier to melt in spring, and the last to freeze in autumn (Dana et al., 1998; Fountain et al., 1998; Lewis et al., 1999). This arises from the solar zenith angle and azimuth dictating that the vertical cliffs of the terminal face present a surface more perpendicular to the sun's rays, compared with the horizontal glacier surface (Fountain et al., 1998), thus increasing meltwater production. The predominantly snow-free cliff faces also have a lower albedo than that of the glacier surface, thus absorbing more incident solar radiation (Lewis et al., 1999).

Hence, for a short period each day, when the sun's rays directly strike the terminal face, incident radiation is greater on vertical faces as opposed to the more horizontal glacial surface (Dana et al., 1998). The temporary increase in solar radiation intensity appears sufficient to melt the ice (Fountain et al., 1998). The terminus cliffs are also at lowest elevation, and closest to the warmer soil surface, thus being warmer than the corresponding upper surface of the glacier (Fountain et al., 1998). Consequently, ablation is further intensified.

Topography and cloud cover

Stream flow variations in the McMurdo Dry Valleys are predominantly controlled by climate, solar position, and geomorphic factors (Conovitz et al., 1998). However, topographic effects and the presence of clouds are also important

modulators of incoming solar radiation in the dry valleys (Dana et al., 1998). Under partly cloudy conditions, cloud fields act to dominate the spatial variability in incoming solar radiation. Conversely, under uniformly clear or cloudy skies, the spatial variability in solar radiation is dictated by topographic effects (Dana et al., 1998). Such effects arise from variations in slope, aspect, terrain reflectance, shadowing, and obstruction by nearby topography.

Other factors relating to solar radiation received also impact on the energy balance within the valleys; such factors exacerbate the inherent spatial variability, and include optical path length, and the scattering and absorbing properties of the atmosphere and their variation with height (Dana et al., 1998).

2.3.4 Habitat provision

Ephemeral streams provide habitats for, in some cases, relatively diverse microbial communities. The microbial communities consist primarily of cyanobacteria, though chlorophytes and diatoms are also found (Wynn-Williams, 1990; Vincent et al., 1993; Niyogi et al., 1997; McKnight et al., 1999). The continuous daylight of the austral summer and its associated stream flow also provides for the growth of algal communities. Algal communities grow in the streams as mats, having different colours due to photosynthetic and accessory pigments (Vincent et al., 1993; McKnight et al., 1999). Such communities are most abundant in stream reaches with armoured stream beds (Fountain et al., 1999). Stream macrofauna are limited to nematodes, rotifers, and tardigrades (McKnight et al., 1999).

2.4 Antarctic soils

Weathering in Antarctica proceeds at a slow rate, though differences in available moisture and surface age have a strong influence on soil development. Consequently, a highly variable soil pattern exists within the McMurdo Dry Valleys, driven predominantly by differences in climate, though also by parent material, surface age, and local relief.

2.4.1 Soil-forming environment

The soil-forming environment of the McMurdo Dry Valleys is characterised by hyper-arid climatic conditions; this is a function of the prevailing low temperatures, low precipitation, and low humidity (Campbell et al., 1997b). Thus available moisture is low, and biological activity is negligible (Campbell et al., 1998b). The landscape is phenomenally stable, and, consequently, the dominant soil-forming processes occurring are salinisation and oxidation (Bockheim, 1990; Campbell et al., 1997b; Campbell et al., 1998b).

Inherent soil variability is predominantly a function of the range of climatic conditions experienced, and, to a lesser extent, the geomorphic and geological differences within the region (Campbell et al., 1998b). The dominant geomorphic surfaces existing within the region include coastal lowland and marine terraces, long, narrow, steep-sided inland and coastal valleys, upland valleys, wide cirques, broad plateaus and high mountains (Campbell et al., 1998b). The soil-forming environment is also influenced by differences in parent materials on the different land surfaces, and by differences in the ages of the glacial deposits (Campbell et al., 1998b), though the influence of organisms on soil development is negligible (Campbell and Claridge, 1987).

2.4.2 Soil morphology

Soils of the McMurdo Dry Valleys are characterised by the presence of a surface pavement of lag gravels, often stained, ventifacted or polished, and underlain by a thin sandy horizon which is apparently formed by the physical disintegration of the surface stones (McCraw, 1967; Bockheim, 1980; Campbell and Claridge, 1982). Desert pavements increase in development with soil age and degree of exposure to katabatic winds; increasing development is seen as clasts packed more tightly together, and evidence of desert varnish, exfoliation, pitting, and ventifaction (Bockheim, 1980).

Below the desert pavement, soils commonly exhibit a zone of salt accumulation which overlies a layer of permanently frozen soil (permafrost) (Campbell and Claridge, 1982). The permafrost generally consists of ice-cemented ground, although in places where there is insufficient moisture to form an ice-cement, the frozen ground is referred to as "dry" permafrost (McCraw, 1967; Bockheim, 1997a). "Dry" permafrost is defined by Bockheim (1980) as ground which remains below the 0°C-isotherm for two or more years in succession but contains insufficient moisture to cause cementation by ice. The depth to ice-cemented permafrost varies with soil age and proximity to glaciers. In older soils located in particularly arid regions, ice-cemented permafrost may recede downwards in the regolith due to sublimation (Bockheim, 1980), thus forming an upper zone of "dry" permafrost above the ice-cemented layer.

Salt encrustations are found beneath coarse fragments in soils older than 18 ka (Bockheim, 1979), while salt flecks ranging from 2 – 5 mm in diameter occur in the matrix of soils older than 135 ka (Bockheim, 1980). Weakly cemented salt-pans are found in soils older than 1.2 Ma, and strongly cemented salt-indurated layers occur in soils older than 3.5 Ma (Campbell and Claridge, 1975).

The soil profile commonly consists of unconsolidated bouldery or pebbly gravels with some horizons weakly cemented by finer textured material (Campbell and Claridge, 1969; Claridge and Campbell, 1977). Physical disintegration and staining of clasts is strongest at the soil surface and in the upper horizons, decreasing with depth down the profile. Soil textures are dominantly controlled by the lithology of the parent material and weathering (Bockheim, 1980). Therefore, the availability of soil moisture plays an important role in influencing textural changes, as it is intimately linked to weathering processes. The fine-earth fraction of soils of the Dry Valleys tends to be dominantly sand, while coarse fragments (>2 mm) commonly comprise between 25 and 75% of pedons in these soils (Bockheim, 1980). Soil structure is generally absent and single-grained (Bockheim, 1980), and organic matter content is negligible (Campbell and Claridge, 1969; Claridge and Campbell, 1977; Campbell et al., 1998b).

2.4.3 Soil chemistry

Soils of the McMurdo Dry Valleys have pH values ranging from neutral to mildly alkaline (Bockheim, 1980). Electrical conductivities are high due to the arid, accretionary environment in which the soils develop. The dominant cation in 1:5 soil: water extracts of soils older than 18 ka is sodium (Bockheim, 1980); this further highlights the arid nature of the soil-forming environment, with the low moisture levels effectively preserving the presence of soluble salts.

Soils located within 75 km of the open sea contain chloride as the dominant anion (Bockheim, 1980), with the distribution of chloride markedly decreasing with distance inland (Keys and Williams, 1981). Ionic ratios of water extracts from these soils indicate that the provenance of sodium, magnesium, chloride, and sulphate ions is most likely marine, while the origin of calcium and potassium is probably from rock weathering (Claridge and Campbell, 1977; Bockheim, 1979; Keys and Williams, 1981). Salt efflorescences are dominantly comprised of sodium salts; such salts often contain chloride, thus reinforcing the dominance of sodium and chloride as the two major ions present in Antarctic soils (Bockheim, 1979).

The clay mineralogy of the McMurdo Valley soils is dominated by mica and iron-chlorite; these are inherited from the felsic nature of the parent material (Bockheim, 1979; 1980). Montmorillonite and vermiculite are also present. Vermiculite may form as a weathering product of the slow hydration of mica, while weathering of vermiculite to montmorillonite can be considered a function of the high pH and low leaching environment that prevails in soils of the Dry Valleys (Claridge, 1965; Bockheim, 1980).

2.4.4 Influence of climate on soil development

Climate is the single most important factor influencing the properties of Antarctic soils (Campbell and Claridge, 1987). The significance of local climatic conditions on soil development are such that they control the rate at which soil-

forming processes operate, with other soil-forming factors such as time and parent material having a comparatively negligible influence on soil genesis.

The dominant component of climate influencing soil development is the extreme cold temperatures. This acts to restrict the availability of water in the landscape, with any water present generally occurring as ice (Claridge and Campbell, 1977; Campbell and Claridge, 1987).

2.4.4.1 Soil moisture

Marked differences in climatic conditions in Antarctica are manifest in the soils as differences in moisture supply. This variation is predominantly seen as a difference in precipitation and its availability, thus being dependent on the length of time a soil is above freezing (Campbell and Claridge, 1982), or its proximity to a meltwater channel. Consequently, soil moisture availability is reflected in the development of soil morphological properties, such as soil depth, horizonation, and salt accumulation.

Individual site characteristics such as aspect and parent material are also important in determining soil moisture availability. Soils developed on northerly aspect sites will be considerably warmer than those on southerly aspect sites, while soils formed from darker coloured parent materials are likely to absorb more heat from incoming radiation than those formed in lighter coloured parent materials due to their lower albedo (Campbell and Claridge, 1987; Campbell et al., 1997a). The presence of snow also acts to increase the surface albedo, resulting in a greater proportion of short-wave solar radiation being reflected (Campbell et al., 1997a).

Soil salinity also influences the water content of Antarctic soils, with the presence of distinct salt horizons acting to produce significantly greater water contents than those in adjacent horizons without accumulations of soluble salts (Campbell et al., 1997b; Campbell, 2003).

The existence of moisture as small ice crystals, vapour, or thin water films (Campbell and Claridge, 1982) limits both physical and chemical weathering

processes, and provides few opportunities for the translocation of materials. The relative absence of moisture also promotes the precipitation and persistence of soluble salts in subsoil horizons, as with increased moisture levels, soluble salts may be dissolved in solution and leached from the soil (Campbell and Claridge, 1975).

2.4.4.2 Soil classification based on moisture regime

The extent of development of soil properties is predominantly dependent on climatic conditions, though soil development is also influenced by individual site characteristics such as aspect, proximity to moisture sources, the age of the land surface, and the characteristics of the parent material (Campbell et al., 1998b). However, the climate zonation system of Campbell and Claridge (1969) can be used to classify soils according to their moisture regime. Three zones are defined: ultraxerous, xerous, and subxerous. The three climatic zones encompass the regional climate variability, though individual site characteristics will appear as deviations from the typical soil chemical and morphological properties.

In each of the three climatic zones, the quantity of soluble salts present is related to the age of the soil and its moisture status, with salt abundance increasing linearly with time (Claridge and Campbell, 1977; Bockheim, 1979; 1990; 1997a).

Ultraxerous soils

Ultraxerous soils are found at high altitudes, dominantly inland, where both temperature and snowfall are low. Consequently, moisture is rarely, if ever, available, and, accordingly, there is no leaching of soluble materials (Campbell and Claridge, 1969; 1982). Ultraxerous soils do not generally exhibit a frozen ground layer except on sites with an aspect favouring warmer and moister conditions.

The presence of a strongly developed horizon of salt accumulations is common in ultraxerous soils. In older soils this may be up to 10 cm thick and consist almost

entirely of water-soluble salts (Campbell and Claridge, 1969). The salts present are dominantly nitrates and sulphates of sodium, magnesium, and calcium, and are representative of the residues remaining after sublimation of the snow cover, combined with the products of rock weathering (Campbell and Claridge, 1969). Chloride concentrations are low as a result of the low proximity to the sea (Campbell and Claridge, 1982).

The effects of chemical weathering on soils of the ultraxerous zone are minimal, with the absence of moisture and low temperatures severely limiting chemical degradation processes. However, some oxidation of iron compounds does occur, along with staining of soil particles. There is also breakdown of some soil minerals, while hydration of micaceous clays produces clay-vermiculites and montmorillonite (Campbell and Claridge, 1969).

Xerous soils

The xerous zone is the most extensive of the three zones, and experiences climatic conditions intermediate between the coastal (subxerous) and plateau (ultraxerous) regions (Campbell and Claridge, 1969; Bockheim, 1997a). Consequently, available moisture is greater than that of the ultraxerous zone. The dominant source of moisture is from summer snow-melt, with sufficient water released to allow some leaching of soluble materials from the profile (Campbell and Claridge, 1969; 1982).

Soils of the xerous zone are characterised by the presence of dry permafrost at a depth of between 45 and 100 cm (Campbell and Claridge, 1969; 1982; Bockheim, 1997a). These soils have a lower soluble salt concentration than ultraxerous soils of equivalent age; this reflects the greater level of moisture available and thus the stronger leaching regime of the environment.

Salts present in xerous soils also tend to be dispersed throughout the profile, rather than being concentrated in horizons as seen in soils of the ultraxerous zone. Those dominant within the soil matrix include nitrates, sulphates, and chlorides of

sodium, calcium, and magnesium, while encrustations of gypsum and calcite can be found on rocks above the soil surface (Campbell and Claridge, 1969). Soil colours tend to be darker and horizonation is distinct (Campbell and Claridge, 1969; Bockheim, 1997a); this is indicative of the slightly greater influence of chemical weathering, again reflecting the greater levels of available moisture.

Subxerous soils

Soils of the subxerous zone occur predominantly in coastal regions, where both temperature and precipitation are higher than in xerous or ultraxerous zones. Consequently, subxerous soils are exposed to greater levels of soil moisture; this is manifested in their morphology as a relative paucity of salt accumulations (Campbell and Claridge, 1969; Bockheim, 1997a). However, surface crusts of gypsum and coatings of carbonate on the undersides of stones are found. This is a function of the lower solubility of gypsum and carbonate, as the higher temperature, higher rainfall environment dictates that more soluble salts such as nitrates and chlorides are generally leached from the soil (Campbell and Claridge, 1969; 1982). Salts found in subxerous soils are generally chlorides, reflecting their low-altitude coastal location (Campbell and Claridge, 1975; Claridge and Campbell, 1977).

Meltwater is sourced from summer snowfalls, along with any remaining winter snow, and areas of permanent ice. Subxerous soils have ice-cemented permafrost within 30 cm of the surface, weak soil horizon development and shallow profiles (Campbell and Claridge, 1969; Bockheim, 1997a).

The weathering of subxerous soils is greater than that of xerous and ultraxerous soils, with soils of equivalent age appearing to be slightly finer textured (Campbell and Claridge, 1969). Soil colours are typically stronger, again highlighting the influence of available moisture on soil morphology. The clay mineralogy is dominated by clays such as montmorillonite, typical of those formed in a base-rich environment (Campbell and Claridge, 1969).

2.4.4.3 Salt accumulation

The influence of climate on soil development is primarily manifested as salt accumulations within profiles (Campbell and Claridge, 1975). A morphogenetic sequence of soluble salt accumulation in cold desert soils has been defined (Table 2.1) (Bockheim, 1990).

Table 2.1. Morphogenetic stages of accumulation of soluble salts in Cold Desert soils. (Source: Bockheim, 1990).

Salt stage	Maximum salt morphology	Electrical conductivity (dS/m)	Numerical age
0	None	<0.6	<10 ka
I	Coatings on stone bottoms	0.6-5.0	10-18 ka
II	Few flecks (<20% of surface area has flecks 1 – 2 mm in diameter)	5-18	18-90 ka
III	Many flecks (>20% of surface area has flecks 1 – 2 mm in diameter)	18-25	90-200 ka
IV	Weakly cemented pan	25-40	250-? ka
V	Strongly cemented pan	40-60	~ 1.7-2.5 Ma
VI	Indurated pan	60-100+	~ >2.5 Ma

The qualitative salt morphology is related to electrical conductivity and soil age (Bockheim, 2002). Soils of salt stages 0 and I are generally found in coastal regions and young surfaces, highlighting the effect of moisture availability and

time of soil development on the accumulation of salts. Greater salt accumulations, and thus salt morphological stages, occur in older soils with climate regimes dictating negligible availability of moisture.

2.5 Ecosystem vulnerability to human impacts

The cold desert environment which characterises the McMurdo Dry Valleys dictates that the ecosystem is particularly vulnerable to impacts from human activity, due to the long time-scales over which processes operate. Disturbances arising from walking, camping, and scientific investigation all have some degree of environmental impact associated with them; recovery time can range from a period of months to millions of years depending on the extent of the initial disturbance, local climatic conditions, and the rate at which natural site evolution processes occur (Waterhouse, 2001). An Environmental Code of Conduct has been developed for the McMurdo Dry Valleys in order to minimise disturbance associated with human activity in the valleys. Guidelines for behaviour within these areas are published in the McMurdo Dry Valleys ASMA Manual (Antarctica New Zealand, 2004).

2.5.1 Streams and lakes: Wright Valley

Streams and lakes in Wright Valley are particularly vulnerable to human impacts, as the hydrological system is closed. All meltwater is ultimately transported, via the Onyx River, to Lake Vanda (Turnbull et al., 1994; Isaac et al., 1996), an enclosed (Fenwick and Anderton, 1975; Chinn, 1980), thermo-haline, stratified lake in which bottom temperatures can be as high as 25.5 °C (Isaac et al., 1996).

The closed nature of the hydrological system within Wright Valley means that there are no opportunities for self-remediation, with all contaminants remaining within the lake (Waterhouse, 2001).

2.5.2 Soils

Soils of the McMurdo Dry Valleys are loose and unconsolidated, making them particularly vulnerable to disturbance (Campbell et al., 1993; Campbell et al., 1998a). Furthermore, natural recovery of disturbed sites in the Dry Valleys is slow due to negligible vegetative cover, the paucity of liquid water, and the limited movement of soil materials within the landscape (Campbell et al., 1993).

Disturbances to the environment can range from large-scale, high impact activities such as deep drilling, to smaller-scale field investigations such as soil and geological mapping (Campbell et al., 1993). Criteria for evaluation of the impact of field parties on the terrestrial environment have been developed; these include assessing the severity and extent of impacts from walking tracks, campsites, and scientific investigations (Campbell et al., 1993). Assessment of impacts can therefore be readily identified, and provide the basis for monitoring of residual impacts, and inter-site comparisons.

The effects of walking on soil disturbance have been monitored through several studies (e.g. Campbell et al., 1993; Campbell et al., 1998a). The degree to which soils are disturbed by walking is dependent on individual soil and site characteristics (Waterhouse, 2001). Older soils commonly show greater evidence of disturbance as contrasts between surface and subsurface material are likely to be greater, as opposed to contrasts in younger, less weathered soils (Campbell et al., 1998a). However, recovery from disturbances can be relatively rapid (~ 1 year), depending on local climatic conditions. Water and wind are the most effective agents of restoration; disturbed sites located in warmer, moister zones where freeze-thaw processes are active have a relatively rapid recovery rate (Campbell et al., 1993; Waterhouse, 2001).

The impact of camping on the soil environment depends on soil characteristics such as age and texture, as well as intensity of use and local the climate (Waterhouse, 2001). Soils with a high proportion of fine textured material (<2 mm) and a desert pavement comprised of small clasts are more susceptible to disturbance than soils with a greater proportion of coarser material (Campbell et

al., 1993; Campbell et al., 1998a), while sites located on areas where there are active fluvial or aeolian processes operating are likely to be rapidly naturally restored (Campbell et al., 1998a; Waterhouse, 2001).

Chapter 3
Study area and methodology

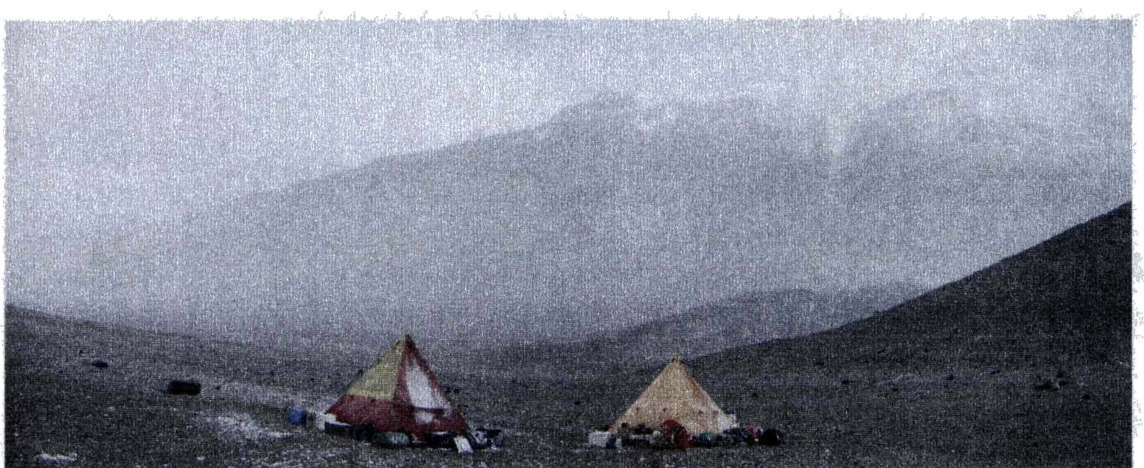

Chapter 3 Study area and methodology

3.1 Wright Valley

Wright Valley is located on the western margin of the Ross Sea embayment (Figure 3.1), forming part of the McMurdo Dry Valley system. Wright Valley is approximately 50 km long, and is bounded to the south by the Asgard Range, west by the polar plateau, north by the Olympus Range, and east by the Wright Lower and Wilson Piedmont Glaciers. The Onyx River flows inland – during the austral summer – for 29 km in the valley floor (Fenwick and Anderton, 1975), from Lake Brownworth, a proglacial lake of Wright Lower Glacier, to Lake Vanda (Hall et al., 1993).

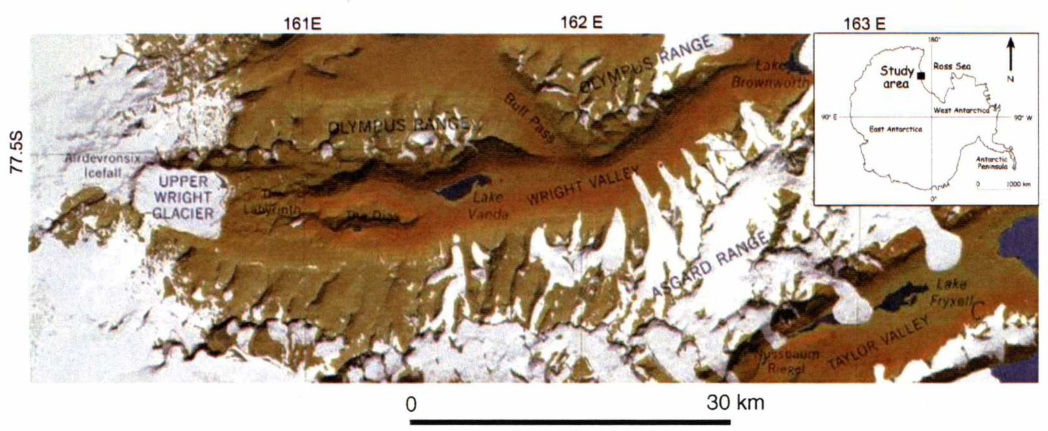

Figure 3.1. Location map of Wright Valley. (Adapted from Potton and Green, 2003)

The Onyx River is fed almost solely by glacial meltwater, the primary source of which is melt from the Wilson Piedmont Glacier (Chinn, 1980). Melt from the Wright Lower Glacier contributes a small proportion of flow in the Onyx River (Chinn, 1980); ephemeral streams from the alpine glaciers along the south wall of Wright Valley are estimated to contribute up to 10% of the Onyx River flow (Chinn, 1980; Chinn, 1981b). Total relief decreases from the western end of the valley, where peaks exceed 2000 m elevation (Bull, 1966), with mountains

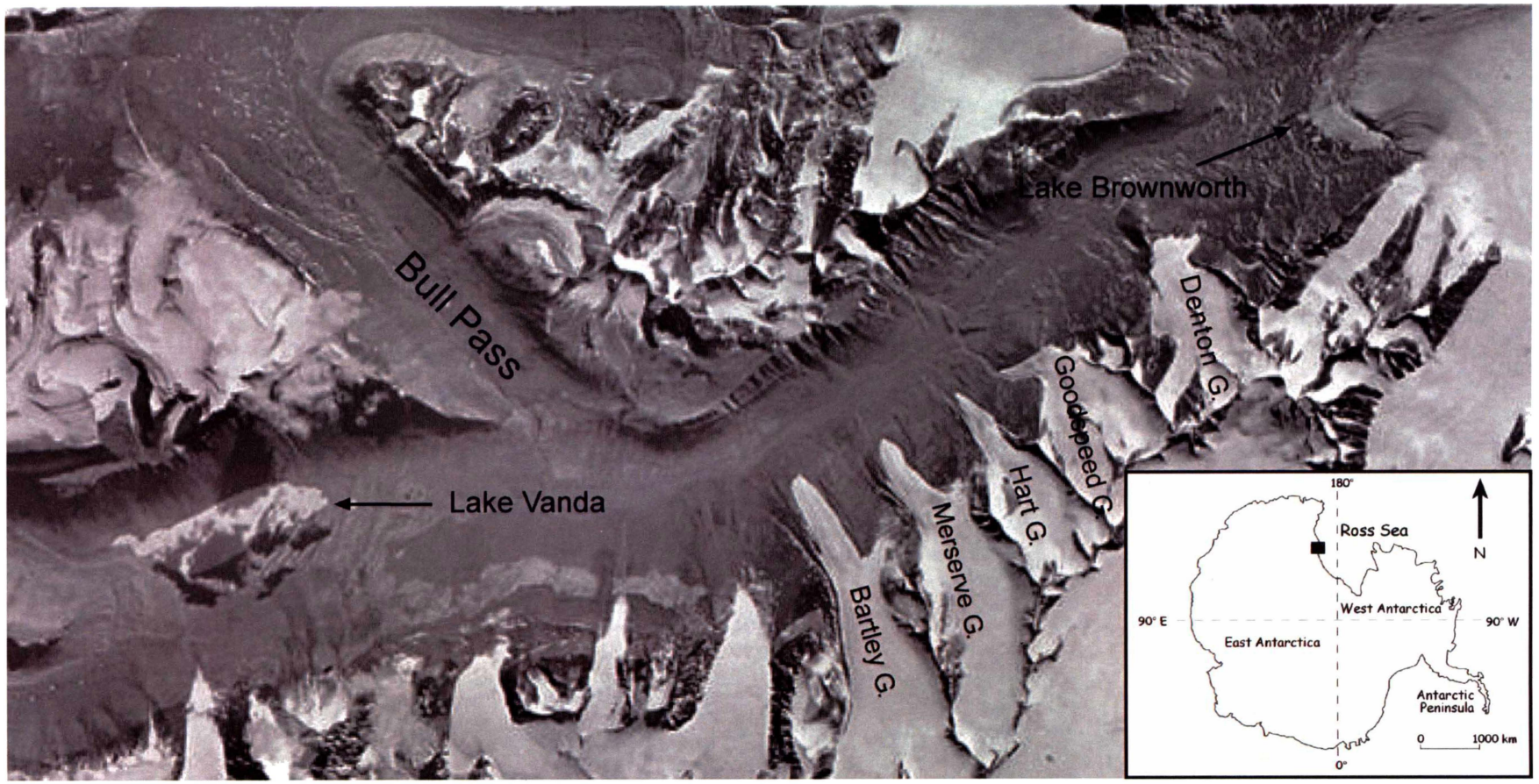

Figure 3.2. Main glaciers and other features of eastern Wright Valley.

becoming progressively dissected towards the coast (Marchant and Denton, 1996).

Towards the eastern end of Wright Valley, the landscape is dominated by cold-based alpine glaciers flowing down the south wall (Figure 3.2) (Hall et al., 1993); the north wall is predominantly scree and exposed bedrock. Mountain slopes have a patchy veneer of glacial till, interspersed with scree and colluvial material. The valley floor is characterised by large expanses of sandy gravel and ventifacted boulders, with the Onyx River bisecting the valley (Figure 3.3).

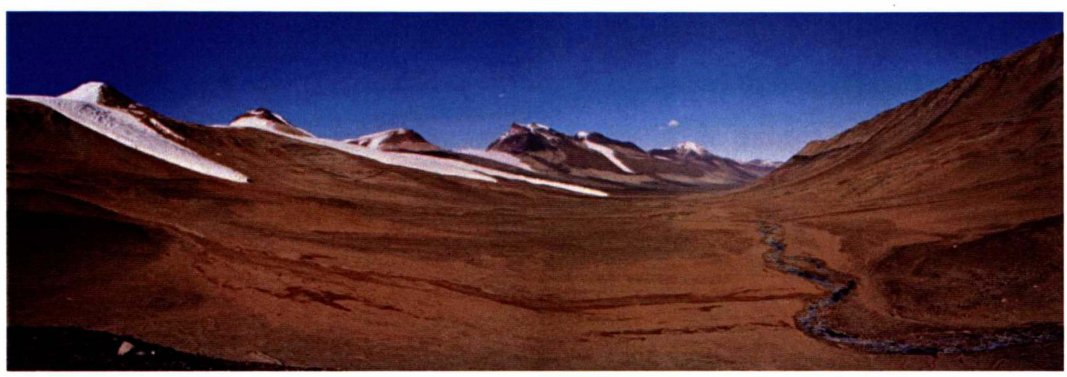

Figure 3.3. View of Wright Valley, looking west from the western side of Loop Moraine. The Onyx River is on the right hand side of the image; dark areas leading towards the Onyx River in the foreground are the Goodspeed Stream hyporheic zones.

3.1.1 Geology and geomorphology

The McMurdo Dry valleys are east-west oriented (Bull, 1966; Hall et al., 1993; Isaac et al., 1996), deglaciated valleys (Nichols, 1966). The topography of the Dry Valleys has remained virtually unchanged since it was carved beneath the last major wet-based overflow of the East Antarctic Ice Sheet, in Late Miocene time (13.6 – 15.2 Ma) (Isaac et al., 1996).

The geology of the Valleys is commonly well exposed. The valley floors are covered with late Cenozoic glacial, fluvioglacial and periglacial deposits (Isaac et al., 1996). Basement rock exposures are complexes of lower Paleozoic igneous and metamorphic rocks (Marchant et al., 1993); in lower Wright Valley these are predominantly the Granite Harbour Intrusives (Isaac et al., 1996). The basement

rocks are overlain by Devonian-to-Triassic sandstones, siltstones and conglomerates of the Beacon Supergroup (Marchant et al., 1993; Isaac et al., 1996). Both the basement and overlying units are intruded by thick sills of Jurassic-age Ferrar Dolerite (Marchant et al., 1993; Isaac et al., 1996).

The gentler slopes, benches and valley floors are almost all covered by tills of variable thicknesses (Isaac et al., 1996), preserving evidence of ice advances from the inland ice sheet, the Wilson Piedmont Glacier and Ross Sea ice, and local alpine glaciers (Hall et al., 1993; Turnbull et al., 1994; Hall and Denton, 2005). The till deposits are mostly pre-Pleistocene in age, though some were deposited during the Mid-Miocene (Isaac et al., 1996). Moraines are present on the valley floors and walls; some, such as Loop Moraine (Pliocene or Miocene in age) (Hall and Denton, 2005); towards the eastern end of Wright Valley have been overridden by subsequent glacial advances (Hall et al., 1993; Hall and Denton, 2005).

The valley walls are mantled by screes which generally thicken and become more extensive towards the heads of the valleys (Isaac et al., 1996). Tills near the valley floors are derived predominantly from granitoid rocks; steeper slopes are mantled by dolerite screes (Turnbull et al., 1994; Isaac et al., 1996).

Most surficial deposits within the valleys have been modified to some extent by cryoturbation, commonly forming polygonal patterned ground (Turnbull et al., 1994; Isaac et al., 1996). However, patterned ground cracks are less common on older surfaces, probably due to their very low soil moisture contents (Nichols, 1966).

The land surface with the Dry Valleys is extraordinarily stable (Denton et al., 1993; Hall et al., 1993; Marchant et al., 1993; Isaac et al., 1996). Consequently, periglacial processes have been operating over long time-scales (Isaac et al., 1996). Peleus till blankets much of the floor and southern wall of Wright Valley (Isaac et al., 1996), and is overlain by Alpine III and IV moraines derived from local alpine glaciers in central Wright Valley (<3.5 and >3.7 Ma, respectively) (Hall et al., 1993). Ages of basalt clasts in Alpine III/IV drift beside the western

margin of Bartley Glacier suggest that Peleus till was deposited at least >3.8 Ma ago, and probably >13.6 Ma ago (Hall et al., 1993). Correlation of Peleus till with Asgard till deposited between 13.6 and 15.2 Ma in the western Asgard Range (Marchant et al., 1993) supports a deposition age for Peleus till of >13.6 Ma (Hall et al., 1993), and suggests long-term stability of the East Antarctic Ice Sheet (Hall et al., 1993; Marchant et al., 1993).

Alluvial deposits occur only in stream channels and as associated fans. As stream channels are currently of an ephemeral nature, and, arguably, show no signs of much larger flows in the past (Isaac et al., 1996), many of the fans are thought to be derived from the melting of a small snow or ice field. Rapid melting of the snow or ice is thought to have produced enough water over a short period for a fan to develop (Isaac et al., 1996, after I. Campbell, written communication).

Ferrar Supergroup dolerites disintegrate over millions of years to form extensive screes (Isaac et al., 1996). More resistant fine grained dolerites develop desert varnish, oxidation rinds and surface pitting. Ventifacts of fine grained Ferrar Dolerite and Beacon Supergroup sedimentary rocks are common on the floors and sides of the valleys (Figure 3.4) (Bull, 1966; Turnbull et al., 1994; Isaac et al., 1996); the ventifacts are formed by strong winter westerly winds, and are often highly polished (Nichols, 1966).

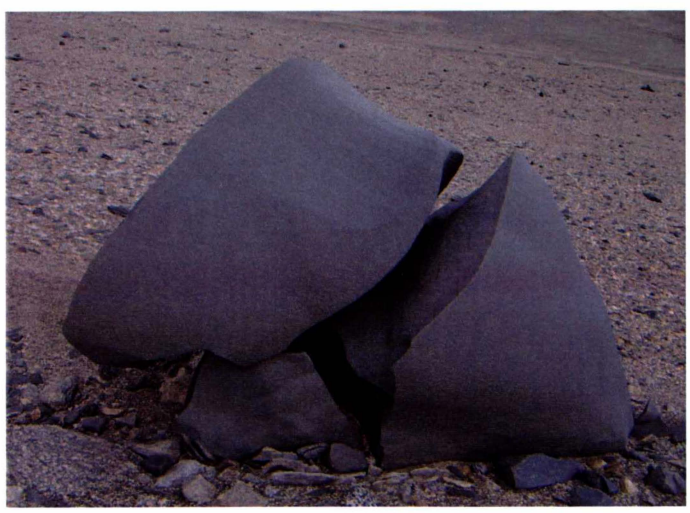

Figure 3.4. Ventifacted dolerite boulder, Wright Valley.

Salt encrustations are common on the undersides of most surface boulders and cobbles (Turnbull et al., 1994; Isaac et al., 1996). The origin of the salts is predominantly marine, though there is also evidence that some salts are derived from rock weathering (Claridge and Campbell, 1977). The crystallisation of salts in pores and fractures within rocks causes pitting and flaking; this typically leads to cavernous weathering (Figure 3.5), particularly in coarser grained dolerites and granitoids (Turnbull et al., 1994; Isaac et al., 1996). Surfaces of cavernously weathered granites are soft and flaky, in contrast to the hard polished surfaces of dolerite ventifacts (Nichols, 1966).

Figure 3.5. Cavernously weathered granite boulder, Wright Valley.

3.2 Goodspeed Stream (W channel)

Goodspeed Stream is an ephemeral stream located towards the eastern (lower) end of Wright Valley. It is sourced from meltwater from the Goodspeed Glacier (Figure 3.6), situated between the Hart and Denton Glaciers. The western channel of Goodspeed Stream (hereafter referred to as Goodspeed Stream, as the eastern channel was not considered in this study) flows for 1.75 km from the terminal face of the Goodspeed Glacier before coalescing with the Onyx River in the valley floor. The stream has an overall drop in altitude of 290 m from the Goodspeed Glacier terminal face to its confluence with the Onyx River, and thus an average gradient of 166 m km^{-1}.

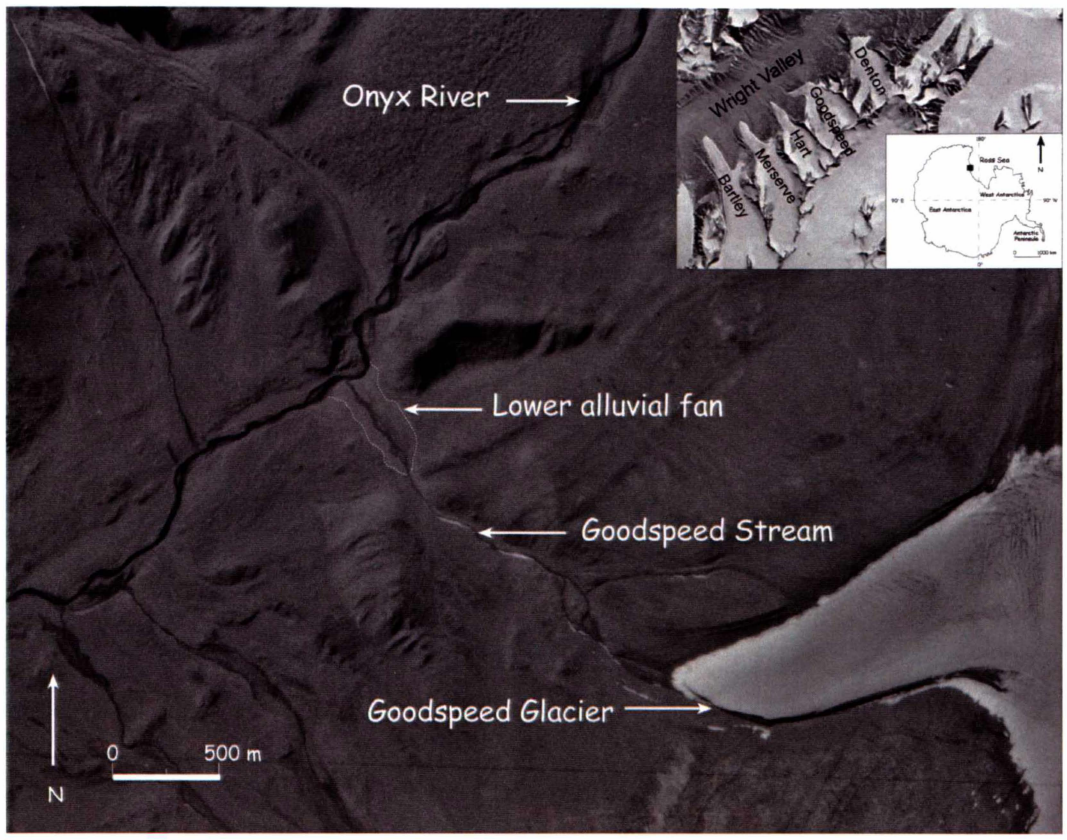

Figure 3.6. Location of Goodspeed Stream.

In January 2005, Goodspeed Stream was first observed on the true left of the Goodspeed Glacier terminal face, emerging onto a broad area of alluvium harbouring subsurface flow. Stream flow was concentrated further downstream where numerous flow paths converged to form a single channel, which ran through a narrow bouldery gully with a gradient of around 10° before emerging onto the lower alluvial fan (Figure 3.7), about 1.25 km from the terminal face of the Goodspeed Glacier. The lateral extent of the extended hyporheic zone visibly increased at the top of the lower alluvial fan; stream flow decreased from this point throughout the lower reaches of Goodspeed Stream as water flowed into the laterally extensive hyporheic zones.

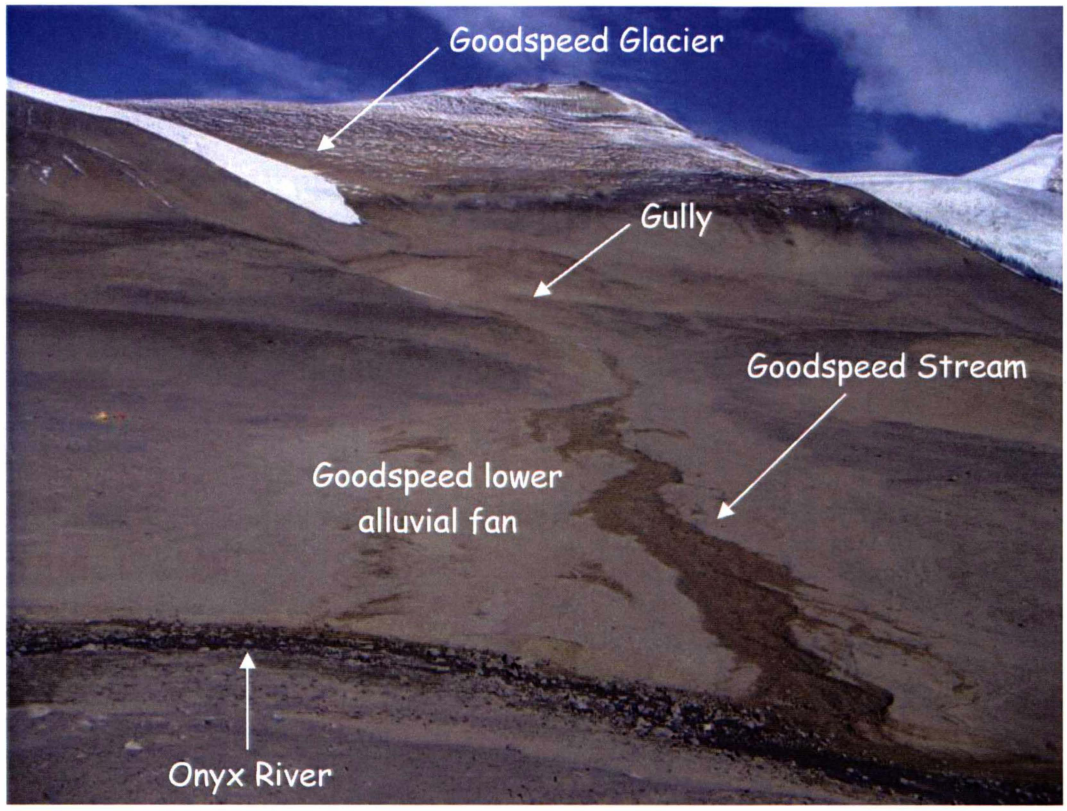

Figure 3.7. Goodspeed Stream hyporheic zones and lower alluvial fan showing the extent of surface expression of the hyporheic zones, viewed from the Loop Moraine photo monitoring point.

On the lower alluvial fan, Goodspeed Stream was predominantly single-channelled. The stream gradient was consistently around 5°, and the stream bed consisted of very coarse gravel and boulders ranging from 10 to 30 cm in length (long axis).

3.2.1 Soils of the Goodspeed lower alluvial fan

The Goodspeed lower alluvial fan is probably Holocene in age (Bockheim, Pers. Comm., 2005), and overlies the Onyx drift (<3.3 Ma) (Hall et al., 1993; Hall and Denton, 2005). The desert pavement on the lower alluvial fan surface is weakly developed, with clasts interspersed with gravel and sand sized material. Soils are relatively weakly weathered into alluvial and colluvial deposits dominated by granite.

3.2.2 Climate

The climate of the Goodspeed Stream area can be considered similar to that generalised for the Wright Valley. Automated Weather Stations (AWS's) are located at Lake Brownworth, east of Goodspeed Stream, at the foot of Bull Pass, west of Goodspeed Stream, as well as at Lake Vanda. The mean annual temperature in Wright Valley is around –20 °C, and mean annual precipitation is less than 100 mm water equivalent (Keys, 1980). Solar radiation is absent between the months of April to August (Nylen et al., 2004). Climate data obtained over the duration of this study are discussed in the following chapter.

3.2.3 Field season

This study was carried out over the period 1 – 31 January, 2005, with climate data recorded at the Goodspeed Stream site over the period 4 – 30 January 2005. At the time of writing, climate data for the Bull Pass climate station were available from January 1999 – 16 January 2005.

3.2.4 Stream and hyporheic zone characterisation

Ten sites, including one daily monitoring site, along Goodspeed Stream were used to characterise Goodspeed Stream and its hyporheic zones (Figure 3.8). At each site, stream depth and width, and width of both the near-stream and extended hyporheic zones were measured; stream flow was estimated using a bucket, measuring cylinder, and stop watch.

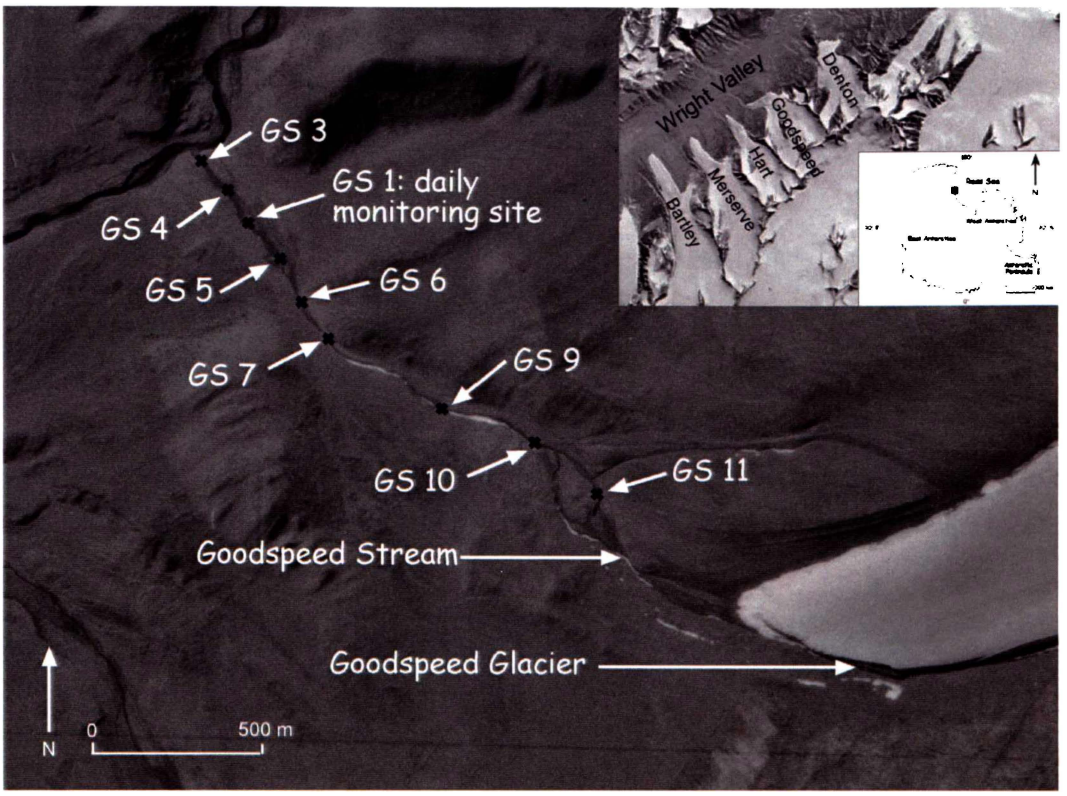

Figure 3.8. Sampling locations along Goodspeed Stream, including the daily monitoring site. Site GS 2 is located 5 m upstream from GS 1.

The height above the stream channel at which moisture was present was measured at the outermost edge of the extended hyporheic zone. Measurements were made by holding a taut string at ground level at the edge of the extended hyporheic zone, ensuring it was level before measuring the height of the string above the stream surface. However, the limited accuracy of this method means that measurements should be treated as indicative.

Surface soil samples (0 – 2 cm) from the Goodspeed Stream extended hyporheic zone and adjacent dry soil were taken for laboratory analyses.

3.2.5 Goodspeed Stream daily monitoring site

A daily monitoring site was established on Goodspeed Stream (77° 29′ 13.9" S, 162° 21′ 27.4" E), c. 230 m above its confluence with the Onyx River. The daily monitoring site was c. 250 m below the emergence of Goodspeed Stream onto the lower alluvial fan.

Data were recorded at the daily monitoring site at least twice a day between 4 and 30 January 2005. Measurements of air temperature and wind speed were made using a Silva hand-held "Atmospheric Data Centre", and percentage cloud cover was estimated at the time of observation. Stream flow was estimated using a bucket, measuring cylinder and stop watch; stream depth and width, and width of the visible extent of both the near-stream and extended hyporheic zones was measured. Markers were placed at the outer limits of the extended hyporheic zone so as to easily measure changes in its lateral extent. The width of a band of visible salt precipitating on the western bank of Goodspeed stream was also measured (Figure 3.9).

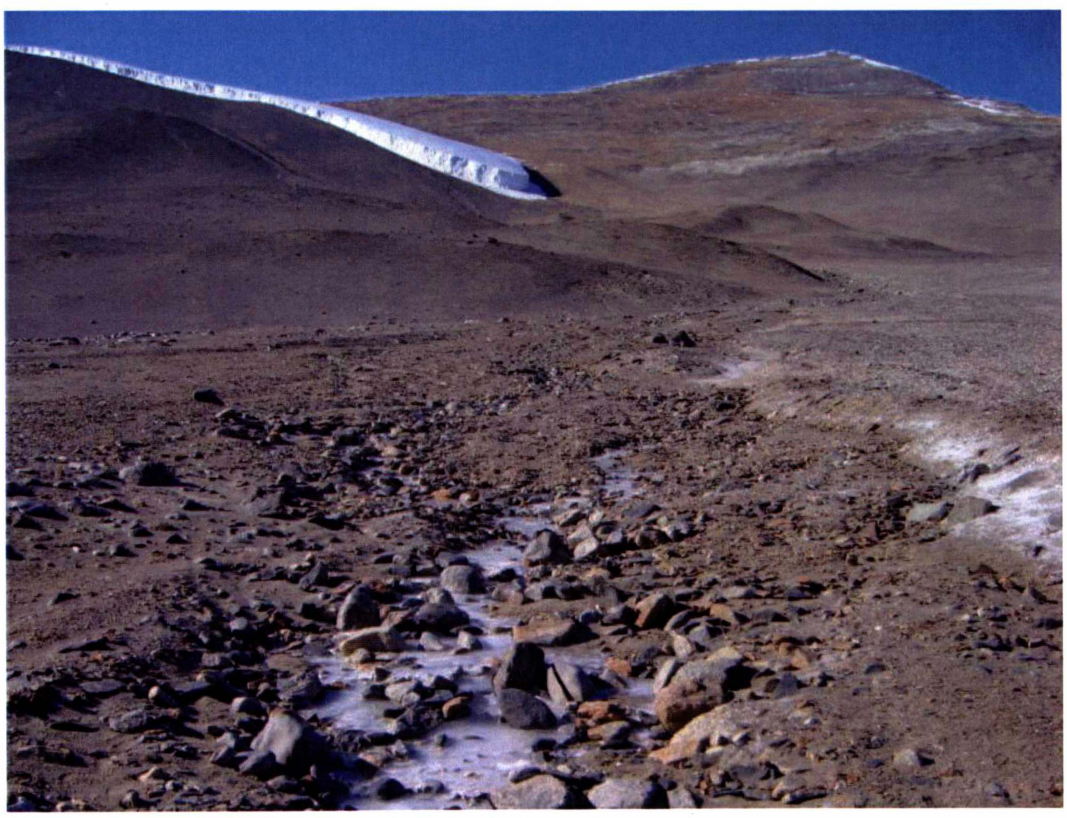

Figure 3.9. View upstream towards Goodspeed Glacier from the Goodspeed Stream daily monitoring site. The stream (frozen) is approximately 60 cm in width. The white area on the right-hand side of the photo is a band of salt precipitating out at the limit of the extended hyporheic zone. Distance to the terminal face of the Goodspeed Glacier is approximately 1.5 km from where this photo was taken.

3.2.6 Loop moraine photo monitoring point

Photo monitoring of Goodspeed Stream and its hyporheic zones over the lower alluvial fan was conducted from the crest of Loop moraine, on the north side of the Onyx River opposite the Goodspeed lower alluvial fan (77° 29′ 05.1" S, 162° 21′ 01.7" E). The photographs taken provided visual corroboration of measurements made at the Goodspeed Stream daily monitoring site.

3.2.7 Goodspeed Stream climate station

A temporary climate station was installed at the Goodspeed Stream daily monitoring site (Figure 3.10). Air temperature and relative humidity were measured by a shielded probe (Skye 2031, Skye Instruments Ltd., Powys, UK), at a height of 0.84 m above ground. Solar radiation flux density was determined using a pyranometer (Eppley PSP, The Eppley Laboratory Inc., Newport, Rhode Island). Soil temperature and moisture content at 5 cm depth (mid-point of probes) in the near-stream and extended hyporheic zones of Goodspeed Stream were measured by two Hydra probes (Stevens Vitel Inc., Chantilly, Virginia). Each parameter was measured every ten seconds, with half hourly averages logged by a data logger (CR10X, Campbell Scientific Inc., Logan, Utah).

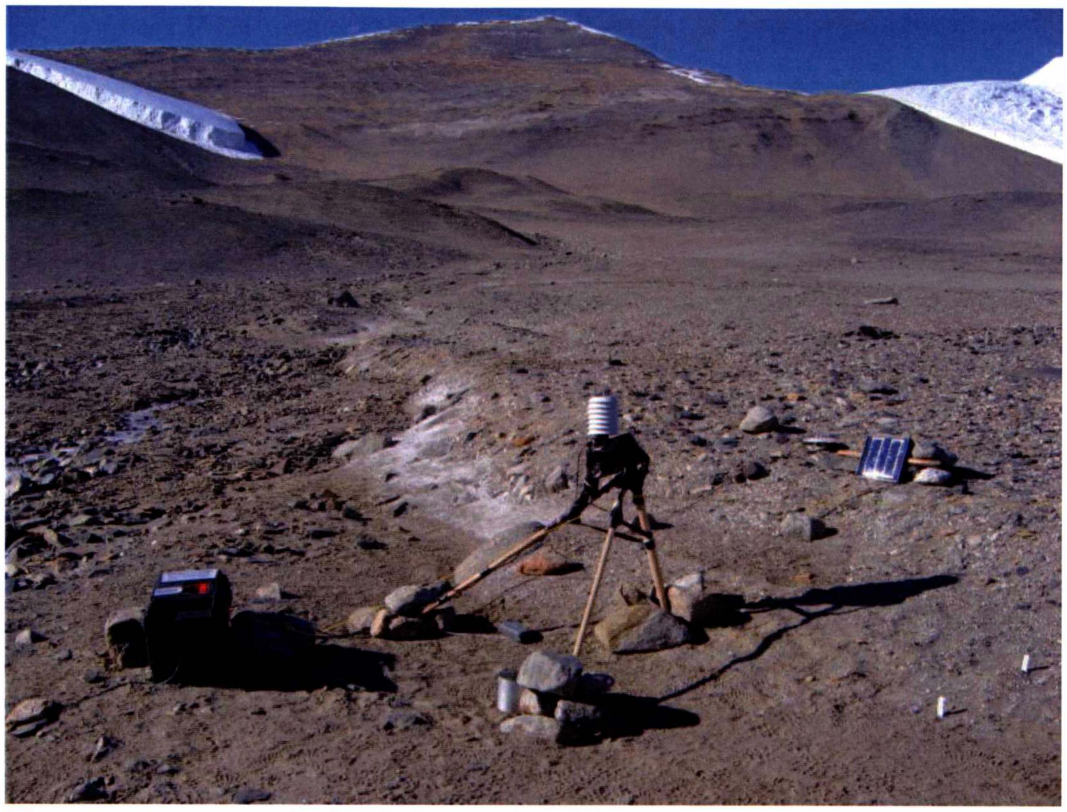

Figure 3.10. Climate station at the Goodspeed Stream daily monitoring site. Goodspeed Glacier is in the top left-hand corner of the image.

3.2.8 Bull Pass climate station

Climate data were also obtained from the Bull Pass climate station, an automated weather station (AWS) located c. 15 km west of the Goodspeed Stream daily monitoring site (77° 31′ 05.7" S, 161° 51′ 57.3" E). However, at the time of writing, data from the Bull Pass site were only available until 16 January 2005, at which time the annual data download occurred.

At the Bull Pass climate station, air temperature was measured by a RM Young RTD sensor situated 1.6 m above the ground surface. Soil temperature and moisture content were determined by Vitel Hydra probes, including 2 replicates at a depth of 2 cm. As the Hydra probes are 5 cm in diameter, the probes installed at 2 cm depth were considered as having the top edge of the probe 2 cm below the soil surface (Balks, Pers. Comm., 2005). Therefore, the mean depth of the probe was considered to be 4.5 cm ± 2 cm. Data from the Hydra probes at Bull Pass were thus comparable to data from 5 cm depth at the Goodspeed Stream site.

A LiCor LI200X pyranometer was used to determine solar radiation. Wind speed and direction were measured by a Met One Sensor, at a height of 3 m above the ground. Atmospheric variables were measured at ten second intervals; soil variables were measured every fifteen minutes (Balks et al., 2002; Guglielmin et al., 2003). All measurements were averaged hourly, with average values subsequently being recorded by a Campbell CR10X data logger.

3.3 Soil sampling

Soil samples were taken along two transects across the Goodspeed alluvial fan (Figure 3.11). At each interval, a small pit was excavated. Care was taken to remove the desert pavement, placing it onto a ground-sheet before excavating the subsoil onto a separate sheet. Soil profiles deemed characteristic of those on the Goodspeed lower alluvial fan were described using the methods of Milne et al. (1995), and classified according to USDA Soil Taxonomy (Soil Survey Staff, 2003) (Appendix I).

Sampling increments were determined by soil morphology, though samples were contiguous within pits. Total depth of sampling was limited by the depth of ice-cemented permafrost. Following sampling, the excavated subsoil was replaced, with special care being taken to 'pedocosmetically' restore the desert pavement as close as possible to its original state. Samples were double bagged and transported back to New Zealand for laboratory analyses.

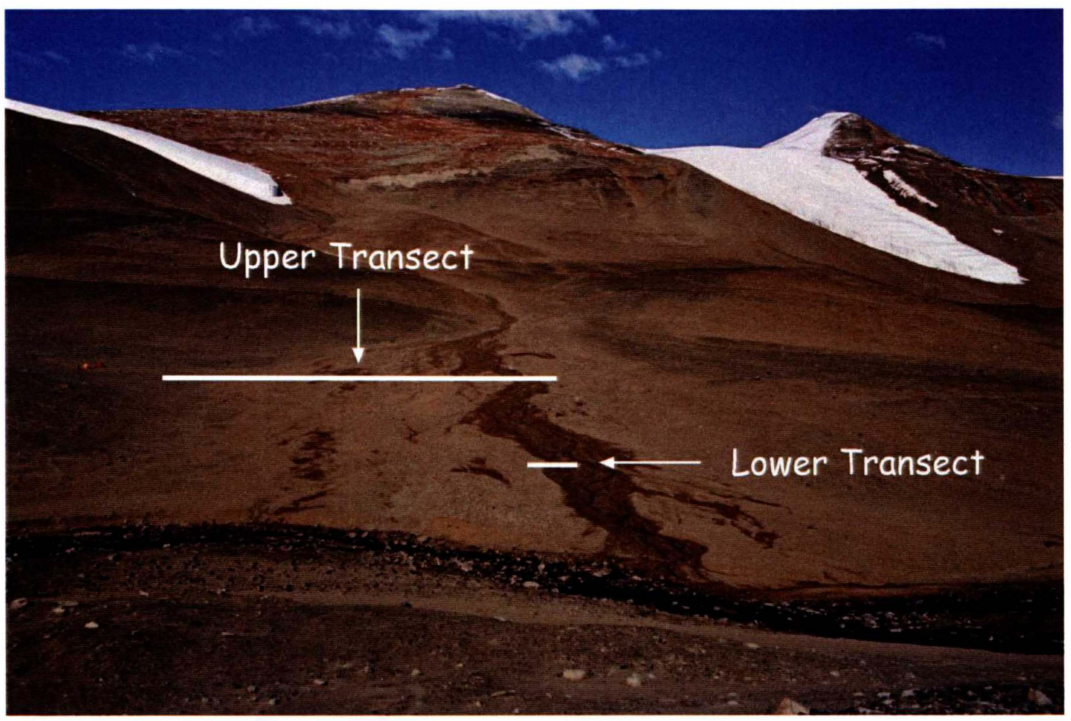

Figure 3.11. Sampling transects across the Goodspeed alluvial fan.

3.3.1 Goodspeed Upper Transect

The Goodspeed Upper Transect spanned 151.5 m across the Goodspeed Stream hyporheic zones and lower alluvial fan (Figure 3.12). 27 soil pits were excavated and sampled across the transect; the first just beyond the western bank of Goodspeed Stream (0 m; 77° 29' 13.9" S, 162° 21' 26.7" E), and the last at the foot of the western side of the Loop moraine (151.5 m; 77° 29' 10.6" S, 162° 21' 42.9" E). Goodspeed Stream intersected the transect at distances of 5.6 and 8.1 m.

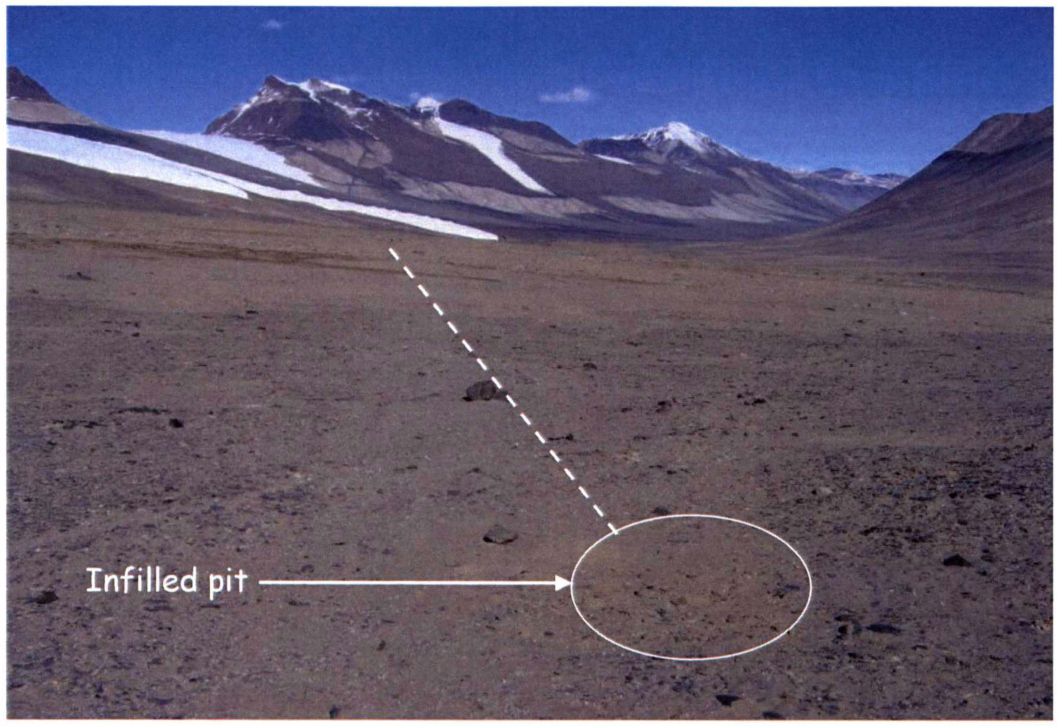

Figure 3.12. View west along the Goodspeed Upper Transect (dashed line). The arrow points to the surface of a pit which has been excavated and restored; disturbance was minimised.

The Goodspeed Upper Transect was sampled between 7 and 16 January 2005, with the upper two increments (0 – 2 and 2 – 5 cm) at each site on the transect being re-sampled on 27 January 2005. The time interval between initial sampling and re-sampling of the upper increments was sufficient that climatic conditions, and conditions within the extended hyporheic zone, had changed. In late January, the extended hyporheic zone was freezing at the surface on a diurnal basis, while also appearing to dry out.

3.3.2 Goodspeed Lower Transect

The Lower Transect on the Goodspeed alluvial fan was much shorter than the Upper Transect, its purpose being to obtain data from another part of the Goodspeed Stream extended hyporheic zone. The Lower Transect extended 18.2 m from the eastern edge of Goodspeed Stream (0 m; 77° 29' 10.9" S, 162° 21' 16.2" E) to about 4.5 m beyond the extended hyporheic zone on the lower alluvial fan (18.2 m; 77° 29' 10.6" S, 162° 21' 17.1" E) (Figure 3.13). Seven pits were excavated and sampled on 25 January 2005.

Figure 3.13. View west across the Goodspeed Lower Transect. The slight surficial whitening in the centre of the photo is evidence of salt precipitation at the soil surface, within the extended hyporheic zone.

3.3.3 Sample preparation

Bulk soil samples were sieved to <2 mm. Gravimetric moisture content was determined before remaining samples were air-dried for subsequent laboratory analyses.

3.4 Laboratory analyses

All analyses were carried out in duplicate, with mean results reported (Appendix II – V).

3.4.1 Gravimetric moisture content

Gravimetric moisture content (θ_g) was determined on both coarse (>2 mm) and fine (<2 mm) material. An approximately 15 g sub-sample was weighed (M_w)

before being dried for a period of 8 – 24 hours at 105 °C. Samples were then cooled in a dessicator before being re-weighed (M_d) and the gravimetric moisture content determined (Eqn. 3.1).

$$\text{Gravimetric moisture content } \theta_g\,(\%) = \frac{M_w - M_d}{M_d} \times 100\,\% \qquad \text{(Eqn. 3.1)}$$

where M_w = mass of moist sub sample

M_d = mass of dry sub sample

3.4.2 Soil pH (H_2O) and electrical conductivity

Soil pH in water, and electrical conductivity were determined using the methods described by Blakemore et al. (1987). Soil pH and electrical conductivity measurements were made on 1:2.5 and 1:5 soil:water slurries, respectively. Soil pH in water was measured using an Orion pH/ISE meter (model 710A). pH measurements did not stablise quickly on all meters tried; the cause of the instability was not identified. Therefore, soil pH data are considered to be indicative only (Appendix II), with a measurement error of ± 1 pH unit. Soil electrical conductivity was determined by an EDT GP 383 Conductivity Meter.

3.4.3 Particle size

The particle size distribution of the <2 mm fraction was determined by hand-sieving and weighing. The size classes used were based on particle-size fractions reported by Milne et al. (1995) (Table 3.1).

Table 3.1. Particle size fractions used in determining the particle size distribution of soils of the Goodspeed lower alluvial fan. (After Milne et al., 1995)

Fraction	Particle size (mm)
Coarse sand	2.0 – 0.6
Medium sand	0.6 – 0.2
Fine sand	0.2 – 0.063
Silt and clay	<0.063

3.5 Estimation of soil moisture potential

The total soil moisture potential (ψ_t) is the sum of three components: gravitational potential (ψ_g), matric potential (ψ_m) and osmotic potential (ψ_s) (Hillel, 2004). The osmotic potential, which relates to differences in solute concentration, has been ignored in this analysis. Gravitational potential relates to the position of a parcel of soil water in relation to the Earth's gravitational field (Hillel, 2004), and decreases with increasing depth in the soil. The gravitational potential is commonly expressed in units of potential energy per unit volume, which is equivalent to units of pressure (k Pa) (Hillel, 2004):

$$\psi_g = \frac{mgh}{V} = \rho_w gh \qquad \text{(Eqn. 3.2)}$$

where m and V are the mass (kg) and volumes (m^3) of the parcel of soil water respectively, g is the acceleration due to gravity (m s^{-2}), and h (m) is the elevation relative to some arbitrary reference level, usually the soil surface (hence it is a negative number, decreasing with increasing depth). ρ_w is the bulk density of water (1000 kg m^{-3}).

Matric potential (ψ_m) arises dominantly from capillary forces (Hillel, 2004); the drier the soil, the lower the matric potential. The soil hydraulic curve relating soil matric potential (ψ_m) to soil moisture content (θ) is time consuming and difficult

to obtain experimentally. However, the hydraulic curve can be estimated by measuring θ at limited values of ψ_m, and fitting equations of an appropriate form, such as the van Genuchten equation (van Genuchten, 1980). Alternatively, the parameters of equations describing the θ versus ψ_m relationship can be estimated independently by using pedotransfer functions. Pedotransfer functions use training datasets to derive empirical relationships between difficult or expensive-to-measure soil properties and more readily measured or available soil data (Minasny et al., 1999; McBratney et al., 2002). Essentially, pedotransfer functions translate data we have into data we need (Bouma, 1989).

To estimate matric potential for the Goodspeed Upper Transect, measured gravimetric moisture contents were first converted to volumetric moisture contents using equation 3.2:

$$\theta_v = \frac{\theta_g \times \rho_b}{\rho_w} \qquad \text{(Eqn. 3.3)}$$

where: θ_v = volumetric water content ($m^3\ m^{-3}$)

θ_g = gravimetric water content ($m^3\ m^{-3}$)

$\rho_b = 1.65 \times 10^3$ kg m^{-3} (Bockheim, Pers. Comm., 2005)

$\rho_w = 1000$ kg m^{-3}

The van Genuchten equation (equation 3.3) was then rearranged to solve for ψ_m (equation 3.4):

$$\theta(\psi_m) = \theta_r + \frac{\theta_s - \theta_r}{(1 + (\alpha|\psi_m|)^n)^{\left(1-\frac{1}{n}\right)}} \qquad \text{(Eqn. 3.4)}$$

where: $\theta(\psi_m)$ = volumetric water content at potential ψ_m (k Pa)

θ_r = residual water content ($m^3\ m^{-3}$)

θ_s = saturated water content ($m^3\ m^{-3}$)

α = scaling parameter (k Pa^{-1})

n = curve shape parameter

$$\psi_m = -\left[\frac{\theta_s - \theta_r}{\theta_v - \theta_r}\right]^{\frac{\left(\frac{1}{n-1}\right)}{\alpha}} \qquad \text{(Eqn. 3.5)}$$

The matric potential was then calculated using equation 3.4, using parameters estimated by the ENR2 parametric pedotransfer function developed by Minasny et al. (1999) from a dataset of hydraulic properties from Australian soils. Minasny et al. (1999) fitted the van Genuchten equation to soil hydraulic curves by application of non-linear regression techniques. Non-linear regression was then used again to derive relationships between the best-fit van Genuchten parameters and more readily available soil data (Minasny et al., 1999) (equation 3.5).

$\theta_r = -0.00092\ P_{<2} + 1.17748\ PWP$ (Eqn. 3.6a)

$\theta_s = 0.00112\ P_{<2} + 0.8331\ \varphi$ (Eqn. 3.6b)

$\alpha = 0.1561 + 1.7046\ d_g$ (Eqn. 3.6c)

$n = 1.3978 + 0.0027\ \sigma_g$ (Eqn. 3.6d)

where: θ_r = residual water content ($m^3\ m^{-3}$)

$P_{<2}$ = mass of particles <2 μm ($dag\ kg^{-1}$)

PWP = water content at permanent wilting point ($m^3\ m^{-3}$)

θ_s = saturated water content ($m^3\ m^{-3}$)

φ = porosity ($m^3\ m^{-3}$)

α = scaling parameter (kPa^{-1})

d_g = geometric mean particle size diameter (mm)

n = curve shape parameter

σ_g = geometric standard deviation (mm)

In applying a pedotransfer function outside the range of the training dataset from which it was derived, care needs to be taken. However, the Australian dataset used by Minasny et al. (1999) included a number of soils with similarly high sand and low clay contents to the soils of the Goodspeed Upper Transect, and should therefore adequately represent the hydraulic curves of these soils. In utilising

Minasny et al.'s (1999) pedotransfer function, several other assumptions were made:

- PWP = 0.002 (Scanlon et al., 2002);
- $P_{<2}$ = 1%, based on particle size distribution across the Goodspeed Upper Transect, and Bockheim's recommendation (Bockheim, Pers. Comm., 2005);
- φ = 0.38 (Bockheim, Pers. Comm., 2005);
- α = 0.050 (Scanlon et al., 2002), therefore d_g was not required;
- n = 1.774 (Scanlon et al., 2002), therefore σ_g was not required.

Scanlon et al.'s (2002) data were measured from a non-vegetated engineered site within the Chihuahuan Desert of Texas; mean annual precipitation is 320 mm (Scanlon et al., 2002). The specific layer from which Scanlon et al.'s (2002) data originated comprised 92% sand, 7% silt, and 1% clay, and is therefore considered a good analogue for the Goodspeed Upper Transect, where the mean sand content was 98%, and the mean silt and clay content was 2% (Section 5.2.1.3).

Finally, the total soil moisture potential (ψ_t) was calculated by summing the matric and gravitational potentials (equation 3.6) (Appendix VI).

$$\psi_t = \psi_m + \psi_g \qquad \text{(Eqn. 3.6)}$$

3.6 Statistical analyses and data smoothing

Correlations between various climatic, hydrologic and pedologic variables were determined using Microsoft Excel 2003.

SigmaPlot version 9.0 was used to create contour plots of data across the Goodspeed lower alluvial fan. Data were smoothed using an inverse distance function with a nearest neighbours bandwidth method.

Chapter 4
Climate and stream flow

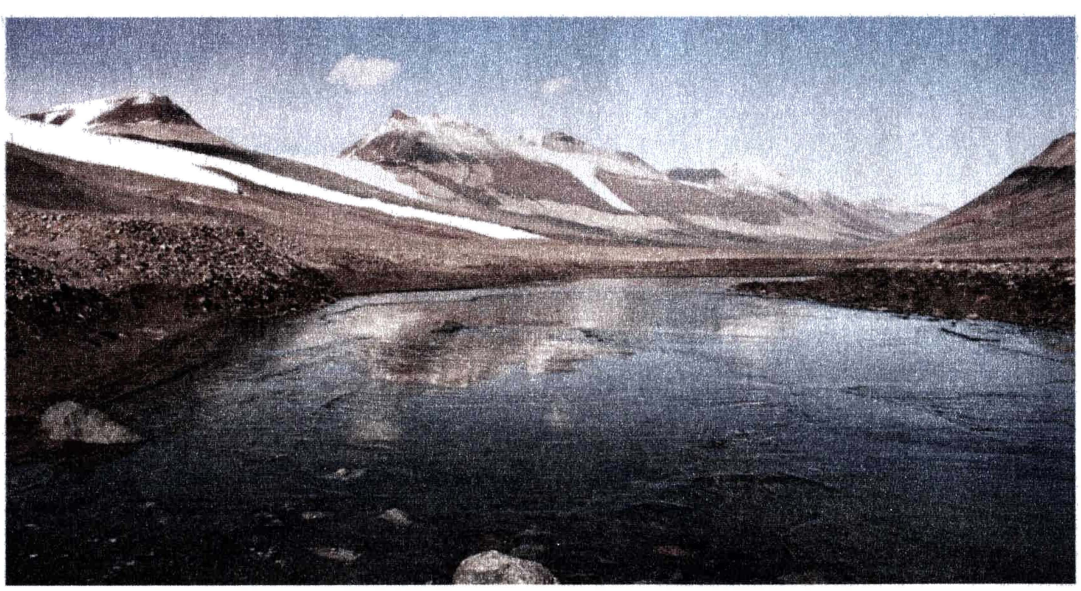

Chapter 4 Climate and stream flow

4.1 Introduction

Data from the Goodspeed Stream climate station, obtained between 4 and 30 January 2005, are presented, with comparisons made to data recorded at the Bull Pass climate station. Observations of long-term trends in data from the Bull Pass site are used to support short-term trends observed at the Goodspeed Stream site.

Stream flow measurements from the Goodspeed Stream daily monitoring site are discussed with respect to climate data. The extent and duration of liquid moisture in the Goodspeed Stream hyporheic zone is also considered in terms of climatic parameters.

4.2 Bull Pass climate data

Climate data have been recorded by an automated weather station (AWS) at Bull Pass since 13 January 1999 as part of K123's programme, with support from the United States Department of Agriculture. Solar radiation and air temperature data provide a clear indication of the seasonal variation in climate; these data also provide a representation of the annual pattern of climate within Wright Valley.

4.2.1 Solar radiation

Solar radiation data recorded at the Bull Pass climate station in 2003 highlight the annual period of winter darkness between the end of April and mid-August (Figure 4.1). The maximum solar radiation recorded in 2003 was 857 Wm^{-2}, recorded on the summer solstice (22 December 2003). Mean annual solar radiation was 97 Wm^{-2}.

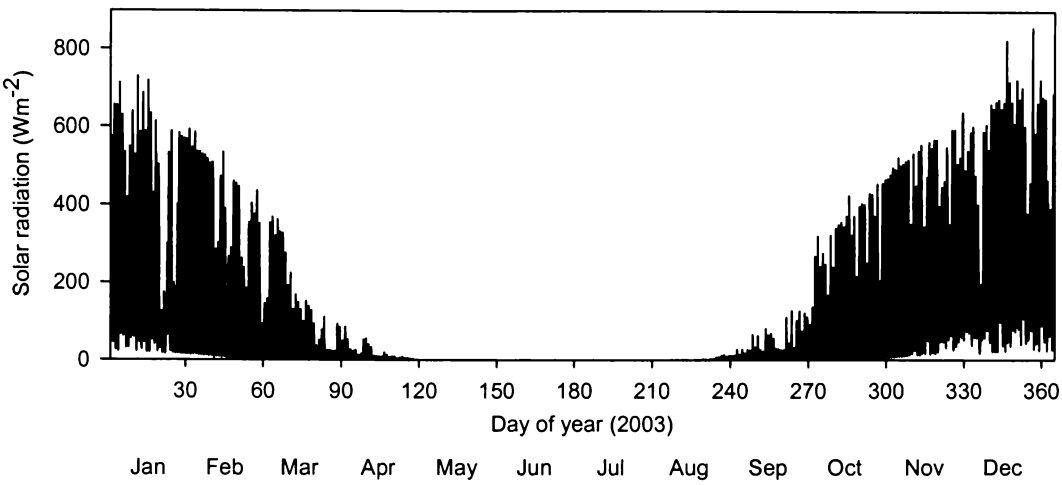

Figure 4.1. Solar radiation recorded at the Bull Pass climate station in 2003.

4.2.2 Air temperature

Air temperature data recorded at the Bull Pass climate station in 2003 show the summer "warm" period which occurs in December and January (Figure 4.2). Air temperature in 2003 ranged from –51.8 °C on 17 August to 10.1 °C on 9 December. Mean annual air temperature was –19 °C.

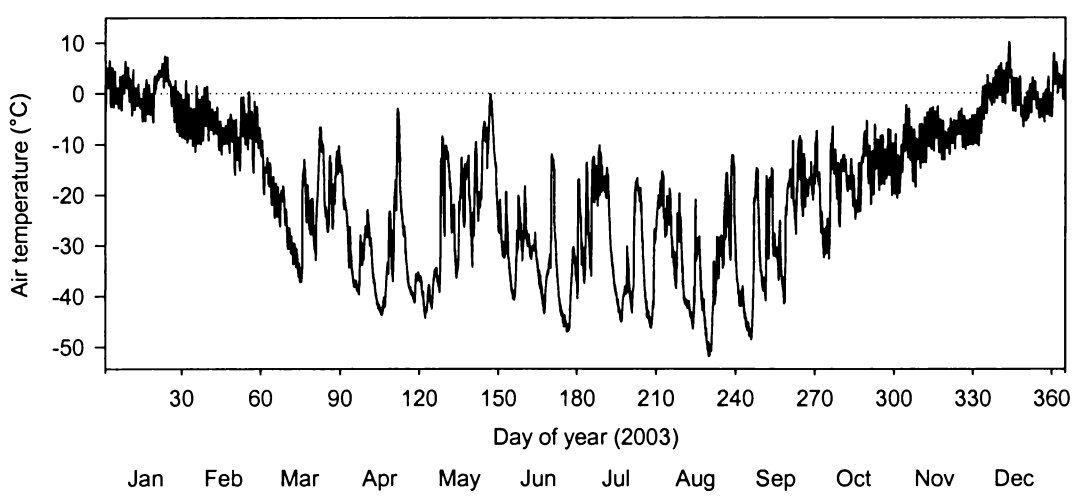

Figure 4.2. Air temperature recorded at the Bull Pass climate station in 2003.

The high frequency variability evident between late October and late February reflects diurnal variation in air temperatures controlled by solar radiation. In the absence of sunlight, variation in air temperature is predominantly driven by the occurrence of westerly katabatic winds (Clow et al., 1988).

4.3 Goodspeed Stream climate data

Climate data were recorded at the Goodspeed Stream temporary climate station between 4 and 30 January 2005.

4.3.1 Solar radiation

Solar radiation flux density showed strong diurnal variability, with the diurnal trend apparent even on cloudy days when solar radiation was low (Figure 4.3). The same trend was evident in data recorded at the Bull Pass climate station (Figure 4.4), although generally, peaks in solar radiation appeared to be systematically greater at Goodspeed Stream than at Bull Pass. The correlation between solar radiation recorded at the two stations was similar (Figure 4.5).

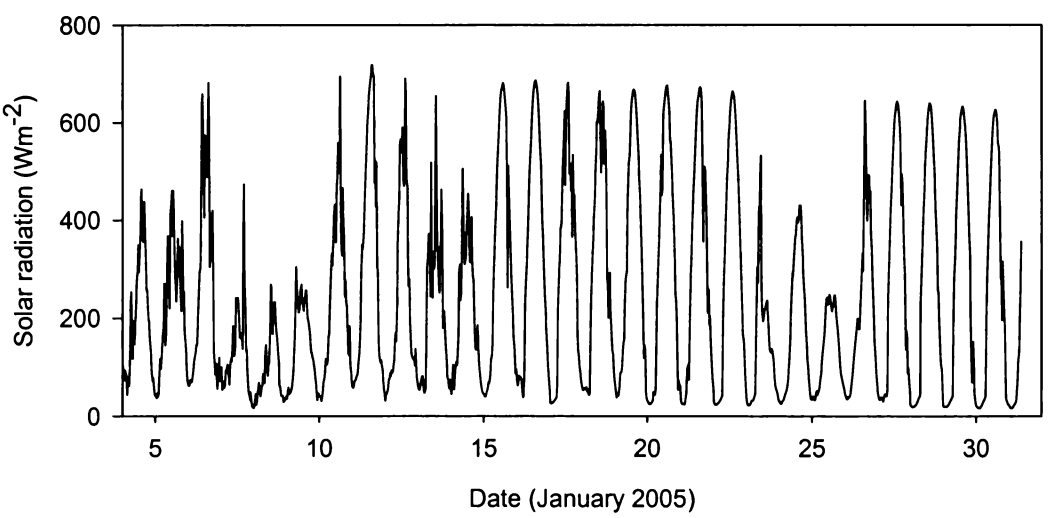

Figure 4.3. Diurnal variability in solar radiation at the Goodspeed Stream climate station.

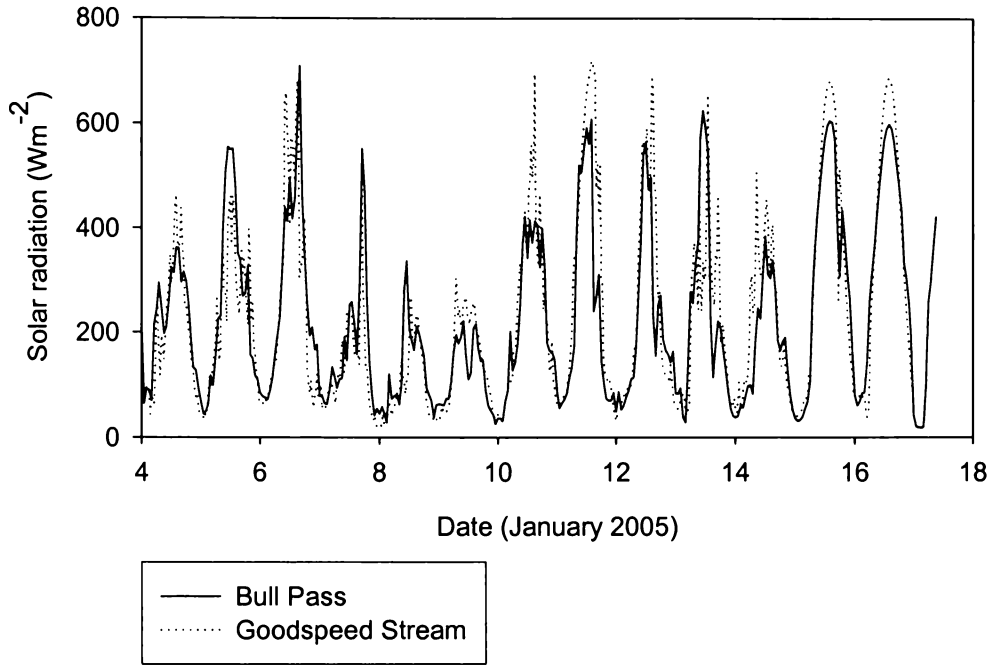

Figure 4.4. Comparison of solar radiation recorded at the Bull Pass and Goodspeed Stream climate stations.

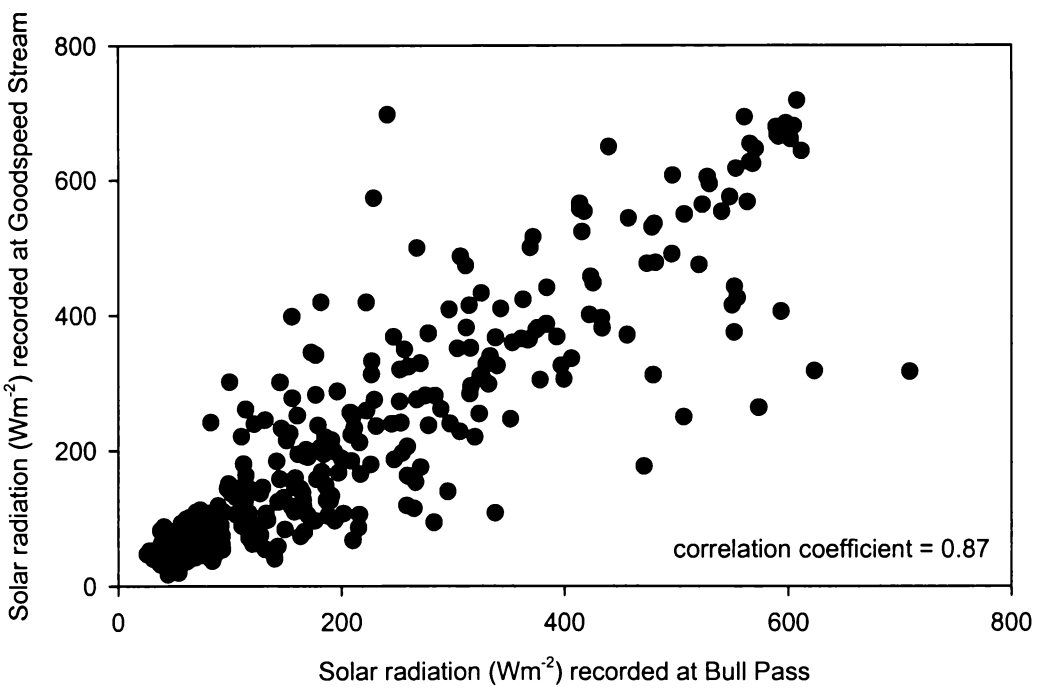

Figure 4.5. Correlation between solar radiation values recorded at the Bull Pass and Goodspeed Stream climate stations over the period 4 – 16 January 2005.

The difference in daily maxima between the Bull Pass and Goodspeed Stream sites may be a result of scratches on the pyranometer installed at Bull Pass, having been subjected to the effects of blowing sediment over a period of 6 years. Similarly, discrepancies could arise from differences in sensor calibration.

The diurnal variability in solar radiation arises from Earth's rotation on its axis. Changes in solar zenith angle during the course of the day, combined with the topographic influence of the Asgard Range meant that, in January, the Goodspeed Stream climate station was shaded for approximately six hours per night, between about 2300 and 0500 hours (NZST) (Figure 4.6); radiative cooling occurs during this period (Thompson et al., 1971a). Towards the end of January, topographic shading became more pronounced, as the sun stayed below the Asgard Range for a longer period each night.

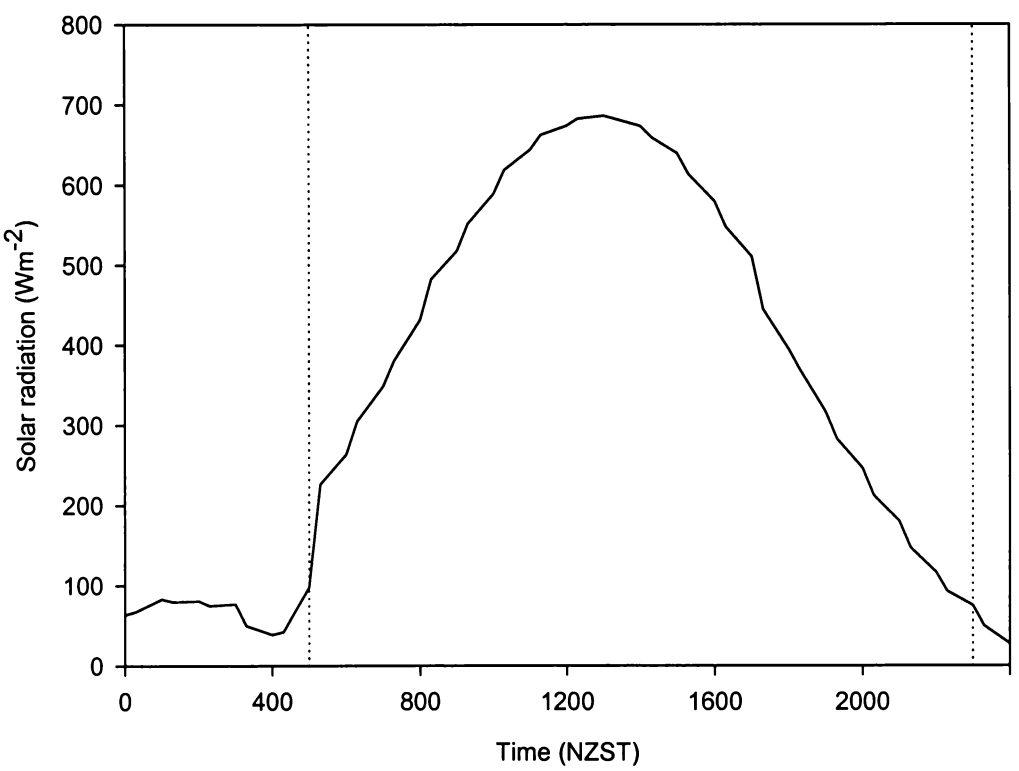

Figure 4.6. Solar radiation recorded at the Goodspeed Stream climate station on 16 January 2005. The dotted lines approximate the period, from about 2300 to about 0500 hours (NZST), over which topographic shading occurred (low values of solar radiation).

During the period of fine weather experienced at the Goodspeed Stream site between 15 – 22 January 2005, the timing of the mean daily peak in solar radiation was 1308 hours (NZST) (n = 7), while the time of minimum mean solar radiation was 0138 hours (NZST) (n = 8).

The timing of the mean daily peak in solar radiation recorded at the Goodspeed Stream climate station corresponded well to the theoretical local noon. Local noon occurs in Wright Valley at about 1300 hours (NZST), though it can be more accurately calculated using the longitude of the site (Eqn. 4.1) (Keys, 1980).

$$Local\ noon = \frac{180 - longitude}{15} \qquad \text{(Eqn. 4.1)}$$

where local noon is the time, in hours, that local noon occurs after 1200 NZST (Keys, 1980).

Therefore, local noon at the Goodspeed Stream climate station, at longitude 162.4° E, is at 1310 hours (NZST); this is almost exactly the time (1308 hours) at which the mean daily peak in solar radiation was recorded.

The mean flux of solar radiation for the period 4 – 30 January 2005 was 250 Wm^{-2}, with daily means ranging from 98 to 347 Wm^{-2} (Figure 4.7). Periods of cloudy conditions are noticeable as distinct troughs in mean daily solar radiation received. The mean daily flux of solar radiation appeared to decrease over the last 3 days of observation, despite having clear sky conditions. This is a function of the decreasing angle of incidence of the solar beam, which results in a decrease in the solar radiation flux density received at Earth's surface.

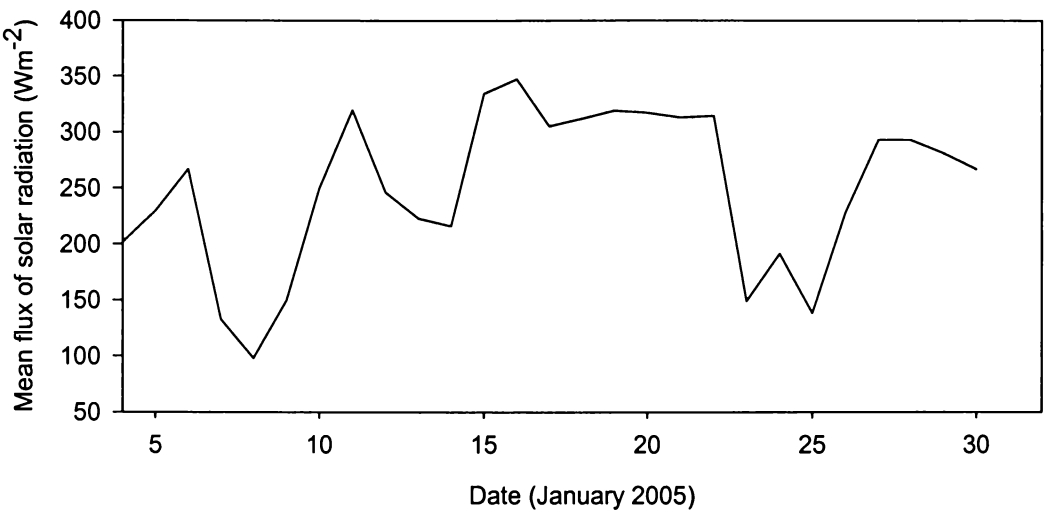

Figure 4.7. Mean daily solar radiation at the Goodspeed Stream climate station.

Solar radiation data from the Bull Pass climate station, recorded over the period 1 November 2003 – 29 February 2004 (Figure 4.8), indicate that mean daily solar radiation decreases sharply as the summer progresses beyond the summer solstice. This supports the trend observed in solar radiation data recorded at the Goodspeed Stream site. The decrease in solar radiation occurs as a result of solar geometry, and is instrumental in influencing both air and soil temperatures in the McMurdo Dry Valleys. Mean daily air temperatures recorded at Bull Pass over the period 1 November 2003 – 29 February 2004 followed the trend evident in mean daily solar radiation (Figure 4.9).

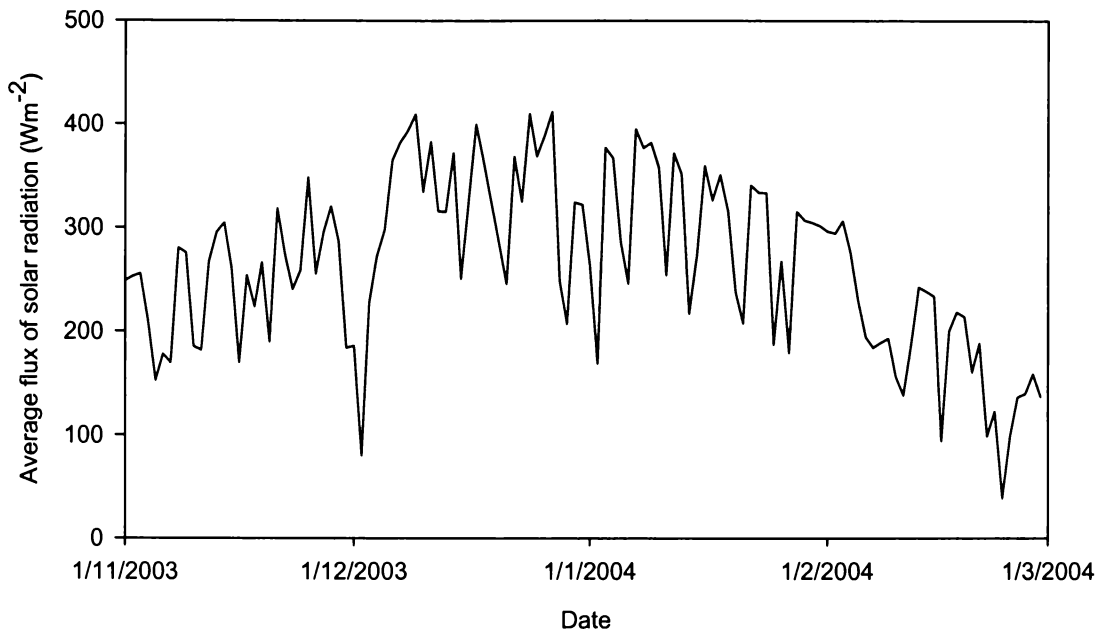

Figure 4.8. Mean daily solar radiation recorded at the Bull Pass climate station over the period 1 November 2003 – 29 February 2004.

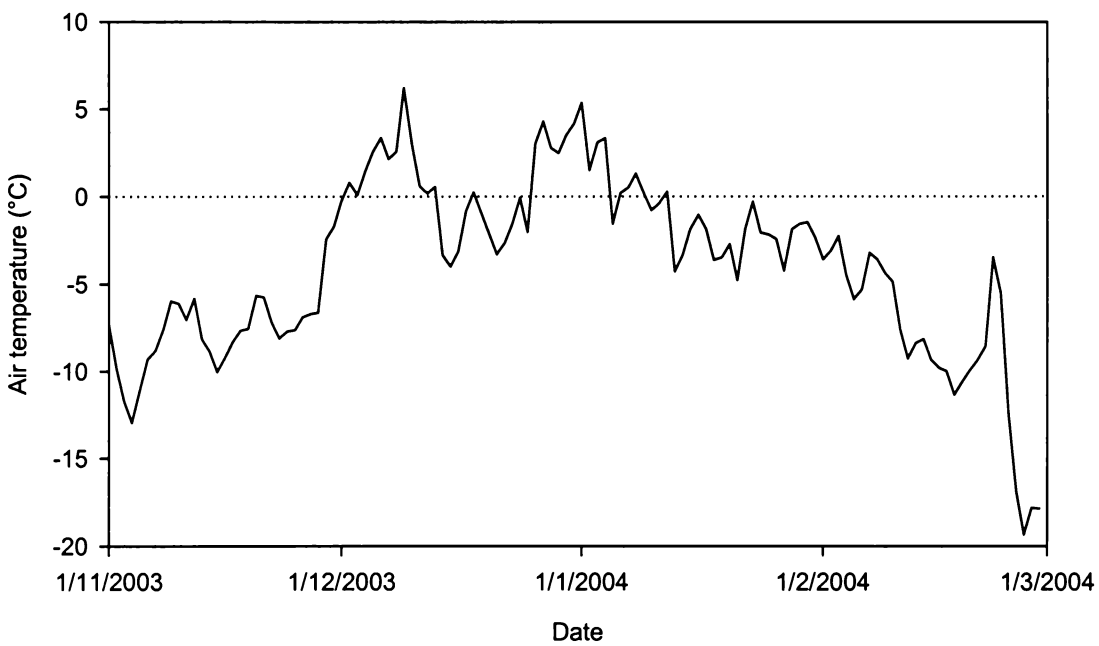

Figure 4.9. Mean daily air temperature recorded at the Bull Pass climate station over the period 1 November 2003 – 29 February 2004.

Some of the differences in solar radiation observed between the Goodspeed Stream and Bull Pass sites may be explained by exposure, though a more detailed

analysis of the variation in radiation flux between the two sites due to topographic effects would require a topographic analysis (Doran et al., 2002). Dana et al. (1998) showed from in-situ measurements and the use of a topographic solar radiation model that topographic features have a large influence on solar radiation patterns within the Dry Valleys. Dana et al. (1998) also proposed differential cloudiness as a mechanism for site-to-site differences in solar radiation. However, the systematic nature of the variation between solar radiation at the Bull Pass and Goodspeed Stream sites suggests that the variation between the two sites is a result of measurement error, and not as a result of differential cloudiness.

4.3.2 Air temperature

The mean air temperature over the period 4 – 30 January 2005 was –1.1 °C. Temperatures ranged from 9.4 °C, recorded at 1230 hours (NZST) on 5 January 2005, to –9.6 °C, recorded at 0530 hours (NZST) on 30 January 2005. As expected, air temperature showed strong diurnal variability (Figure 4.10), with the timing of daily air temperature decreases generally coincident with declining solar radiation.

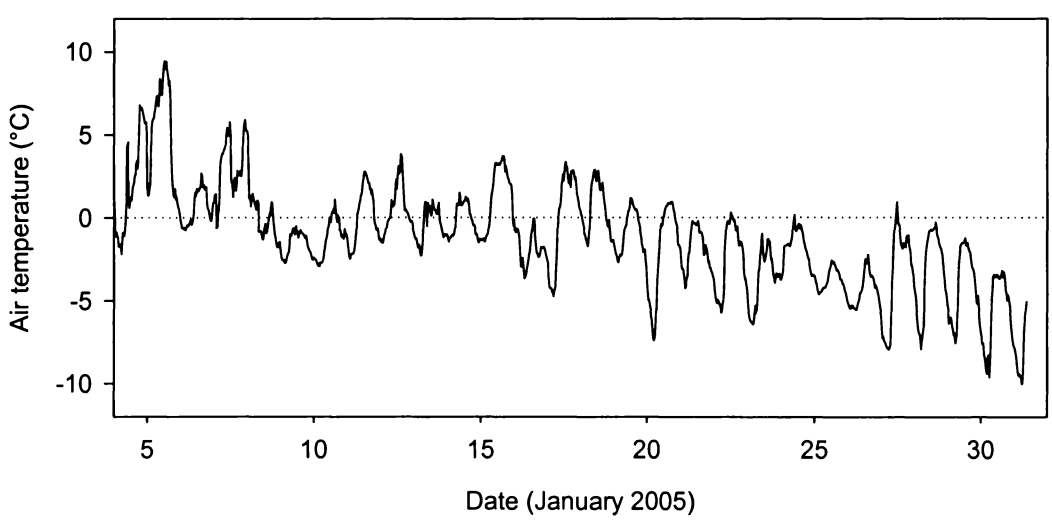

Figure 4.10. Air temperature recorded at the Goodspeed Stream climate station.

Figures 4.11 and 4.12 highlight the decreasing trend in air temperatures recorded at the Goodspeed Stream climate station during January 2005. In early January, air temperature was greater than 0 °C almost all day, while during mid-January, temperatures greater than 0 °C only occurred for approximately 50% of the day. Beyond 20 January, air temperature was seldom above 0 °C.

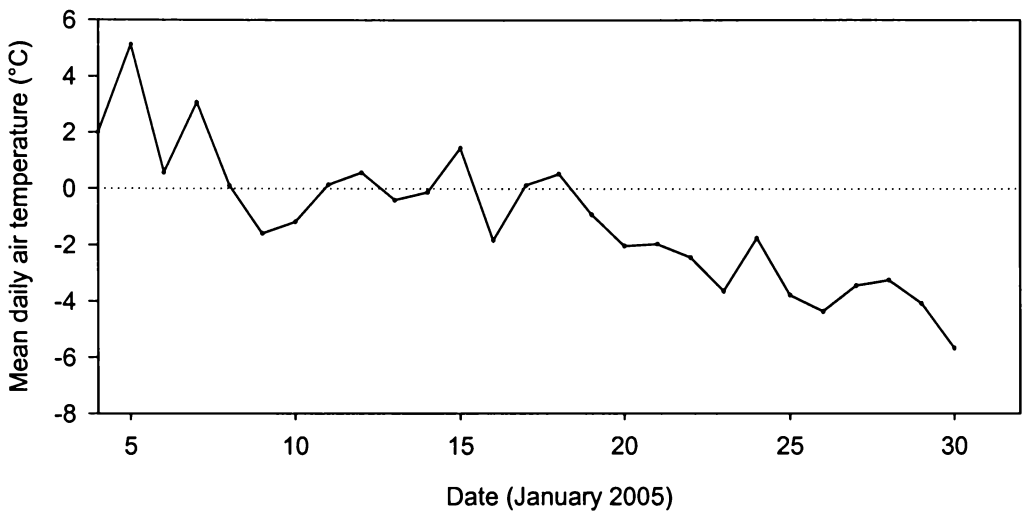

Figure 4.11. Mean daily air temperature recorded at the Goodspeed Stream climate station.

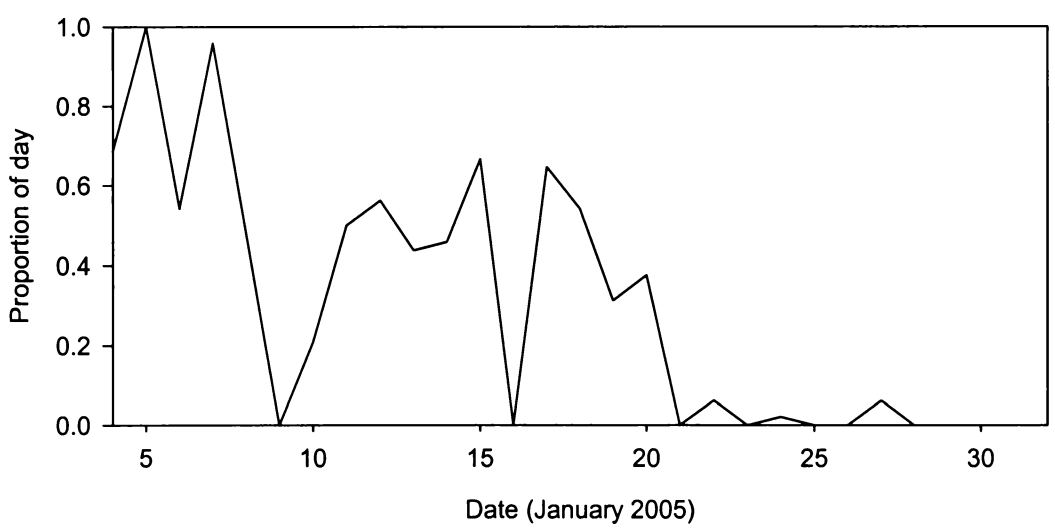

Figure 4.12. Proportion of day with air temperature >0 °C.

The decline in the proportion of the day for which air temperature was greater than 0 °C can be primarily attributed to solar geometry. As the austral summer

progresses beyond the summer solstice, the angle of incidence of the solar beam decreases, thus reducing the intensity of solar radiation received at Earth's surface. Therefore, air temperatures decline. However, the correlation between air temperature and solar radiation recorded at the Goodspeed Stream climate station (Figure 4.13) indicates that there were other variables, most likely wind speed and direction, acting to substantially influence air temperature.

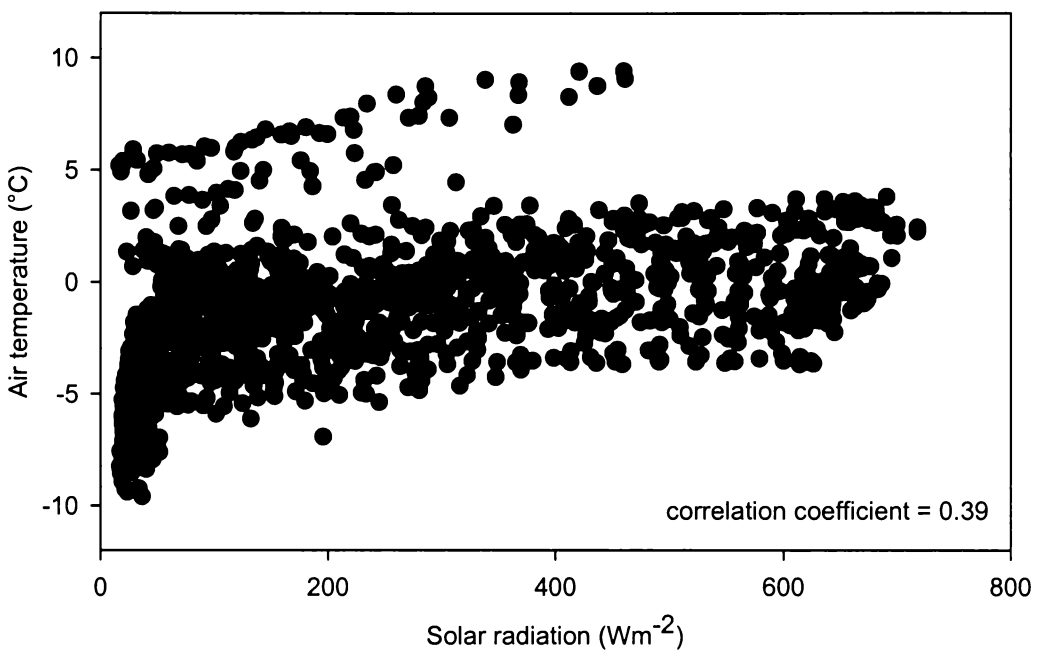

Figure 4.13. Correlation between air temperature and solar radiation recorded at the Goodspeed Stream climate station between 4 and 30 January 2005.

The weak correlation between solar radiation and air temperature may also be due to a lag between the timing of maximum solar radiation and maximum air temperature, on both daily and seasonal time-scales. Lags exist because of diurnal and seasonal imbalances between incoming and outgoing solar radiation (Keys, 1980). Keys (1980) suggests that the lag of the warm peak from the summer solstice is up to 15 – 20 days. Therefore, the intensity of the solar beam decreases from the summer solstice, whereas air temperature reaches a maximum some time in January, and decreases after that time.

From the data recorded at the Goodspeed Stream climate station in January 2005, it appears that the peak in air temperature occurred on 5 January 2005. Assuming

the maximum solar radiation for the season was recorded on 21 December 2004 (the summer solstice), the lag period between maximum solar radiation and maximum air temperature at the Goodspeed Stream climate station for the 2004/2005 summer was 15 days.

Long-term data from the Bull Pass climate station verify that solar radiation decreases beyond the summer solstice, while the maximum air temperature is generally recorded in the first week of January, giving a lag of around 15 – 20 days. This supports Keys' (1980) suggested lag period, and corroborates the lag observed at the Goodspeed Stream climate station in 2004/2005.

4.3.2.1 Comparison of air temperature at Goodspeed Stream and Bull Pass

Air temperature data obtained from the Bull Pass climate station showed a similar trend in diurnal variation to air temperature recorded at the Goodspeed Stream site (Figure 4.14). Air temperatures recorded at the Goodspeed Stream climate station were, on average, 1.65 °C lower than those recorded at the Bull Pass climate station over the period 4 – 16 January 2005. This could result from either: 1) a systematic difference in measurement, being a function of differences in probes, their calibration, shielding, and the height of measurement, 2) a difference in mean wind direction, with a greater frequency of warm katabatic winds recorded at Bull Pass, 3) an up-valley increase in air temperature, or 4) cold air drainage from the Goodspeed Glacier producing cross-valley winds, acting to locally reduce air temperatures.

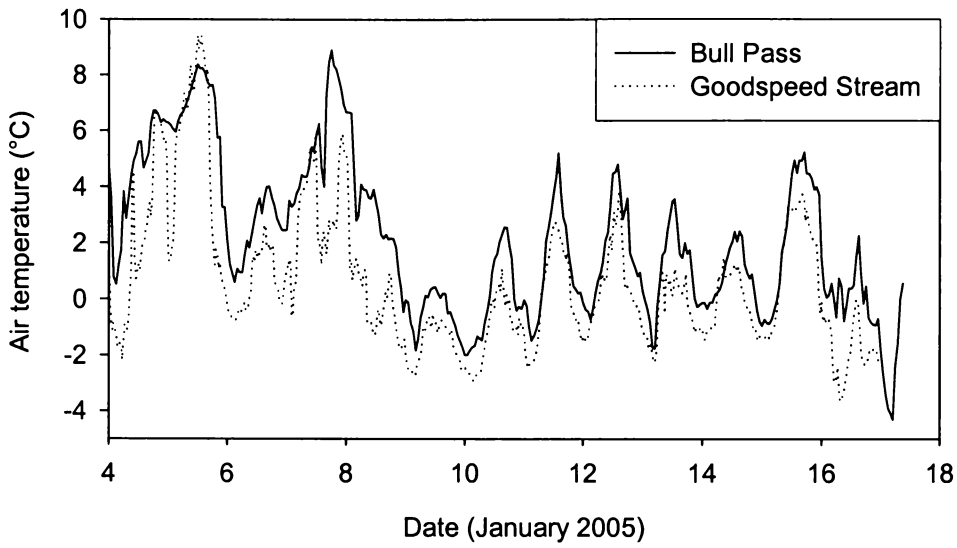

Figure 4.14. Air temperature recorded at Bull Pass and Goodspeed Stream climate stations.

During the period 4 – 16 January 2005, both the Goodspeed Stream and Bull Pass climate stations received predominantly easterly winds (Figure 4.15). Mean wind speed at the Goodspeed Stream site, measured using a hand-held anemometer, was 6.2 m s^{-1} for the period 4 – 16 January 2005. Mean wind speed at the Bull Pass site, calculated from automated measurements, was 6.0 m s^{-1} over the same period.

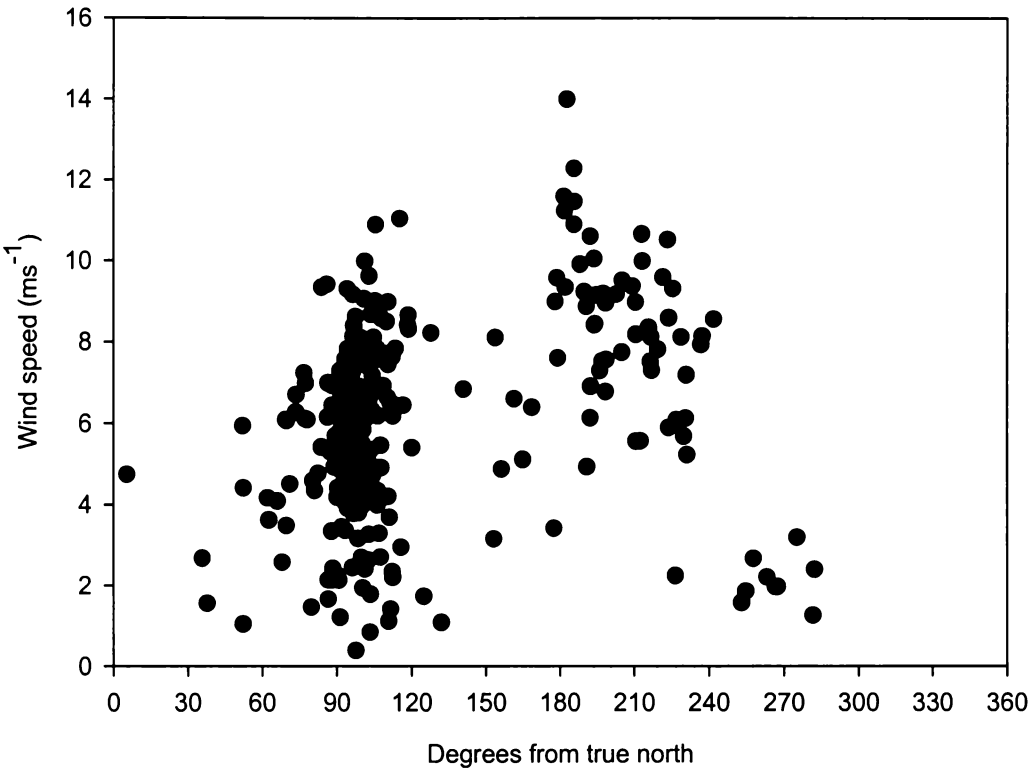

Figure 4.15. Wind speed and direction recorded at the Bull Pass climate station during the period 4 – 16 January 2005.

Recent work by Doran et al. (2002) has established a relationship between summer air temperature and distance inland. The relationship was derived using data from a network of 7 automated weather stations located in the Wright, Taylor and Victoria Valleys, and can be used to account for temperature differences between the Goodspeed Stream and Bull Pass climate stations. The dominance of easterly winds in summer is associated with a 0.09 °C km^{-1} inland warming in air temperature (Doran et al., 2002). Applying this relationship in comparing air temperatures recorded at Goodspeed Stream and Bull Pass, it would be expected that air temperatures at Bull Pass, c. 15 km up-valley from Goodspeed Stream, should be 1.35 °C warmer, very similar to the mean measured difference of 1.65 °C. The effect of cold-air drainage from the Goodspeed Glacier may account for the remainder of the measured difference.

4.3.3 Soil temperatures

Diurnal variability in soil temperature at 5 cm depth was more pronounced in the Goodspeed Stream extended hyporheic zone than in the near-stream hyporheic zone immediately adjacent to Goodspeed Stream (Figure 4.16). This is a result of the greater quantity of water present in the near-stream hyporheic zone having a strong buffering effect on soil temperatures, due to the large specific heat capacity of water. However, for reasons unknown, soil moisture content data from the Hydra probe located within the near-stream hyporheic zone were erroneous; therefore, no comparison of soil moisture content between the near-stream and extended hyporheic zones could be made.

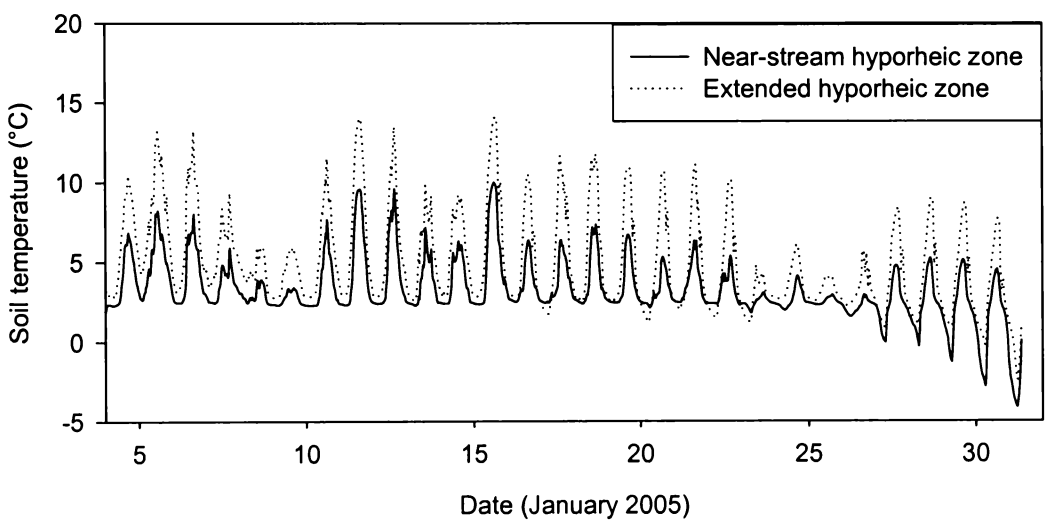

Figure 4.16. Soil temperatures at 5 cm depth recorded at the Goodspeed Stream climate station.

Soil temperatures recorded within the near-stream hyporheic zone over the period 4 – 30 January 2005 ranged from 10.0 to –4.1 °C, with a mean of 3.4 °C, while mean soil temperature in the extended hyporheic zone was 4.9 °C and varied between 14.1 and –2.5 °C over the same period. Periods of cloudy conditions were evident in the data, with the amplitude of diurnal variation being low in comparison to variability under clear-sky conditions.

A sharp decrease in soil temperatures in both the near-stream and extended hyporheic zones occurred around 26 January 2005, and coincided with visual evidence of freezing conditions. Sub-zero temperatures were recorded in the near-stream hyporheic zone on 27 January 2005, and in the extended hyporheic zone on 30 January 2005. As with air temperature, the timing of diurnal fluctuations in soil temperatures corresponded to decreases in solar radiation.

The mean soil temperature of the near-stream and extended hyporheic zones, at 5 cm depth, showed a clear correlation with air temperature (Figure 4.17), and exhibited a similar decreasing trend in late January 2005. The correlation between mean soil temperature (near-stream and extended hyporheic zones) and solar radiation was also important (Figure 4.18), showing a much stronger relationship than that between air temperature and solar radiation (correlation coefficient = 0.39). The stronger correlation between soil temperature and solar radiation highlights the greater thermal stability of the soil mass, being minimally affected by wind speed and direction. Conversely, the nature of the air mass is more fluid, being subjected to incessant winds, the source of which can have a substantial influence on air temperature.

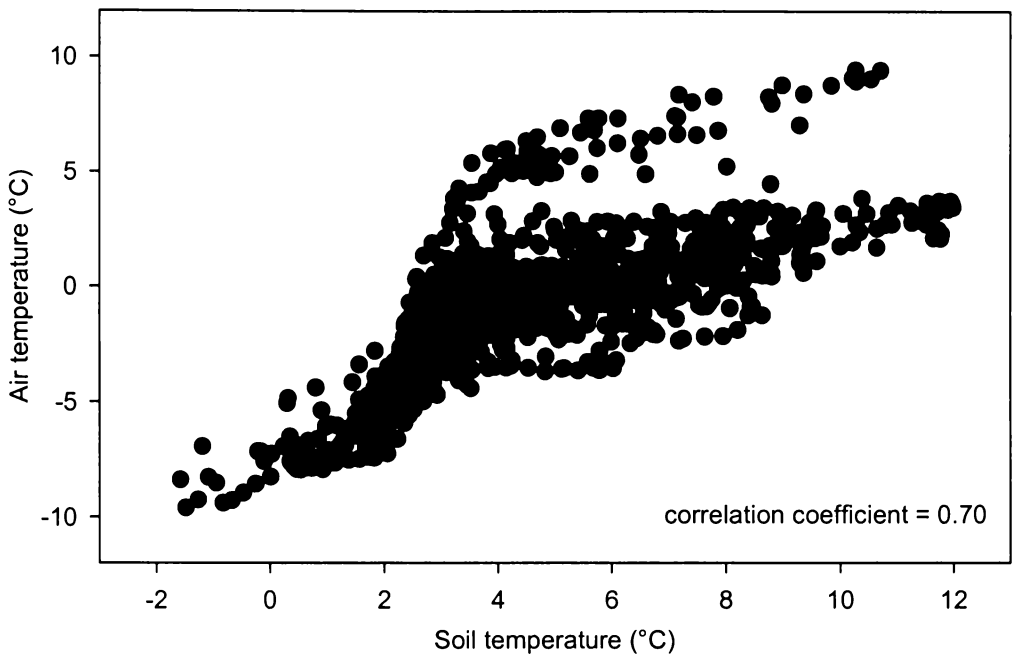

Figure 4.17. Correlation between air temperature and soil temperature (mean of near-stream and extended hyporheic zones) recorded at the Goodspeed Stream climate station between 4 and 30 January 2005.

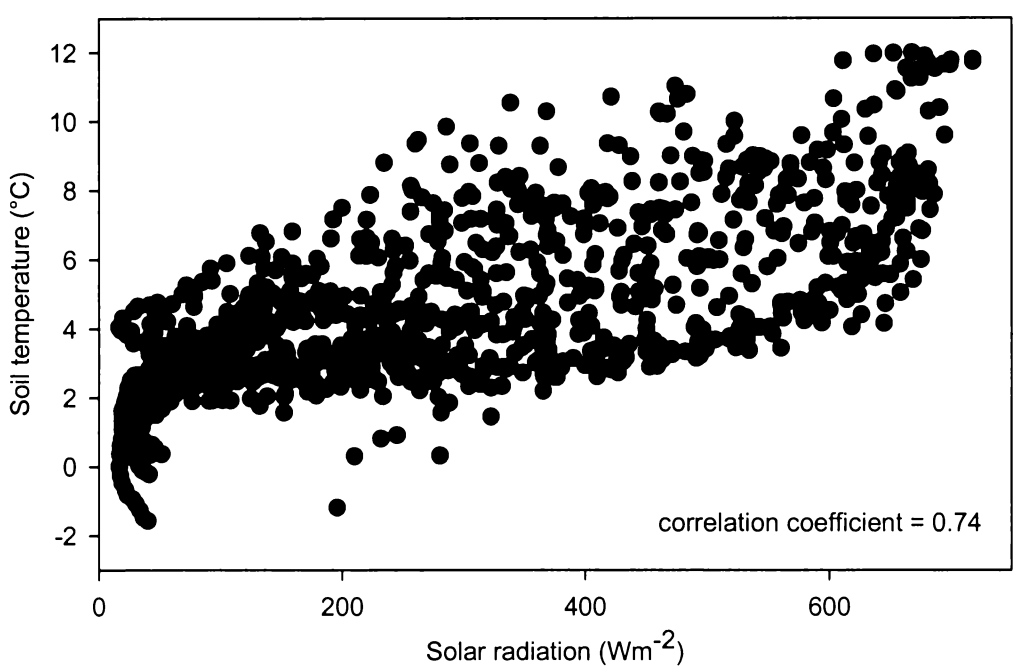

Figure 4.18. Correlation between soil temperature and solar radiation recorded at the Goodspeed Stream climate station between 4 and 30 January 2005.

4.3.3.1 Comparison of soil temperatures at Goodspeed Stream and Bull Pass

A comparison between soil temperatures at 5 cm depth at Goodspeed Stream and Bull Pass shows diurnal fluctuations in soil temperatures at both sites to be similar (Figure 4.19). As with air temperature, soil temperatures at the Goodspeed Stream site were appreciably lower than those recorded at Bull Pass. The mean soil temperature at Bull Pass over the period 4 – 16 January 2005 was 6.5 °C; the mean soil temperature of the near-stream hyporheic zone adjacent to Goodspeed Stream was 4.0 °C over the same period, while the mean soil temperature of the extended hyporheic zone was 6.0 °C.

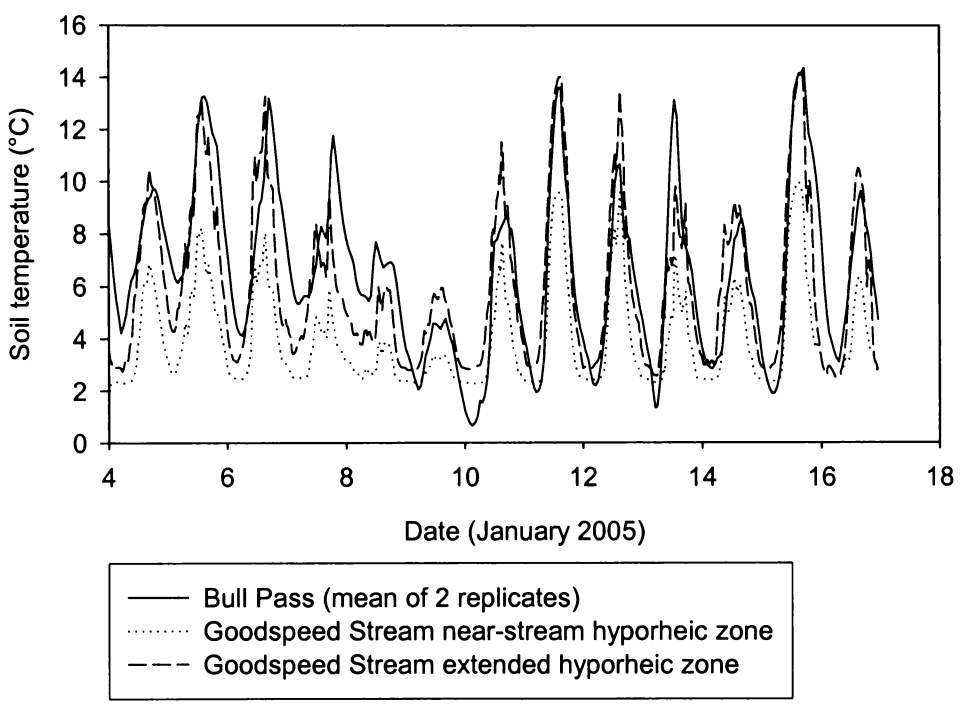

Figure 4.19. Comparison of soil temperatures at 5 cm depth, recorded at the Bull Pass and Goodspeed Stream climate stations.

The differences in soil temperatures between the Bull Pass and Goodspeed Stream sites are likely to result from differences in soil moisture content. Over the period 4 – 16 January 2005, mean soil volumetric moisture content at 5 cm depth at the Bull Pass site was 0.02%, whereas mean soil volumetric moisture content at 5 cm depth in the Goodspeed Stream extended hyporheic zone was 7.6% over the same period.

The lower soil moisture content at the Bull Pass climate station enables rapid heating of the soil, though similarly promoting rapid cooling. However, the low soil moisture content dictates that the soil has a low thermal diffusivity, making diurnal fluctuations in soil temperature more pronounced, as heat transfers are unregulated by the high specific heat capacity of water. Conversely, the greater soil moisture content within the Goodspeed Stream extended hyporheic zone, combined with the high heat capacity and high thermal conductivity of water, acts to impose a thermoregulatory effect on soil temperature, making diurnal fluctuations less pronounced.

Differences in soil moisture content between the Bull Pass and Goodspeed Stream climate stations cannot be attributed to differences in probe type, as at both sites, Stevens Vitel Hydra probes were used. The validity of data obtained from Hydra probes under Antarctic conditions was verified by Wall et al. (2004). As with air temperature, the influence of cool coastal breezes (easterlies) or cold air drainage from the Goodspeed Glacier could contribute to the lower soil temperatures recorded at the Goodspeed Stream site.

4.3.4 Soil volumetric moisture content in the extended hyporheic zone

Soil volumetric moisture content in the Goodspeed Stream extended hyporheic zone was around 8% until mid-January 2005 (Figure 4.20). The first freezing event was recorded on 17 January 2005, with soil moisture content appearing to decrease. The apparent decrease in moisture content was a function of a decrease in the bulk dielectric constant of the soil as the water froze, thus decreasing the volumetric water content as measured by the Hydra probe (Wall et al., 2004).

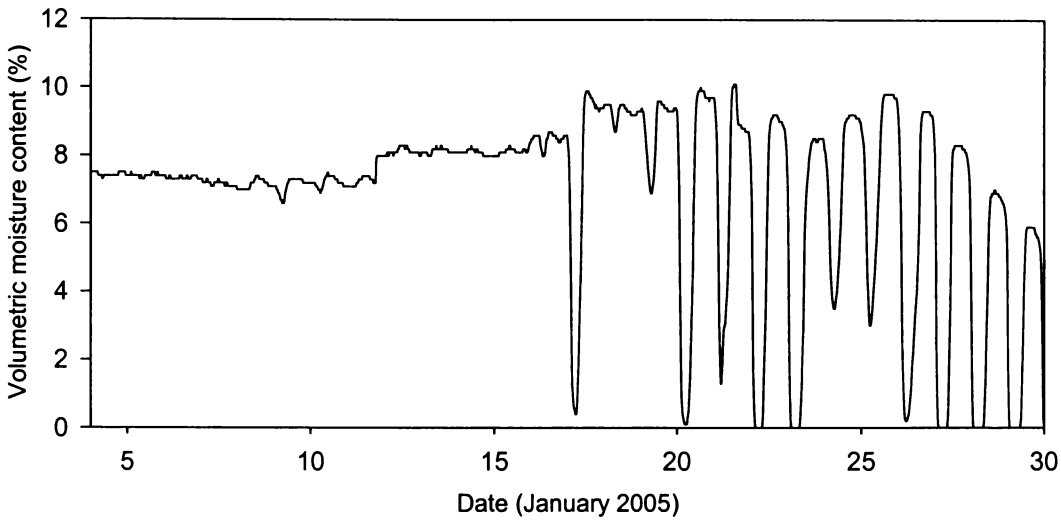

Figure 4.20. Soil volumetric moisture content within the extended hyporheic zone, recorded at the Goodspeed Stream climate station.

Freezing within the extended hyporheic zone occurred nightly from 20 January 2005, and from 25 January, volumetric moisture content began to decrease. The measured decrease in moisture content supported observations that the extended hyporheic zone was visibly drying out.

4.4 Goodspeed Stream

Goodspeed Stream exhibited substantial variation in stream flow, width, and depth during the period 4 – 30 January 2005. Unfortunately, flow had begun before observations commenced. It is not known how long liquid water had been present in the stream channel, though it is likely that the most pronounced changes in stream characteristics occurred during the January 2005 observation period. It is assumed that the maximum discharge for the season was attained during this time, with observations also encompassing a period during which the stream froze and flow ceased completely.

4.4.1 Stream flow

Between 4 and 30 January 2005, flow within Goodspeed Stream ranged from 0 – 2.5 ℓs^{-1} (Figure 4.21). Moderate discharges (up to 1.25 ℓs^{-1}) were recorded between 5 and 10 January, before diminishing to very low flows averaging 0.08 ℓs^{-1} between 10 and 15 January. Stream flow increased from 15 January onwards, reaching a maximum discharge on 17 January, before ceasing, presumably for the season, on 25 January, with all water remaining in the stream having frozen. As the dataset does not extend beyond 30 January 2005, it is impossible to say with complete certainty that Goodspeed Stream did not flow again. However, based on previous documentation of stream flow in Wright Valley (Table 4.1), it is unlikely that flow in Goodspeed Stream would have been re-initiated.

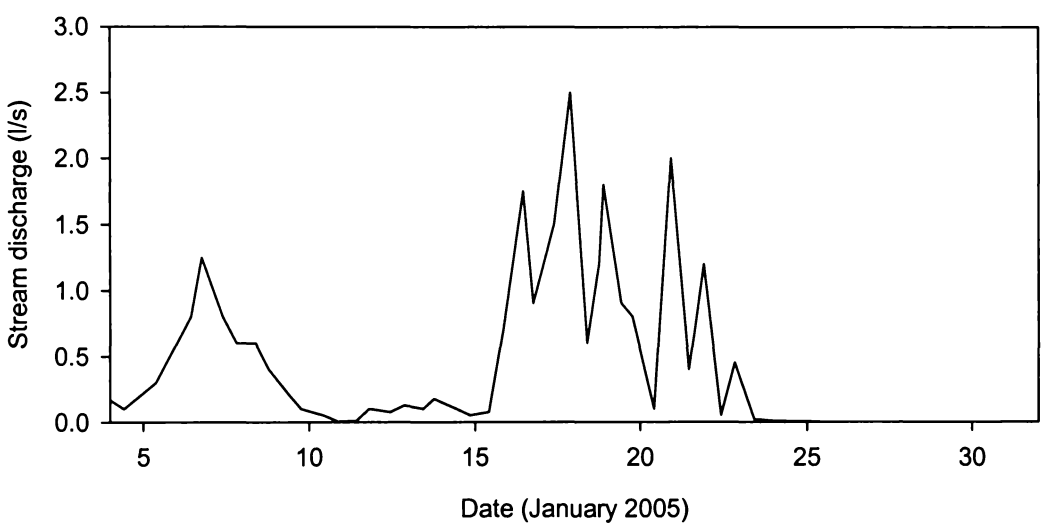

Figure 4.21. Stream flow at the Goodspeed Stream daily monitoring site. Discharge was estimated twice daily using a bucket, measuring cylinder and stop watch. Hence data should be treated as indicative, as the timing of measurements (approx. 0900 and 1900 hours NZST) may not have encompassed the true variability in stream flow; greater flows may have occurred between measurements.

The width and depth of Goodspeed Stream at the daily monitoring site varied in accordance with stream flow. The maximum stream width recorded at the daily monitoring site was 91 cm; mean stream width was 46 cm.

The low flow observed between 10 and 15 January 2005 coincided with a period of greater solar radiation intensity than that experienced over the previous five days (Figure 4.3). Similarly, the comparatively high flow that occurred between 5 and 10 January appears out of phase with solar radiation. The apparent anti-phase relationship between solar radiation and stream flow in early January may be a result of cloud acting to trap long-wave radiation, thus promoting glacial melt. However, from 15 – 22 January both solar radiation and stream flow were high. Therefore, there may be a lag after a period of relatively high solar radiation before stream flow is maximised. This could also be considered as the relaxation time of the system, whereby the system experiences change, and intrinsic thresholds must be crossed before a response is seen.

Stream flow in Goodspeed Stream did not appear to respond synchronously with changes in solar radiation. This may be a result of the hyporheic zones providing sufficient storage to moderate stream flow. Assuming vast quantities of water are stored within the hyporheic zones on the fan, fluctuations in solar radiation may not always be apparent in stream flow. For example, if some of the water stored in the hyporheic zones during periods of high solar radiation had been released from storage (in the hyporheic zones) during a period of cloudy conditions, the storage area would have to be re-filled before meltwater produced under clear-sky conditions appeared as surface stream flow. Thus, considerable lags may exist between changes in solar radiation and stream flow.

A similar lag period probably exists at the beginning of each flow season, with the porous stream bed alluvium becoming saturated as stream flow progresses down the channel (Conovitz et al., 1998; Gooseff et al., 2003). Furthermore, lags in stream flow at the beginning of the season are dependent on the fate of water stored in the hyporheic zone over winter. Two contrasting opinions are reported. Conovitz et al. (1998) suggest that water in the hyporheic zone is largely lost to evaporation and sublimation rather than remaining until the next summer, whereas Gooseff et al. (2003) use stable isotope data to show that some water persists in the hyporheic zone from one flow season to the next. These contrasting views are important in terms of stream flow, as the fate of water in the hyporheic zones over

the winter season has implications for how much meltwater must be produced before surface stream flow occurs the following summer.

The concept of thresholds can also be applied in explaining the cessation of stream flow. A period of diminished solar radiation occurred from 23 – 25 January; 24 January was the last day in which flow was observed in Goodspeed Stream. Beyond 25 January, air temperatures were consistently below 0 °C, and, although solar radiation increased again, the stream remained frozen and began to sublimate. Thus it can be postulated that extrinsic thresholds pertaining to solar radiation, air temperature, and perhaps other factors that influence stream flow had been crossed, with Goodspeed Stream therefore being unable to flow, despite apparently favourable solar radiation conditions.

Chinn's (1981b) observations and other data (Table 4.1) pertaining to the timing of onset and cessation of flow for the Onyx River indicates that stream flow in Wright Valley does occur beyond the end of January, though ceasing by mid-February at the latest. Since flow from ephemeral streams sourced from alpine glaciers, such as Goodspeed Stream, contributes an estimated 10% of flow in the Onyx River (Chinn, 1981b), it can be inferred that the Onyx River continues to flow for a period of time after the cessation of flow in ephemeral streams. This is supported by observations in January 2005 when the Onyx River continued to flow after flow in Goodspeed Stream had ceased. Earlier observations of stream flow in Goodspeed Stream also indicate that flow in Goodspeed Stream ceased before the cessation of flow in the Onyx River (Chinn, 1981a; Chinn and Maze, 1983; Chinn and Oliver, 1983).

Table 4.1. Timing of the onset and cessation of flow in the Onyx River, recorded at the weir located 0.5 km upstream from Lake Vanda.

Season	Onset	Cessation	Maximum instantaneous flow	Approx. duration of flow (days)
1970 – 71[a]	5 Dec. 1970	>11 Feb. 1971	3 Jan. 1971	67
1972 – 73[b]	14 Dec. 1972	6 Feb. 1973	25 Dec. 1972	54
1973 – 74[c]	31 Dec. 1973	13 Feb. 1974	6 Jan. 1974	43
1974 – 75[d]	10 Dec. 1974	>31 Jan. 1975	17 Jan. 1975	53
1975 – 76[e]	13 Dec. 1975	>6 Feb. 1976	22 Jan. 1976	56
1976 – 77[f]	11 Dec. 1976	>3 Feb. 1977	22 Jan. 1977	59
1977 – 78[f]	No flow at weir	No flow at weir	No flow at weir	0
1978 – 79[g]	30 Dec. 1978	1 Feb. 1979	4 Jan. 1979	37
1979 – 80[h]	5 Dec. 1979	2 Feb. 1980	27 Dec. 1979	65
1980 – 81[i]	14 Dec. 1980	4 Feb. 1981	1 Jan. 1981	54
1981 – 82[j]	9 Dec. 1981	5 Feb. 1982	7 Jan. 1982	70
1982 – 83[k]	11 Dec. 1982	2 Feb. 1983	29 Dec. 1982	59

[a](Chinn, 1980); [b](Fenwick and Anderton, 1975); [c](Anderton and Fenwick, 1976); [d](Chinn, 1975); [e](Chinn, 1981a); [f](Chinn, 1983); [g](Chinn and Cumming, 1983); [h](Chinn and Oliver, 1983); [i](Chinn and Maze, 1983); [j](Chinn and Woods, 1984); [k](Chinn and Dickson, 1986)

While there is some temporal variation in the timing of onset and cessation of stream flow, the data above suggest that stream flow in the Onyx River generally commences in December, and ceases for the season by mid-February, with the timing of maximum discharge being variable. Therefore, based on observations of stream flow in Wright Valley during January 2005, and the fact that air temperature and solar radiation were decreasing relatively rapidly in late January, it would be very unlikely for Goodspeed Stream to have re-commenced flow after the end of January.

4.4.1.1 Climatic influence on stream flow

There were no strong correlations between mean daily air temperature, solar radiation and stream flow (Figure 4.22). While both solar radiation and air temperature are known to influence stream flow in the Dry Valleys (e.g. Conovitz et al., 1998; Lewis et al., 1999), there are many other variables which may also contribute to meltwater production. These include surface albedo and the net radiation balance. Furthermore, solar radiation flux density is influenced by the

solar zenith angle, cloud cover, and topography (Dana et al., 1998), while air temperature is influenced by wind direction, elevation, and proximity to the coast (Doran et al., 2002).

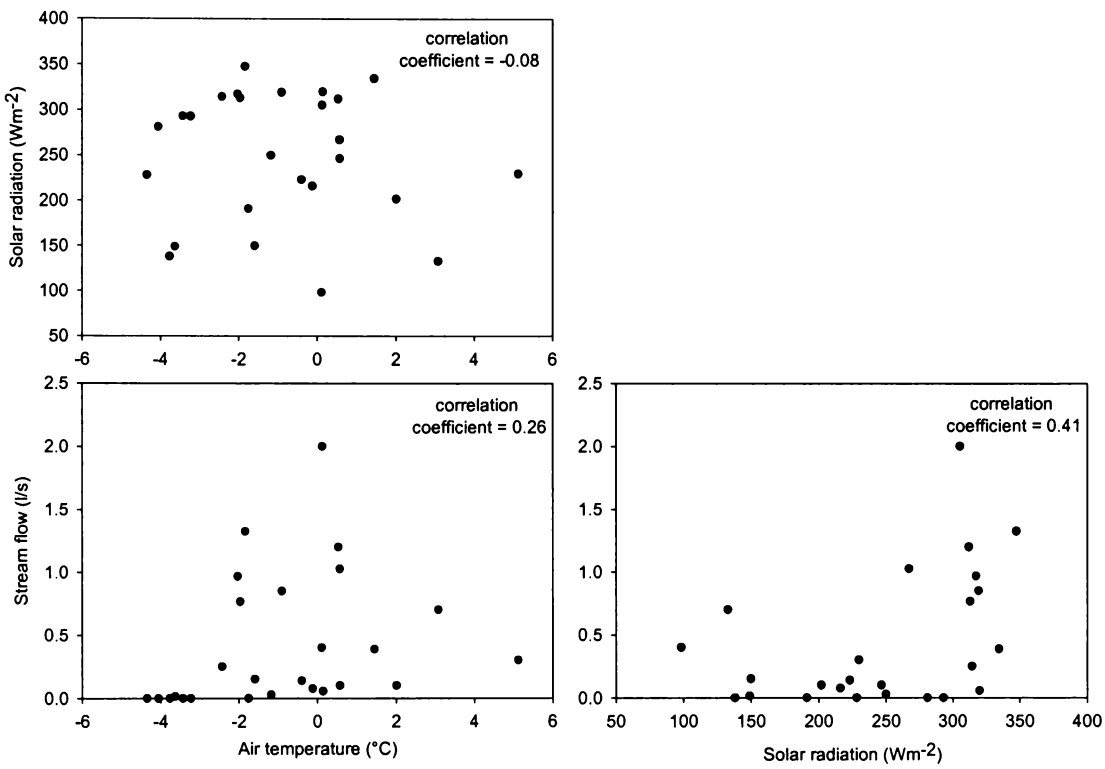

Figure 4.22. Correlations between mean daily air temperature, solar radiation and stream flow at the Goodspeed Stream daily monitoring site for the period 4 – 30 January 2005.

Conovitz et al. (1998) report solar radiation as the primary driver of glacial melt (and hence stream flow) in the Dry Valleys, though note that stream flow is extremely sensitive to changes in air temperature and other climatic factors. Lewis et al. (1999) show that temporal variations in glacial melt are driven by air temperature. The situation at the Goodspeed Stream site can thus be considered too complex to find a coherent relationship highlighting the dominant controls on stream flow, with too few data on potentially influential variables exacerbating the situation.

The data available for deducing the relationship between climate and stream flow in Goodspeed Stream are limited to solar radiation and air temperature.

Furthermore, these data were measured 1.5 km downstream from the terminal face of the Goodspeed Glacier, and at an elevation 235 m lower than that at the base of the terminal face. Compounding this is the fact that no data were recorded at or in the vicinity of the terminal face; this is where the majority of glacial melt in cold-based glaciers occurs. Stream flow data were based on two estimates per day, which is unlikely to provide an accurate representation of diurnal variability, particularly under clear-sky conditions.

4.5 Goodspeed Stream hyporheic zones

Based on work by Gooseff et al. (2003) and observations of moisture present on the Goodspeed lower alluvial fan in January 2005, three hyporheic zones associated with Goodspeed Stream were defined for use in this study. The near-stream hyporheic zone is the area of saturated soil adjacent to Goodspeed Stream, in which water and solutes are rapidly exchanged with those in the main stream channel. Adjacent to the near-stream hyporheic zone is the extended hyporheic zone, which comprises visibly moist soil; exchanges occur over a period of weeks to months (Gooseff et al., 2003).

Areas of visibly moist soil occurring further out on the Goodspeed lower alluvial fan, separated from the extended hyporheic zone by visibly dry soils, represent distal components of the extended hyporheic zone (Figure 4.23). The distal components of the hyporheic zone were replenished with moisture from Goodspeed Stream via subsurface flow paths down the fan, though the time-scale over which exchange processes occur is uncertain.

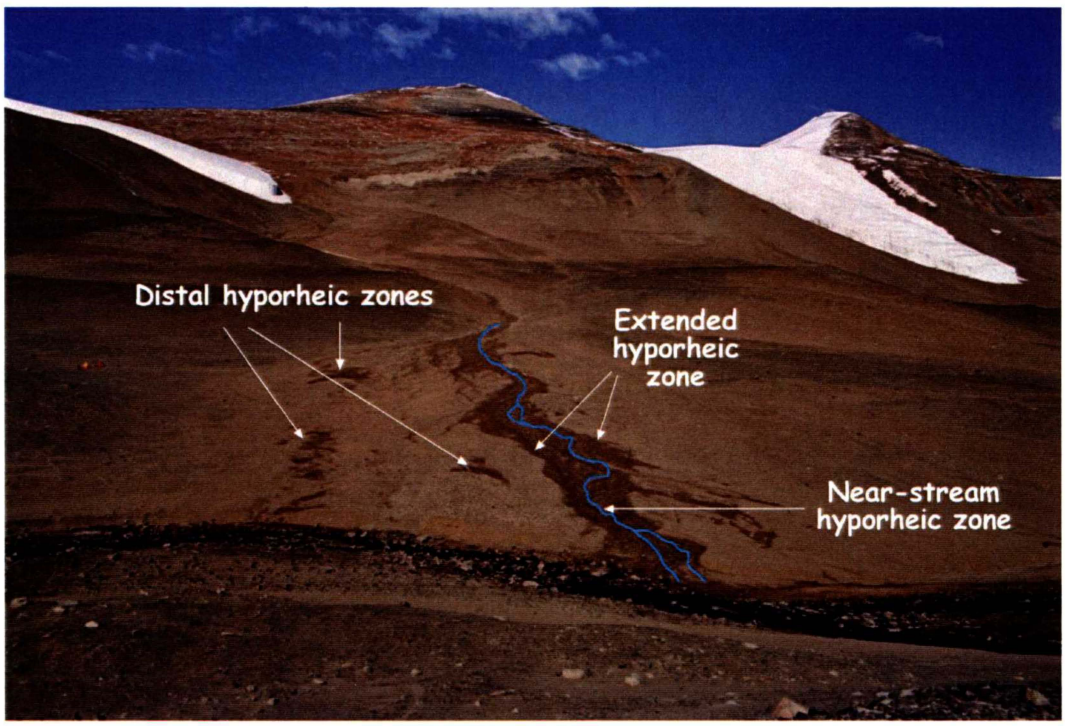

Figure 4.23. Hyporheic zones associated with Goodspeed Stream.

4.5.1 Lateral extent

4.5.1.1 Near-stream hyporheic zone

The near-stream hyporheic zone, measured twice daily at the Goodspeed Stream daily monitoring site, had a mean total width of 0.44 m over the period 4 – 22 January 2005. The distribution of the near-stream hyporheic zone was relatively even, extending 0.19 m beyond the true left of Goodspeed Stream, and 0.25 m beyond the true right of the stream.

4.5.1.2 Extended hyporheic zone

The lateral extent of the Goodspeed Stream extended hyporheic zone, also measured twice daily at the Goodspeed Stream daily monitoring site, showed small fluctuations (Figure 4.24), though its variability was not diurnal, nor did it appear to be directly related to stream flow. The total width of the extended hyporheic zone changed suddenly in mid-January 2005, decreasing from a total

mean width of 8.7 m between 4 and 16 January, to 7.6 m during the period 17 – 30 January 2005.

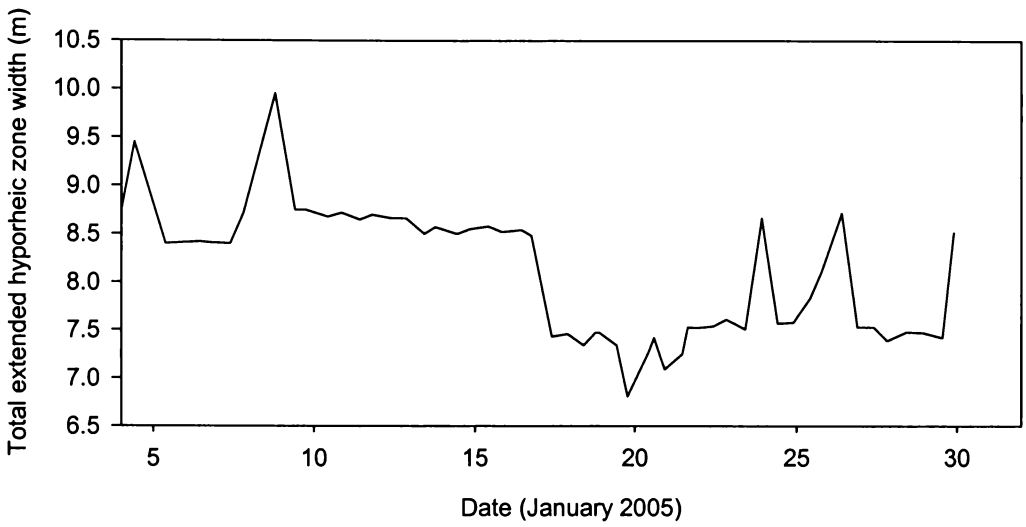

Figure 4.24. Lateral extent of the Goodspeed Stream extended hyporheic zone at the daily monitoring site.

Correlations between air temperature, solar radiation, stream flow and the lateral extent of the extended hyporheic zone were weak, thus not providing any useful insight into the factors controlling the width of the extended hyporheic zone.

The maximum extent of the Goodspeed Stream extended hyporheic zone was observed 110 m upstream from the confluence of Goodspeed Stream with the Onyx River. At this point, the width of the Goodspeed Stream extended hyporheic zone was 20.5 m, including Goodspeed Stream (0.3 m). However, the distribution of the extended hyporheic zone was skewed, stretching 15.6 m from the true right of Goodspeed Stream, and only 4.6 m from the true left of the stream.

The disproportionate lateral extent of the extended hyporheic zone on the true right of Goodspeed Stream was consistent throughout the lower alluvial fan, except at the site (GS 3) closest to the Onyx River (Table 4.2). The greater expanse of the extended hyporheic zone on the true right of the stream was probably related to the topography of the fan. Stream banks were generally

steeper on the true left of Goodspeed Stream, thus an equivalent rise of moisture through capillarity dictates that a greater lateral extent was observed on the true right of the stream.

Table 4.2. Lateral extent of the Goodspeed Stream extended hyporheic zone and height at which the soil surface was visibly moist at sites along Goodspeed Stream, January 2005.

Site	Distance upstream from Onyx River (m)	Ext. hypo. zone width (L bank) (m)	Ext. hypo. zone width (R bank) (m)	Height of ext. hypo. zone above stream surface (L bank) (cm)	Height of ext. hypo. zone above stream surface (R bank) (cm)
GS 3[a]	29	7.10	3.80	65	60
GS 4[a]	100	5.80	12.90	45	65
GS 1[a]	230	4.20	5.25	40	65
GS 2[a]	235	3.80	4.15	65	60
GS 5[a]	430	4.40	5.80	75	60
GS 6[b]	580	3.30	1.40	45	40
GS 7[b]	c. 700	3.60	2.70	45	40
GS 9[b]	c. 1050	3.84	2.80	45	65
GS 10[b]	c. 1300	2.95	2.90	25	45
GS 11[c]	c. 1500	0.85	2.51	35	50

[a] determined on 4 January 2005; sites are on the Goodspeed lower alluvial fan.
[b] determined on 15 January 2005; sites are within the incised middle reach.
[c] determined on 21 January 2005; site is within the incised middle reach.

The presence of moisture in the extended hyporheic zone at a greater height above the stream surface did not necessarily correspond to an extended hyporheic zone of greater width (Table 4.2). This may result either from differences in particle size, or from measurement inaccuracies. Differences in particle size distribution on the stream banks would favour the presence of moisture at a greater height above the stream surface on the bank with the greatest proportion of small size classes, as capillary rise would be more effective.

The true left stream bank on the lower alluvial fan appeared to have a slightly greater proportion of fine sediment than the right bank; this is probably a result of

snow accumulating in the lee of the left bank, trapping aeolian sediments which remain after the snow sublimates.

4.5.1.3 Distal extended hyporheic zone

The occurrence of distal components of the extended hyporheic zone, as observed from the Loop Moraine photo monitoring point, appeared to increase throughout January (Figure 4.25). The effect of the lateral transfer of moisture (across the fan) via subsurface flow paths was evident as a reduction in stream flow at sites below the emergence of Goodspeed Stream onto the lower alluvial fan. This is indicative of stream flow in influent streams, such as Goodspeed Stream, where water is lost from the stream through lateral transfers and evaporation.

4.5.2 Vertical extent

The vertical extent of the Goodspeed Stream extended hyporheic zone was limited by the presence of ice cement at a mean depth of 28 cm (Figure 4.26). Depth to ice cement was measured during sampling of the Goodspeed Upper Transect; samples were taken between 7 and 9 January 2005. Therefore, the vertical extent of the extended hyporheic zone should have been close to its seasonal maximum at this time, as maximum air temperature was recorded on 5 January 2005.

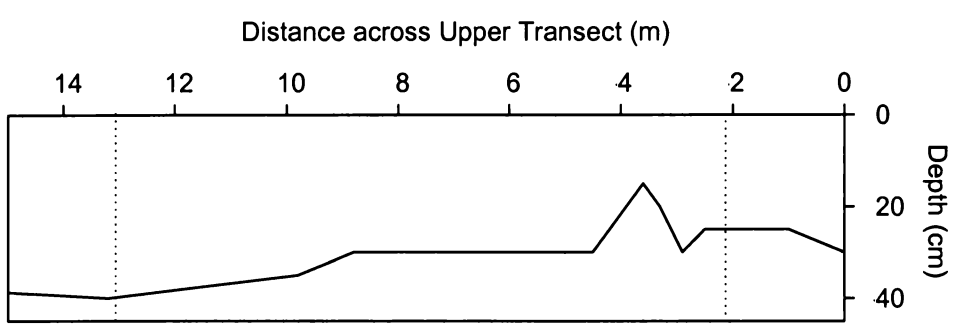

Figure 4.25. Depth to ice cement within the Goodspeed Stream extended hyporheic zone between 7 and 9 January 2005. The extended hyporheic zone occurs between the dotted lines on the graph, from 2.1 – 13.2 m on the Goodspeed Upper Transect.

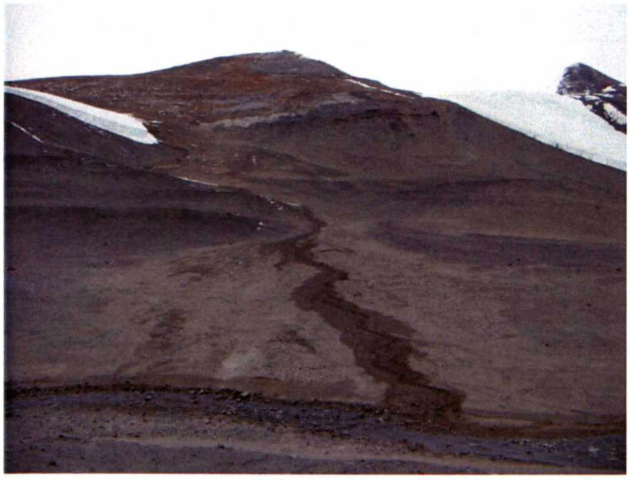

4 January 2005

7 January 2005

10 January 2005

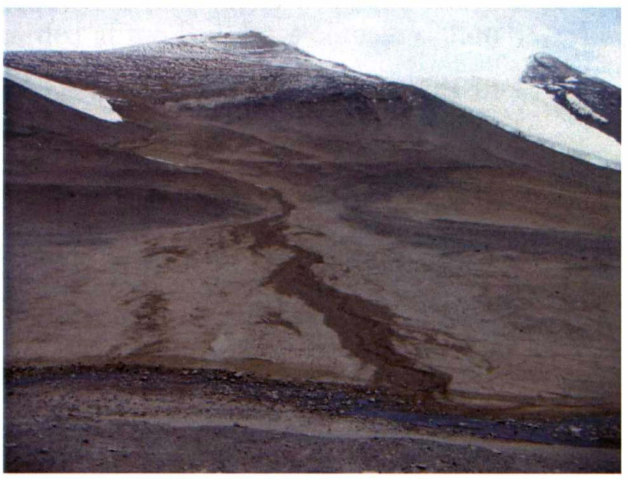

12 January 2005

16 January 2005

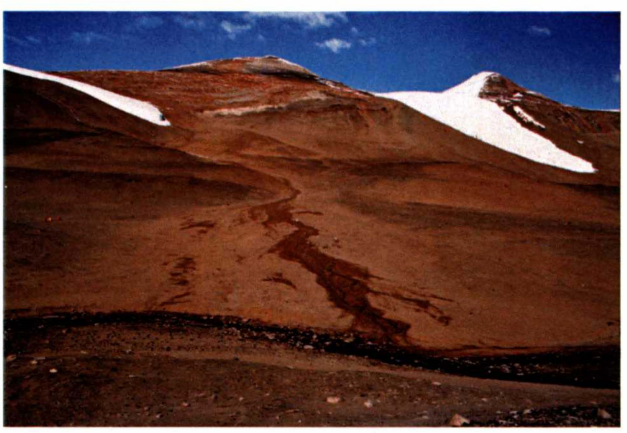

21 January 2005

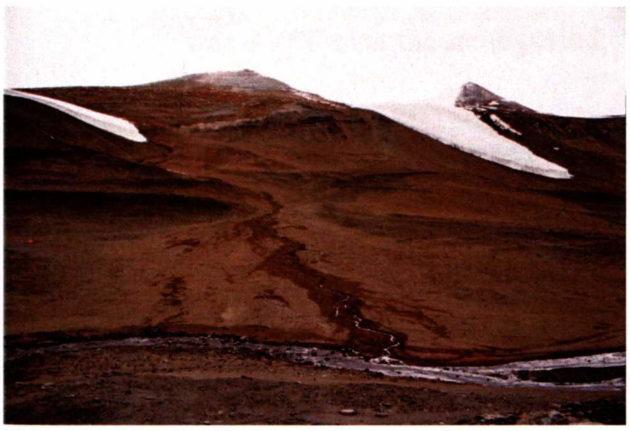

25 January 2005

28 January 2005

Figure 4.25. Time-series of photographs taken from the Loop Moraine photo monitoring point.

4.6 Summary and conclusions

Data recorded at the Goodspeed Stream climate station between 4 and 30 January 2005 showed strong diurnal variability in all parameters. The variability observed in air and soil temperatures was driven by solar radiation, which varied as a result of solar geometry, cloud cover and the topographic influence of the Asgard Range.

Solar radiation and air temperature data recorded at the Bull Pass climate station corroborated the trends shown at the Goodspeed Stream site. Differences in measured values of solar radiation flux density recorded at the two sites was most likely a result of measurement inaccuracies, though there were also differences in cloud cover. The higher air temperatures recorded at the Bull Pass climate station reflect an up-valley warming in summer air temperature.
The following conclusions can be drawn from this chapter:

- Solar radiation flux density recorded at the Goodspeed Stream climate station showed strong diurnal variability due to changes in solar zenith angle and shading from the Asgard Range;

- Mean air temperature recorded at the Goodspeed Stream climate station was –1.1 °C over the period 4 – 30 January 2005;

- Mean soil temperature at 5 cm depth in the near-stream hyporheic zone adjacent to Goodspeed Stream was 3.4 °C over the period 4 – 30 January 2005; mean soil temperature at 5 cm depth in the extended hyporheic zone was 4.9 °C over the same period;

- Stream flow in Goodspeed Stream ranged from 0 to ~ 2.5 $\ell\ s^{-1}$ during the period 4 – 24 January 2005. Stream flow ceased, presumably for the season, on 24 January 2005;

- The mean width of the extended hyporheic zone at the Goodspeed Stream daily monitoring site was 8 m (including Goodspeed Stream and the near-

stream hyporheic zone) over the period 4 – 30 January 2005. The near-stream hyporheic zone had a mean width of 0.44 m over the period 4 – 22 January 2005;

- Ice cement was present within the extended hyporheic zone at a mean depth of 28 cm;

- Correlations between mean daily air temperature, solar radiation and stream flow were poor.

Chapter 5
Soil moisture and salt variability in the Goodspeed Stream hyporheic zones and lower alluvial fan

Chapter 5 Soil moisture and salt variability in the Goodspeed Stream hyporheic zones and lower alluvial fan

5.1 Introduction

Soil moisture and electrical conductivity data obtained along the length of Goodspeed Stream and across the lower alluvial fan are presented. Data pertaining to the Goodspeed Stream extended hyporheic zone are discussed separately, as the moist hyporheic zone is distinctly different from the predominantly dry landscape that characterises Wright Valley. Relationships between soil moisture content and electrical conductivity are considered. A pedotransfer function is used to predict soil moisture potential across the Goodspeed lower alluvial fan, with soil moisture potential providing an indication of the direction of water movement across the fan.

5.2 Goodspeed lower alluvial fan

5.2.1 Upper transect

The Upper Transect on the Goodspeed lower alluvial fan was 151.5 m in length. It extended from just beyond the western bank of Goodspeed Stream, across the fan to the base of the Loop moraine. All distances reported are distances across the transect, in a west to east direction, unless stated otherwise. Two branches of Goodspeed Stream intersected the transect at distances of 5.6 and 8.1 m.

Soil samples along the Goodspeed Upper Transect were taken between 7 and 16 January 2005; the upper two increments were re-sampled on 27 January 2005.

5.2.1.1 Soil gravimetric moisture content

Soil gravimetric moisture content across the Goodspeed Upper Transect (Figure 5.1) ranged from 0.15% at the surface of the eastern-most pit on the transect (151.5 m), to 21.7% at the surface of a former stream channel within the extended hyporheic zone (3.6 m across transect; 2 m from Goodspeed Stream).

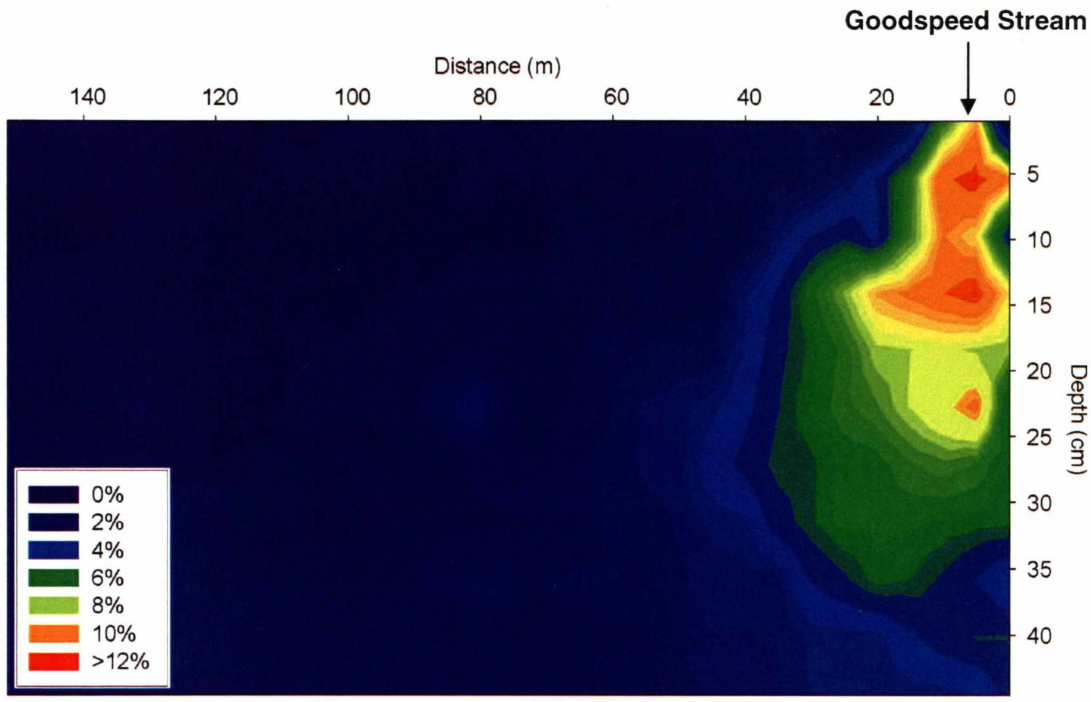

Figure 5.1. Soil gravimetric moisture content across the Goodspeed alluvial fan (Upper Transect).

Soil moisture content was highest close to Goodspeed Stream, within the extended hyporheic zone (2.1 – 13.2 m). Subsurface moisture (up to 4%) was present at a distance of 82.4 m across the transect; mean moisture content at all depths between 15.8 and 82.4 m was 1.6%. From the outer edge of the Goodspeed lower alluvial fan, at 88 m, to the eastern-most end of the transect at 151.5 m, the mean soil moisture content at all depths was 0.4%. This is typical of ambient soil moisture levels in Wright Valley (0.4 – 1%), as determined by Campbell et al. (1997b) for soils in the vicinity of Vanda Station.

Soil moisture content strongly reflected the observed trends in surface moisture content. Distal components of the hyporheic zone were recorded at 29, 67 and 82

m across the Upper Transect (Figure 5.2); these zones contrasted the mean background moisture content of 0.6% at all depths in all profiles across the transect, excluding the extended hyporheic zone and the distal components of the hyporheic zone at 29, 67 and 82 m.

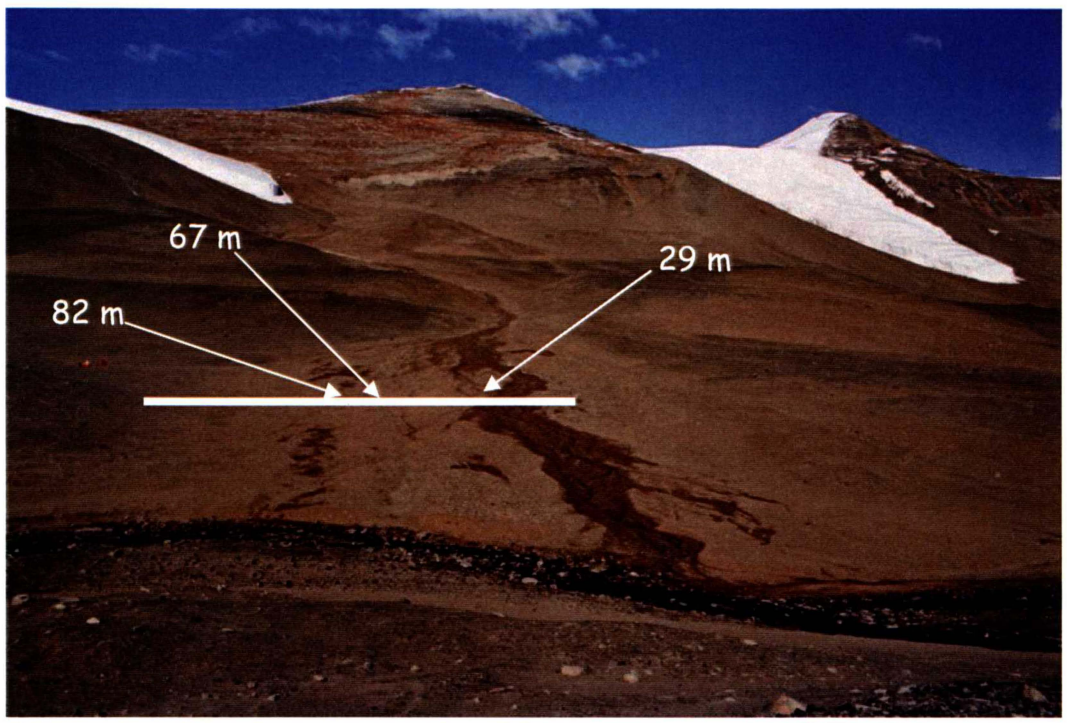

Figure 5.2. Areas of visible moisture on the Goodspeed alluvial fan. The line indicates the Goodspeed Upper Transect; arrows point to distal components of the hyporheic zone across the transect.

As sampling was undertaken predominantly in early January, soil moisture content was likely to be at a maximum. Sampling prior to or after this period may not have provided data representative of the period of maximum melt; thus the observed extent of moisture in the Goodspeed lower alluvial fan can be considered broadly reflective of moisture supply in a moderate-to-low-flow season.

Implications under higher flow conditions

The surficial moistening of soil at various distances across the Goodspeed alluvial fan is important in terms of the potential for contamination of streams. In higher flow years, or during periods of intense melting, distal components of the

hyporheic zone that exist under relatively low flow conditions may become flowing stream channels. Thus, under higher flow conditions, the Goodspeed lower alluvial fan could exhibit multiple flowing stream channels, with the greater extent of liquid water having the potential to mobilise contaminants spilled on the fan.

The presence of moisture visible at the soil surface is also evidence of greater areas of subsurface moisture movement within the fan. Therefore, large spills migrating downwards under saturated flow may reach the top of the ice cement, and be transported down-slope by moisture moving along the top of the ice cement.

Extended hyporheic zone

The visibly moist extended hyporheic zone (2.1 – 13.2 m across the Upper Transect) had a mean soil moisture content of 10.2% at all depths, in contrast to the 0.5% mean moisture content over all depths at all sites outside the extended hyporheic zone. Soil moisture content within the extended hyporheic zone tended to increase with depth (Figure 5.3). The mean surface soil moisture content at the outermost edges of the extended hyporheic zone was 2%, suggesting that this was close to the lower moisture limit at which the soil surface appeared visibly moist. Mean moisture content at the outermost edges of the extended hyporheic zone was 4.3%.

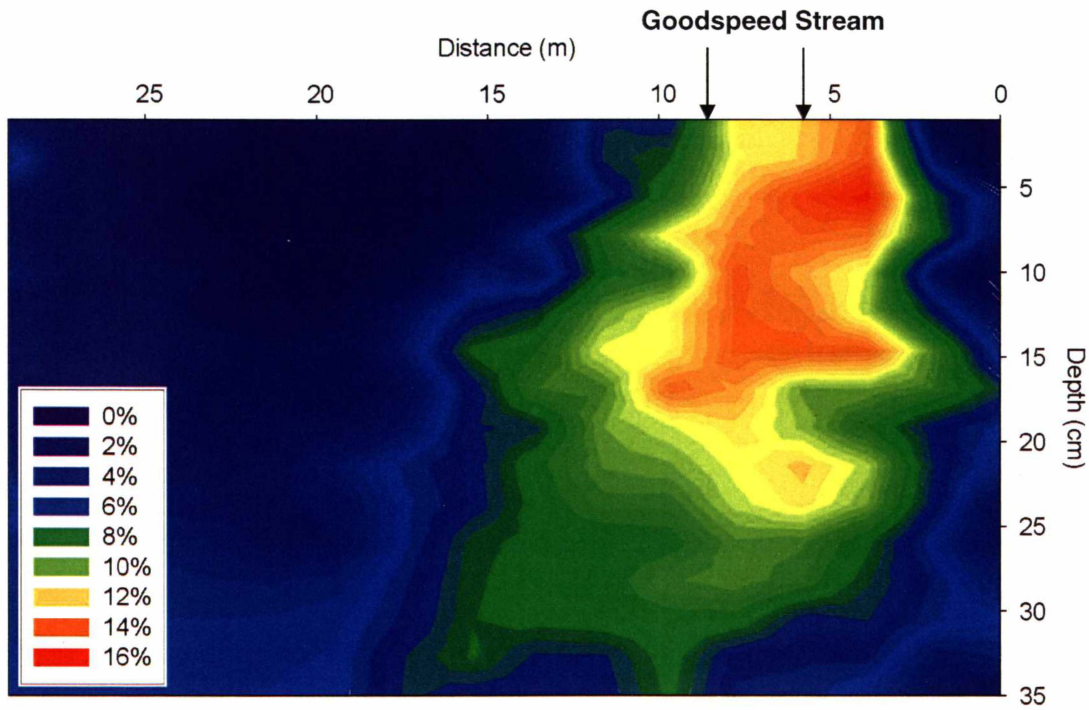

Figure 5.3. Soil gravimetric moisture content in the Goodspeed Stream extended hyporheic zone (Upper Transect; sampled between 7 and 10 January 2005).

Moisture content – re-sampled

In samples taken between 7 and 16 January 2005, the mean soil moisture content of the extended hyporheic zone between 0 and 5 cm depth was 9.4% (Figure 5.4a), slightly lower than the 10.2% averaged over all depths within the extended hyporheic zone. However, moisture content had decreased at the surface by 27 January 2005; mean soil moisture content of the extended hyporheic zone between 0 and 5 cm was 6.4% (Figure 5.4b).

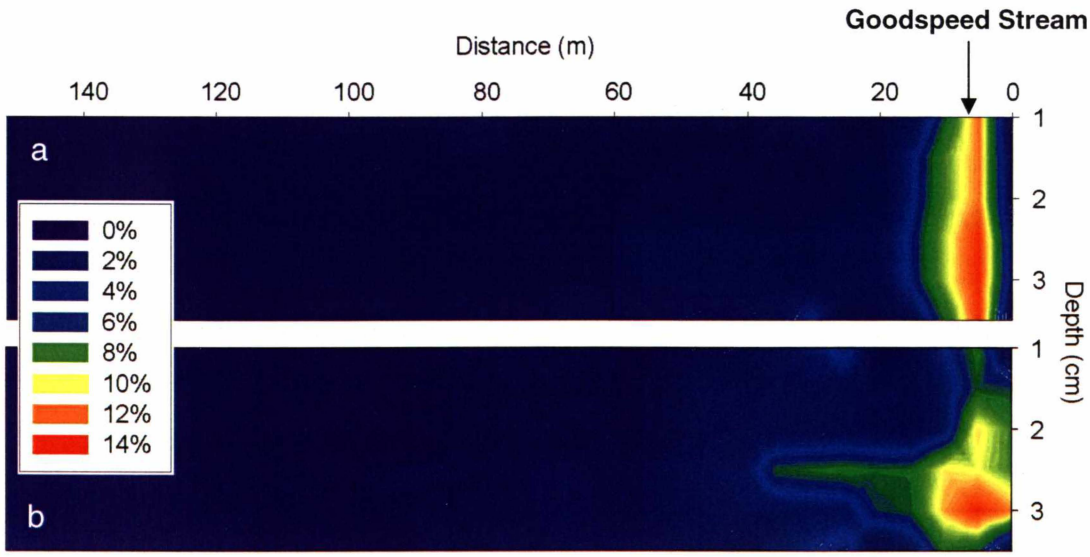

Figure 5.4. Soil gravimetric moisture content in the upper 5 cm. a) Upper Transect sampled between 7 and 16 January 2005; b) Upper Transect sampled on 27 January 2005.

The decrease in near-surface moisture content supported the visible decline in moisture content and width of the extended hyporheic zone. Confounding this, however, was an increase in soil moisture content in the upper 5 cm across the Upper Transect (excluding the hyporheic zone) from 0.7% in early January, to 1.1% in late January.

The increase in soil moisture content across the transect in late January may be a result of decreased air temperatures and hence decreased evaporation of soil moisture. Furthermore, in late January, a lateral spread of moisture at about 2.5 cm depth was observed, and may be a result of lower air temperatures causing freezing at the surface and subsequently forcing moisture laterally through unfrozen pore spaces. The lateral expansion in subsurface moisture could also arise from gradients in soil moisture potential acting to drive moisture laterally, away from areas with greater moisture content.

5.2.1.2 Soil electrical conductivity

Soil electrical conductivity (EC) varied both horizontally and vertically. The maximum salt concentration recorded was 10520 μS/cm in the sample from 5 – 15 cm in the pit at the western-most edge of the transect (0 m). However, this was

a localised maximum, with electrical conductivities of 2270 and 3885 µS/cm recorded in the samples from 2 – 5 cm and 15 – 30 cm in the same pit. Another local high (9660 µS/cm) occurred at 2.1 m along the transect, which coincided with a zone of visible salt precipitation at the western edge of the extended hyporheic zone.

Consistently high electrical conductivity values (>5000 µS/cm) were recorded between 66.6 and 82.4 m on the Goodspeed Upper Transect, averaging 6590 µS/cm at the soil surface (Figure 5.5).

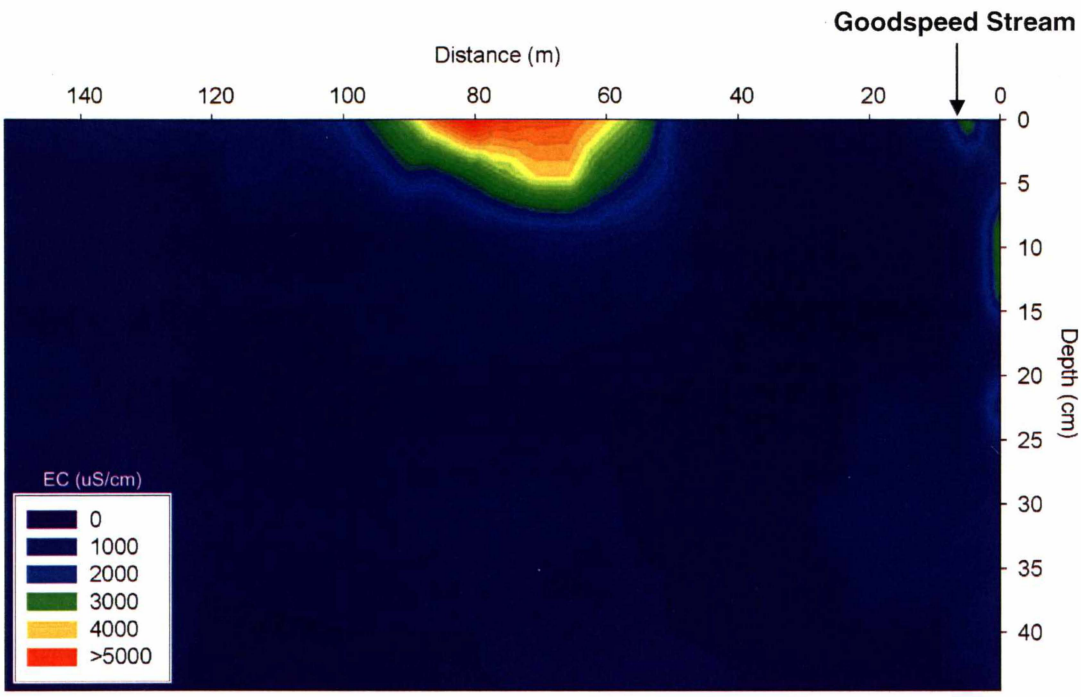

Figure 5.5. Soil electrical conductivity across the Goodspeed Upper Transect. The values shown in the key are lower than the measured values due to the interpolation technique used in producing the contour plot.

The high electrical conductivity values between 66.6 and 82.4 m were coincident with areas of very low soil moisture potential (Figure 5.16, Section 5.2.1.6), though they may also be a function of the microtopography of the fan. Across the fan, there was evidence of former channel and bar patterns. The area between 66.6 and 82.4 m was a former bar, thus being higher in the landscape relative to the relict channels at 66.6 and 82.4 m which were visibly moistened at the surface, and represented distal components of the hyporheic zone. Therefore, the high electrical conductivity values recorded on the raised bar probably reflect greater

movement and evaporation of soil moisture, acting to concentrate salts at the limit of the moisture movement.

At pits located between 2.1 and 104 m across the transect, soil electrical conductivity values decreased with depth, in contrast to previous documentation of soil electrical conductivity in the Dry Valleys (e.g. Bockheim, 1979; 1980; Bockheim, 1997b). In pits with high surface EC values the decrease with depth was sharp, in one instance decreasing from 7800 μS/cm in the 0 – 2 cm increment, to 285 μS/cm in the 2 – 5 cm increment. Conversely, in pits from 0 – 2.1 m and 104 – 151.5 m, electrical conductivity values tended to be lowest at the surface, and increased with depth.

The increase in electrical conductivity with depth in pits at the outermost edges of the transect (0 – 2.1 m and 104 – 151.5 m across the transect) can be explained by greater soil development. The landsurfaces on the extremities of the fan are more stable and soils are more strongly developed. Thus salinisation processes in the soils have operated over a greater timescale, acting to concentrate salts in subsurface horizons, with the greatest accumulations of salts occurring at the limit of the wetting front (Bockheim, 1997b).

One of the most strongly developed soils sampled, at the eastern-most extent of the transect, had a relatively low value of electrical conductivity in all horizons, with a mean of 250 μS/cm throughout the profile. Thus, in a relatively dynamic environment such as that of the Goodspeed lower alluvial fan, it is evident that the presence of summer meltwater drives the accumulation of salts within soils. Soil moisture, replenished from Goodspeed Stream, is drawn to areas of lower moisture potential (Section 5.2.1.6) and evaporated from the soil surface, drawing with it soluble salts which are precipitated out following evaporation of sufficient moisture (Figure 5.6). This mechanism of transport and evaporation results in greater electrical conductivities at or near the soil surface.

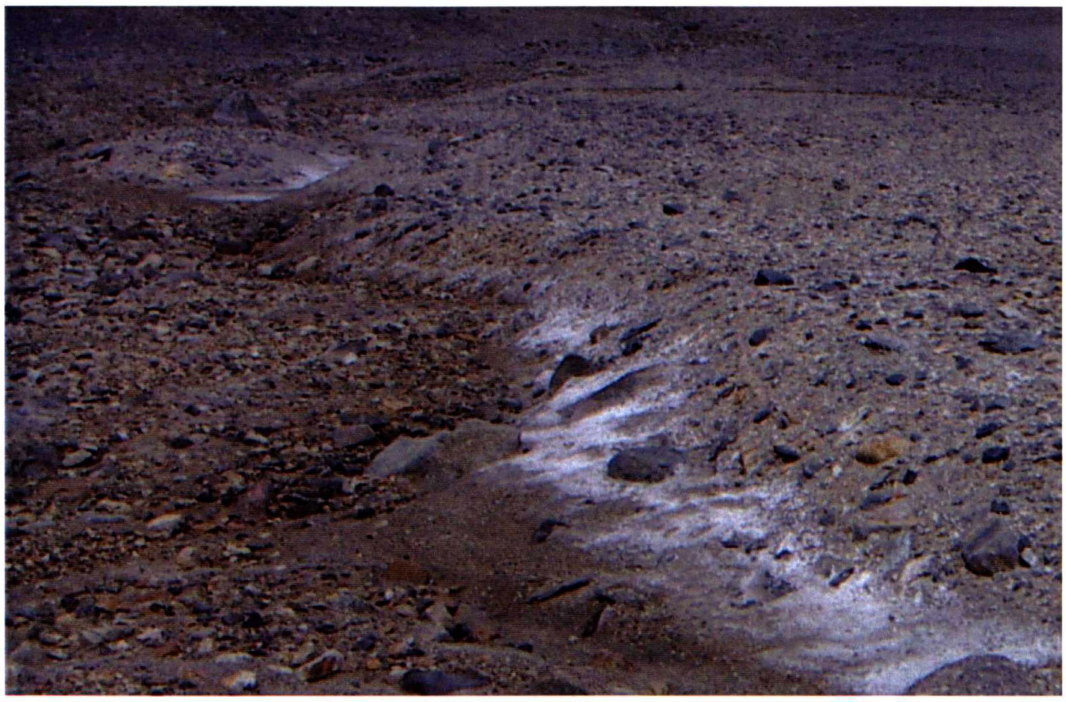

Figure 5.6. Precipitation of salts on the western bank of Goodspeed Stream. The width of the salt band varied in accordance with fluctuations in the width of the hyporheic zone. In this photo, the width of the salt band is approximately 45 cm.

Extended hyporheic zone

Evidence of salt precipitation was observed at the soil surface at the western limit of the Goodspeed Stream extended hyporheic zone. The precipitation of salts at the soil surface represented the limit of lateral moisture movement, with salts precipitating at the soil surface following evaporation of soil moisture. However, there was no correlation between the width of the salt band and the mean moisture content of the extended hyporheic zone (Figure 5.7). The width of the salt band was negatively correlated to the width of the extended hyporheic zone on the true left of Goodspeed Stream (Figure 5.8); salts decreased with increasing hyporheic zone width.

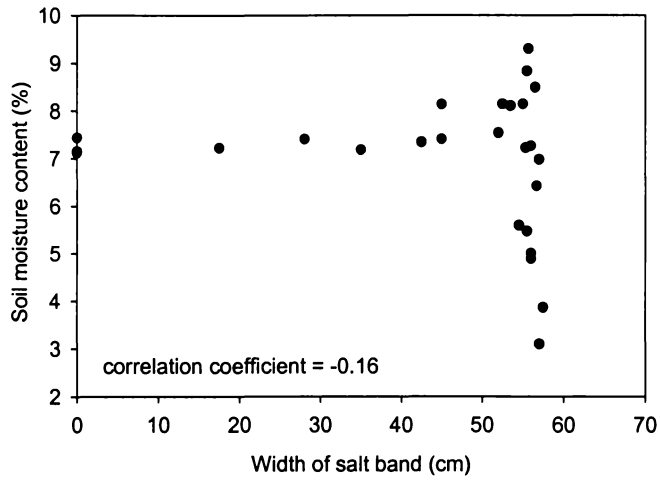

Figure 5.7. Correlation between width of the salt band precipitating at the western-most edge of the extended hyporheic zone and mean soil moisture content of the extended hyporheic zone.

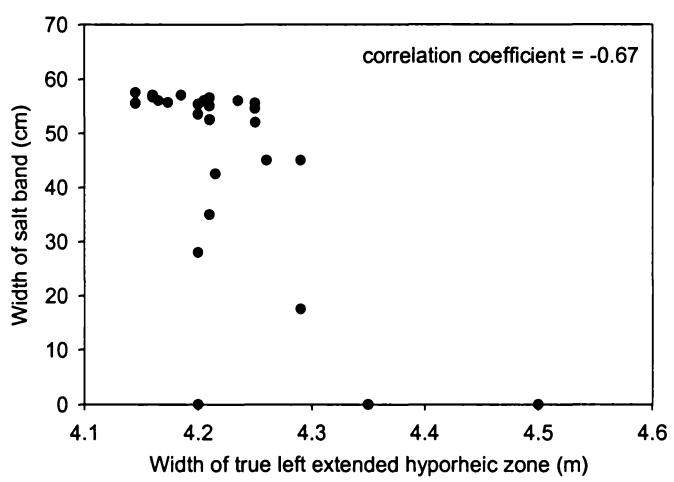

Figure 5.8. Correlation between width of the salt band precipitating at the western-most edge of the extended hyporheic zone and width of the true left extended hyporheic zone.

5.2.1.3 Particle size distribution

Particle size data from the Goodspeed Upper Transect indicate that there was little variability in the <2 mm fraction across the Goodspeed lower alluvial fan (Table 5.1). The dominant size class of the <2 mm fraction was medium sand, comprising just over 45% of the mean sample. The total proportion of sand (2 –

0.06 mm) was almost 98%, and the mean silt and clay content of the samples was low (~2%). These data were consistent with other reported particle size data for the Dry Valleys (e.g. Bockheim, 1979; 1980; Bockheim, 1997b).

Table 5.1. Mean particle size distribution of the <2 mm fraction across the Goodspeed Upper Transect.

Particle size class	% coarse sand (2 – 0.6 mm)	% medium sand (0.6 – 0.2 mm)	% fine sand (0.2 – 0.06 mm)	% silt and clay (<0.06 mm)
mean	34.5	45.3	17.9	2.3
s.d.	9.9	5.7	5.6	1.7
n	53	53	53	53

Mean particle size data for the <2 mm fraction in the Goodspeed Stream extended hyporheic zone were typical of the relatively uniform mean particle size distribution observed across the entire Upper Transect (Table 5.2). Therefore, soils of the extended hyporheic zone have no greater moisture-retaining capacity than those further out on the fan; the extended hyporheic zone was wetted purely as a result of proximity to the stream and capillarity.

Table 5.2. Mean particle size distribution of the <2 mm fraction in the Goodspeed Stream extended hyporheic zone (Upper Transect).

Particle size class	% coarse sand (2 – 0.6 mm)	% medium sand (0.6 – 0.2 mm)	% fine sand (0.2 – 0.06 mm)	% silt and clay (<0.06 mm)
mean	36.1	45.7	16.4	1.8
s.d.	10.1	6.4	5.2	0.8
n	19	19	19	19

5.2.1.4 Depth to ice cement

The depth to ice cement across the Goodspeed lower alluvial fan ranged from 15 cm immediately adjacent to Goodspeed Stream, to 54 cm at the eastern-most extent of the Goodspeed Upper Transect (Figure 5.9). Ice cement in Wright Valley is generally sparse, being predominantly located within younger surfaces or those with a seasonal moisture supply (Campbell et al., 1997b). Hence the

occurrence of ice cement on the Goodspeed alluvial fan reflects the greater availability of moisture at sites proximal to ephemeral streams.

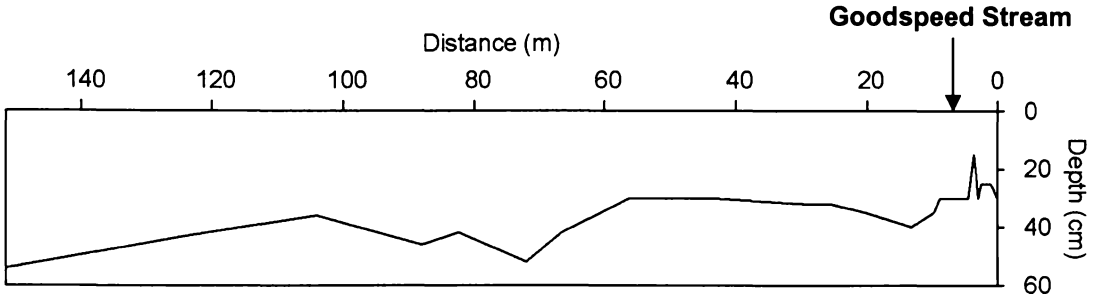

Figure 5.9. Depth to ice cement across the Goodspeed alluvial fan (Upper Transect).

The increase in depth to ice cement between 57 and 72 m across the Upper Transect coincided with a decrease in mean soil gravimetric moisture content from 1.2% to 0.4%, respectively. The mean soil gravimetric moisture content of all samples in each pit was negatively correlated to depth to ice cement in the pit (Figure 5.10), with the depth to ice cement increasing with decreasing gravimetric moisture content.

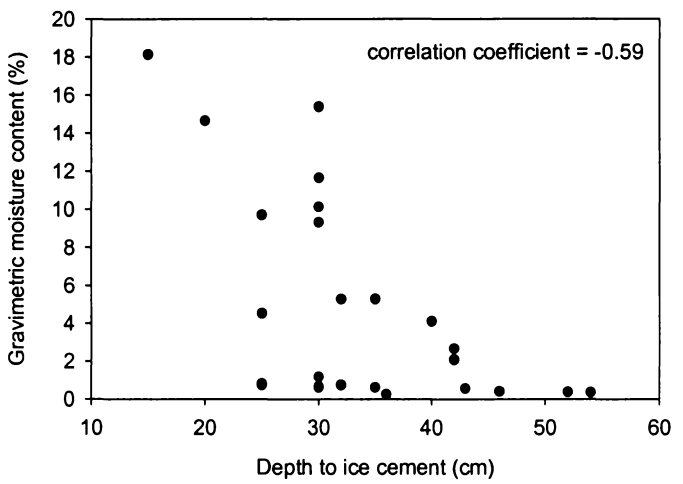

Figure 5.10. Correlation between mean soil gravimetric moisture content and depth to ice cement across the Goodspeed Upper Transect.

The correlation between gravimetric moisture content and depth to ice cement was improved by relating the moisture content of visibly dry soils, thus excluding those within the extended and distal components of the hyporheic zone, to the

depth to ice cement (Figure 5.11). Similarly, the relationship between gravimetric moisture content and depth to ice cement was considered for soils within the extended hyporheic zone (Figure 5.12).

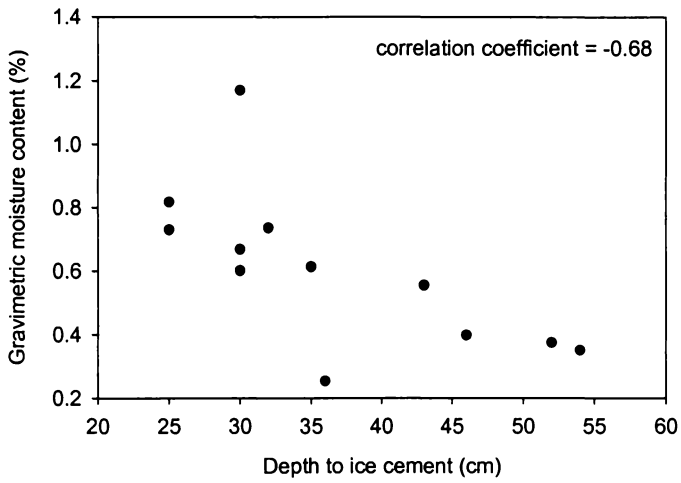

Figure 5.11. Correlation between mean soil gravimetric moisture content and depth to ice cement in visibly dry soils across the Goodspeed Upper Transect.

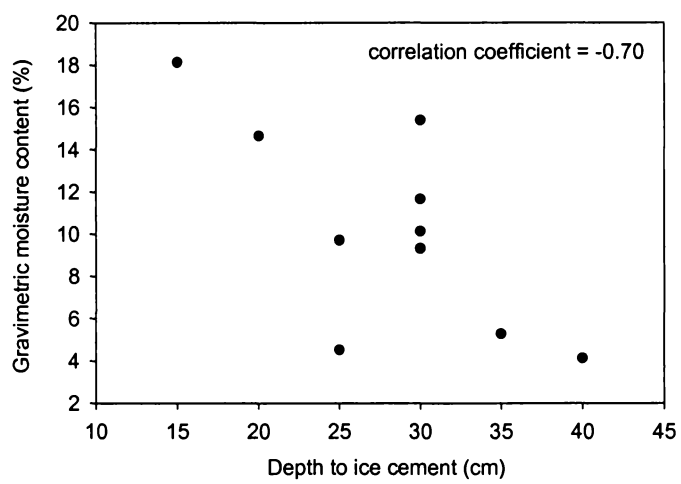

Figure 5.12. Correlation between mean soil gravimetric moisture content and depth to ice cement within the extended hyporheic zone on the Goodspeed Upper Transect.

The correlation between soil gravimetric moisture content and depth to ice cement indicates that soil gravimetric moisture content and the depth at which soils become ice cemented are inversely related. Lower soil moisture contents are related to greater depths to ice cement, and vice-versa. Thus the extent and

distribution of moisture across the Goodspeed lower alluvial fan influences the depth at which soil becomes ice cemented.

5.2.1.5 Relationship between soil gravimetric moisture content and electrical conductivity

Soil gravimetric moisture content was weakly correlated to soil electrical conductivity across the Goodspeed Upper Transect (Figure 5.13). The weak relationship between soil gravimetric moisture content and electrical conductivity was probably a function of a high degree of spatial variability in the evaporation regimes of soils across the fan. Evaporation is reliant on the presence of soil moisture, and subsequently depends on solar radiation and air temperature.

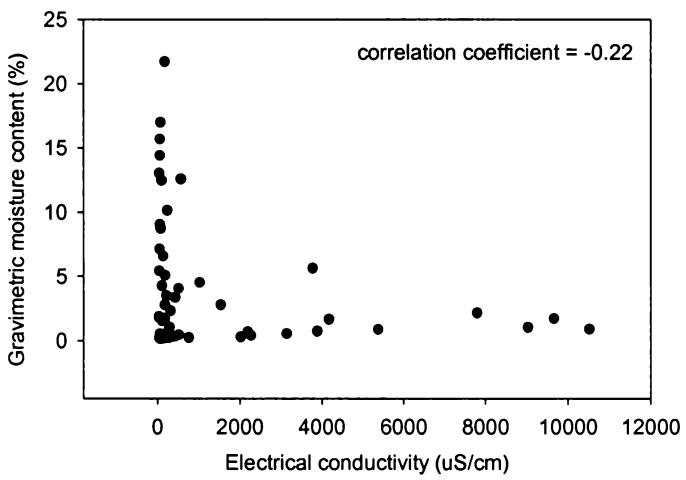

Figure 5.13. Correlation between soil gravimetric moisture content and soil electrical conductivity across the Goodspeed Upper Transect.

The relationship between soil moisture content and electrical conductivity was positive, although weak, when values from soils within the extended and distal components of the hyporheic zone were excluded (Figure 5.14). The positive correlation suggested that greater soil moisture contents (up to 2%) were related to higher salt concentrations.

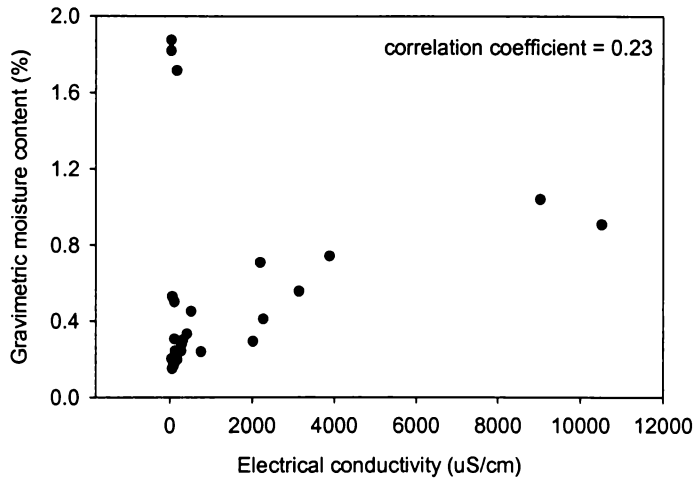

Figure 5.14. Correlation between soil gravimetric moisture content and soil electrical conductivity across the Goodspeed Upper Transect, excluding values within the extended and distal components of the hyporheic zone.

Soil gravimetric moisture content and electrical conductivity within the extended hyporheic zone were also correlated (Figure 5.15). The negative correlation was poor, though it suggested that greater soil moisture contents were related to lower electrical conductivity values. The change from a positive to negative relationship using data from within the extended hyporheic zone may be a result of too few data to adequately represent the nature of the relationship, or it may be indicative of a threshold condition pertaining to soil moisture content and salt concentration.

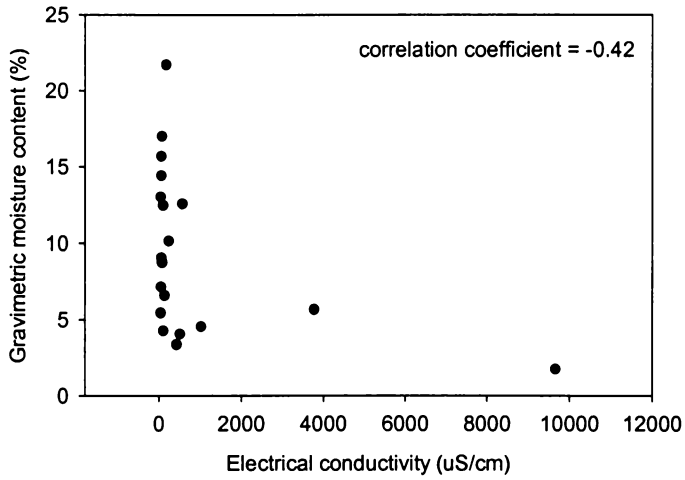

Figure 5.15. Correlation between soil gravimetric moisture content and soil electrical conductivity within the extended hyporheic zone (2.1 – 13.2 m) on the Goodspeed Upper Transect.

There may be a soil moisture content threshold, above which salts are transported within the soil matrix, either laterally or vertically. Thus, soil moisture contents and electrical conductivities both increase to some point, but beyond a certain moisture content, salts are effectively remobilised, and will likely re-precipitate at a site where moisture content is lower (Section 5.2.1.6).

5.2.1.6 Soil moisture potential

Soil moisture potential across the Goodspeed Upper Transect was estimated using a pedotransfer function (Equations 3.3 – 3.6) developed by Minasny et al. (1999). The data used to develop the pedotransfer function were from Australian soils, thus data predicted across the Goodspeed alluvial fan should be treated as indicative. Nonetheless, soil moisture potential, as estimated by Minasny et al.'s (1999) model, greatly decreased with distance from Goodspeed Stream (Figure 5.16).

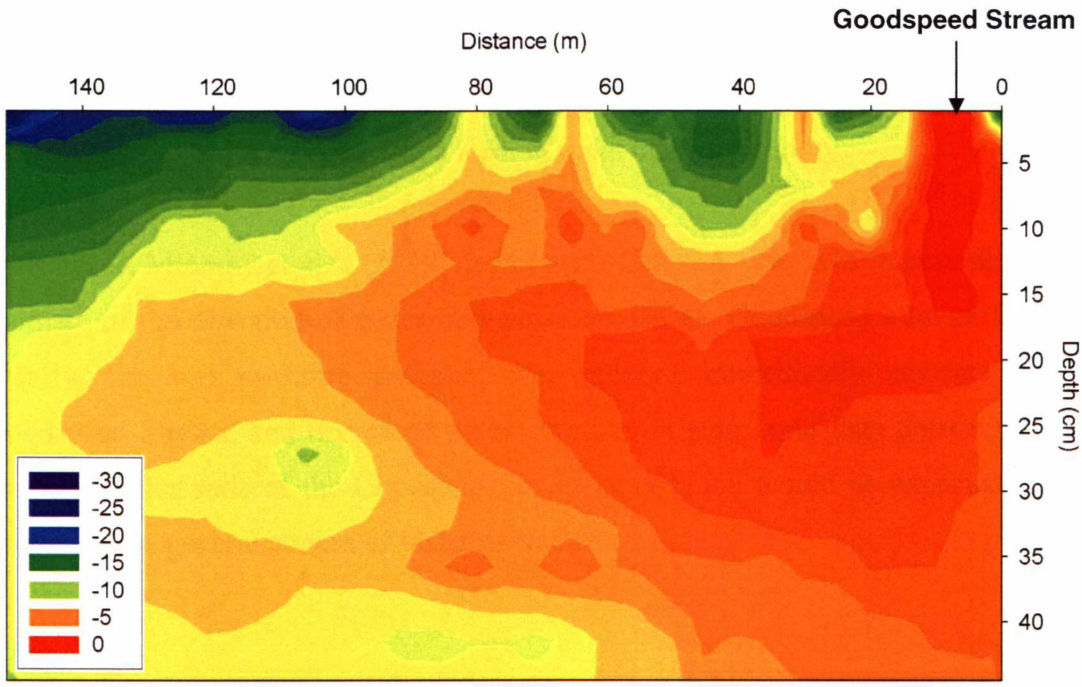

Figure 5.16. Two-dimensional representation of soil moisture potential (kPa) across the Goodspeed alluvial fan (Upper Transect).

Soil moisture moves from areas of high to low potential energy. Therefore, moisture present near Goodspeed Stream would be driven laterally across the fan due to the gradient in soil moisture potential. Similarly, moisture would be drawn towards the soil surface, where soil moisture potential is lower.

The movement of soil moisture from areas of high to low potential also draws with it soluble salts. Consequently, salts are re-precipitated in soils where the soil moisture content is sufficiently low to allow precipitation; this may arise from either evaporation of soil moisture and/or a decrease in soil moisture potential.

Potential error in predicted soil moisture potential

Potential sources of error in the transfer function output data arise primarily from two sources: 1) the model, and 2) input data (McBratney et al, 2002, Minasny and McBratney, 2002). The predictive data used to develop the pedotransfer function were from Australian soils, thus encompassing a broader range of soil types than the predominantly sandy soils which dominate in Antarctica. Therefore, the modelled function may be biased towards soils with greater proportions of silt and

clay. Assumed input data were typical of sandy soils (Section 3.5), rather than being specifically measured for soils of the Goodspeed alluvial fan. Hence spatial variability in soil properties is also a form of input data uncertainty.

In this case, Minasny et al.'s (1999) pedotransfer function was used to provide an estimate of the direction of water movement across the Goodspeed alluvial fan. Clearly, the soil moisture potential was greatest immediately adjacent to Goodspeed Stream, and decreased across the fan. Using input data determined specifically for soils of the Goodspeed lower alluvial fan would be expected to give a similar general pattern of water movement.

Implications for contamination of streams

The gradient in soil moisture potential observed in the Goodspeed Upper Transect has important implications pertaining to the potential for accidental spills to contaminate streams. While Figure 5.16 indicates that spills outside the extended hyporheic zone will be driven laterally across the fan, away from the stream, the representation is purely two-dimensional, and does not encompass down-slope water movement, nor does it take into account the volume of the spill.

Although the gravitational potential component of the soil moisture potential is minimal when using the model to represent moisture potential in two-dimensional space across the fan, lobes of moisture present on the Goodspeed lower alluvial fan were observed to be moving down-slope towards the Onyx River in the valley floor, suggesting that the gravitational potential component on the broader fan was significant. Based on a decrease in altitude of approximately 50 m from where Goodspeed Stream emerges onto the lower alluvial fan to its confluence with the Onyx River, it would be expected that the gravitational potential component of the soil moisture potential would be important in influencing water movement down the fan.

Experimental work in Wright Valley by Claridge et al. (1997) suggests that migration of large spills (e.g. 10 ℓ) is primarily dependent on the soil moisture

content immediately prior to the spill. Spills on "dry" surfaces with a moisture content of ~0.6% showed little migration from the origin of the spill, as they were adsorbed to the dry soil surfaces. However, spills on soils with moisture contents of ~4% moved downwards to the ice cement, before progressing down-slope. Spills on sites with even greater moisture contents (8.5%) were shown to move greater distances down-slope (Claridge et al., 1997). Thus spills of relatively large volume in an area where soil gravimetric moisture content was greater than ~4%, such as that determined on the Goodspeed lower alluvial fan – up to 74 m from Goodspeed Stream, would be expected to migrate downwards to the ice cement before moving down-slope along the surface of the ice cement.

Smaller spills, such as spills of urine or kerosene, are likely to have volumes less than 1 ℓ and would likely be adsorbed to soil particles, and thus driven laterally or to the surface as a result of evaporation and gradients in soil moisture potential.

Extended hyporheic zone

A substantial decrease in the soil moisture potential was observed just beyond the extended hyporheic zone, at around 15 m (Figure 5.17). The observed decrease in soil moisture potential highlights the sharp reduction in soil moisture content beyond the eastern-most edge of the extended hyporheic zone (13.2 m). The gradient in soil moisture potential between the moist extended hyporheic zone and the visibly dry soil on the Goodspeed lower alluvial fan acts to drive soil moisture laterally, away from the extended hyporheic zone. Consequently, small spills within the extended hyporheic zone are likely to be driven away from the stream channel.

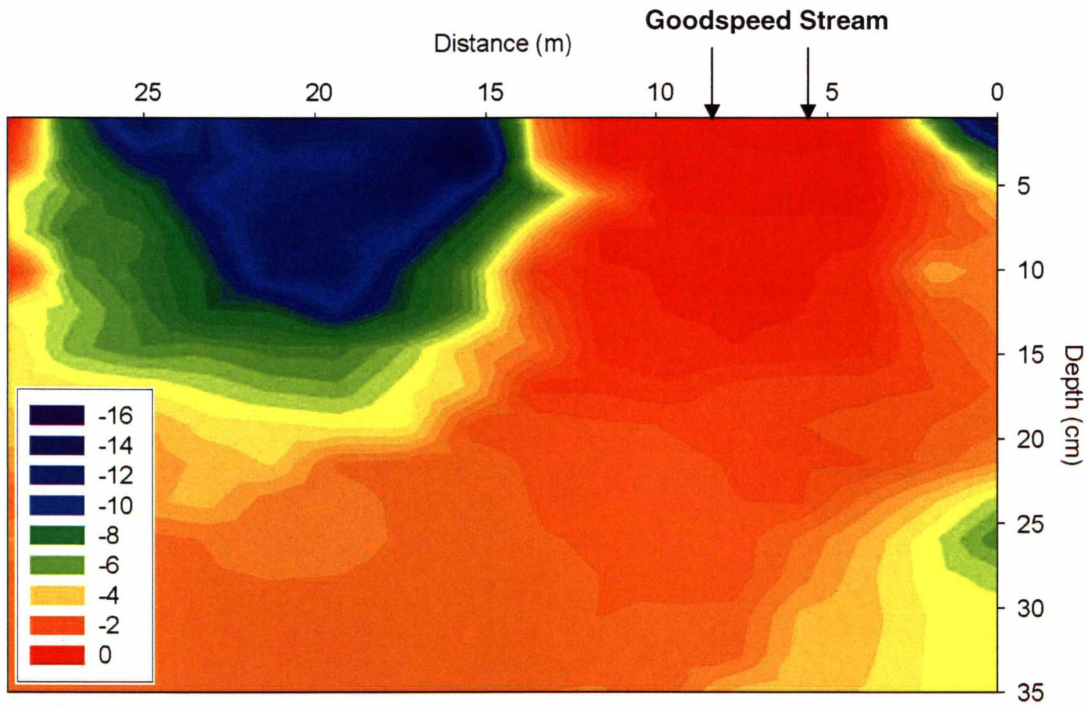

Figure 5.17. Soil moisture potential (kPa) in the Goodspeed Stream extended hyporheic zone (2.1 – 13.2 m across the Upper Transect).

Despite the decrease in soil moisture potential beyond the extended hyporheic zone, the hyporheic zone itself is particularly vulnerable to contamination from spills. Any large spills within the extended hyporheic zone are likely to be incorporated into the stream and transported to the Onyx River, and on to Lake Vanda.

5.2.2 Lobe of moisture

Monitoring of one lobe of moisture extending out from the extended hyporheic zone on the true right of the Goodspeed lower alluvial fan showed considerable down-slope progression of moisture. On 4 January 2005, markers were placed to indicate the maximum visible extent of the moisture (Figure 5.18), with the increase in distance down-slope being measured from the markers on 28 January 2005.

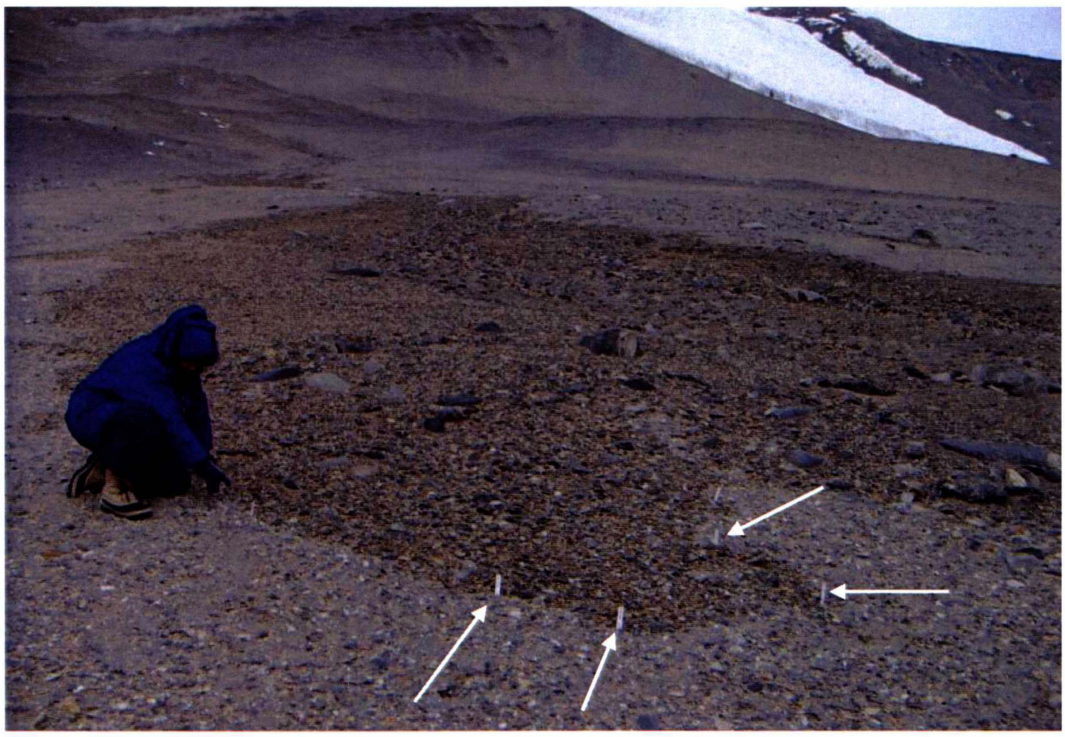

Figure 5.18. Lobe of moisture on the right hand side of the Goodspeed Stream extended hyporheic zone, taken 4 January 2005.

Over the 24 day observation period, the lower-most extent of the moisture increased by a maximum of 7.5 m, while the eastern-most extent of the moisture increased by between 2.75 and 3.5 m (Figures 5.19 and 5.20). Therefore, the mean migration down-slope was 0.3 m per day, though such down-slope progression may not have occurred in a linear fashion. Similarly, the lateral expansion of the moistened area occurred at a maximum rate of 0.15 m per day, presumably primarily as a result of differences in the soil moisture potential acting to drive moisture towards areas of lower moisture content.

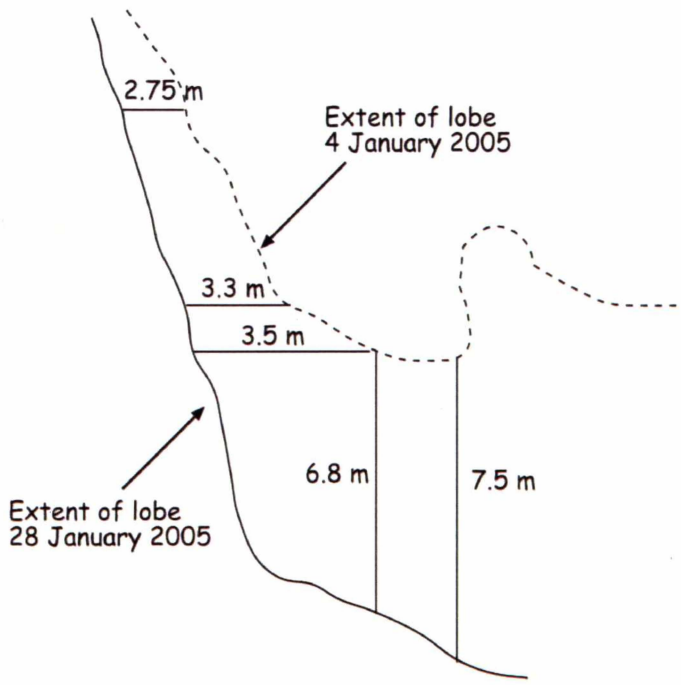

Figure 5.19. Diagram showing down-slope and lateral progression of moisture. (Not drawn to scale)

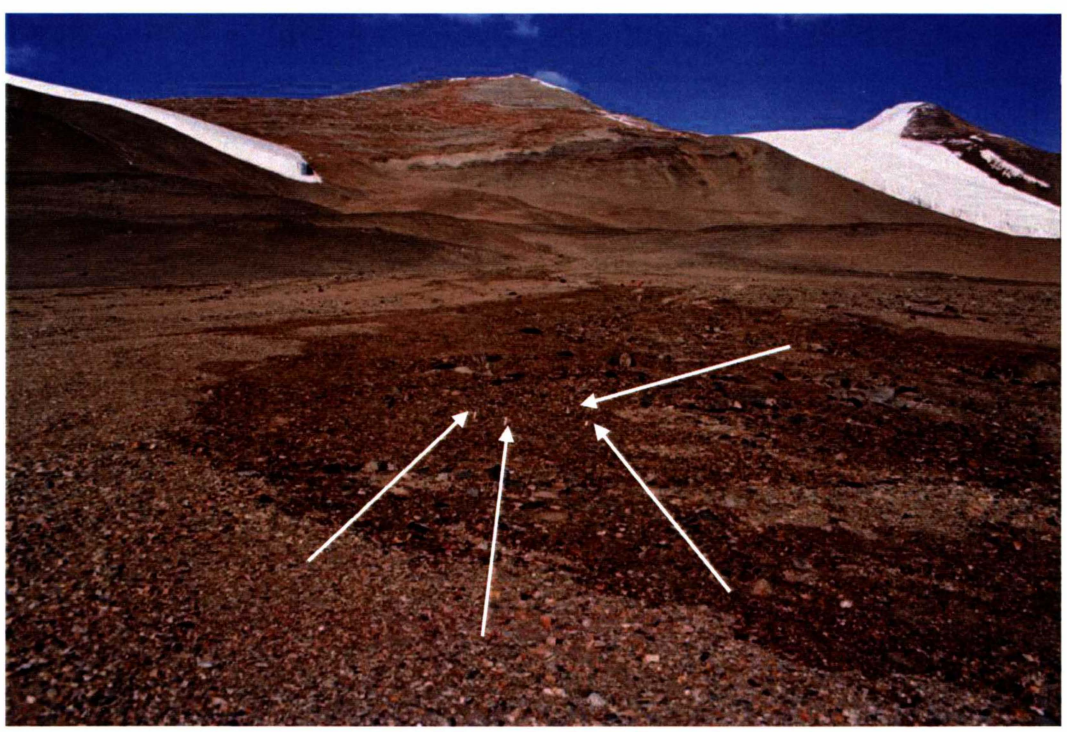

Figure 5.20. The eastern-most extent of the lobe of moisture on the right hand side of the Goodspeed Stream extended hyporheic zone, taken 28 January 2005. The arrows point to the same white markers shown in Figure 5.18.

5.2.3 Lower transect

The Goodspeed Lower Transect was considerably shorter than the Upper Transect. The Lower Transect began on the eastern edge of Goodspeed Stream, spanning a distance of 18.2 m across the fan. As with the Upper Transect, all distances reported are distances across the transect, in a west to east direction, unless stated otherwise.

Soil samples along the Goodspeed Lower Transect were taken on 25 January 2005.

5.2.3.1 Soil gravimetric moisture content

Soil gravimetric moisture content in the Goodspeed Lower Transect was greatest (17.6%) at a distance 6.3 m from Goodspeed Stream. In contrast, the greatest soil moisture content recorded on the Upper Transect was at a distance of 2 m from the stream. The distribution of soil moisture within the Goodspeed Lower Transect showed a different pattern to that observed across the Upper Transect, with high values of soil moisture recorded near the soil surface throughout the extended hyporheic zone (Figure 5.21).

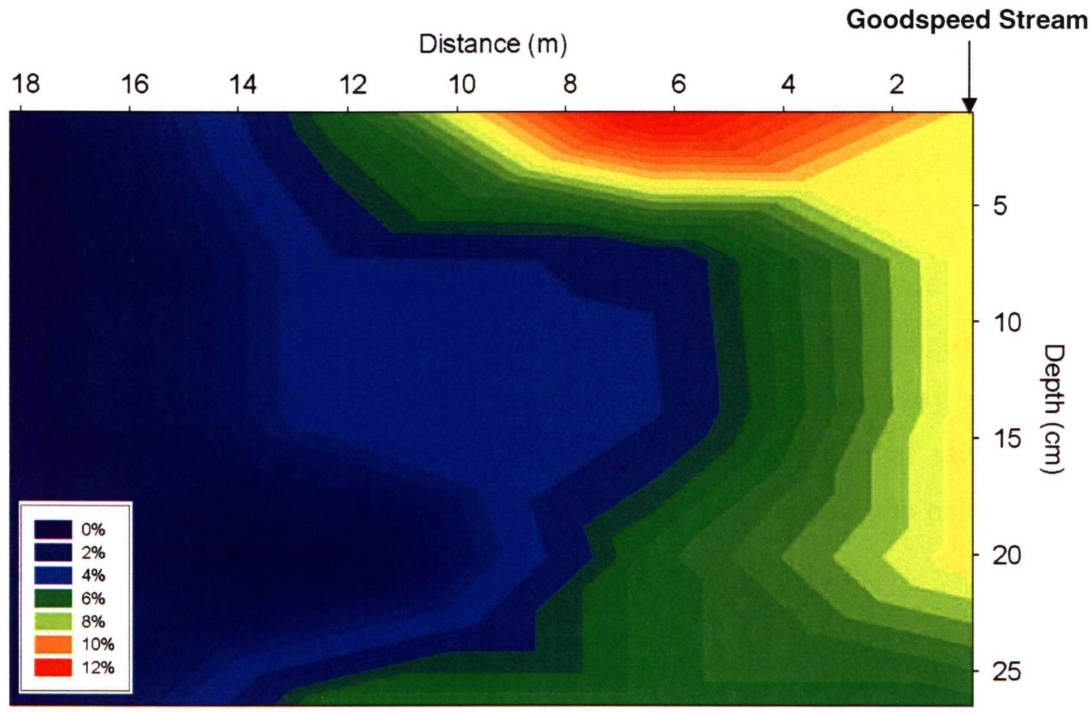

Figure 5.21. Soil gravimetric moisture content across the Goodspeed Lower Transect.

Soil moisture content generally increased with depth. Mean soil moisture content of the extended hyporheic zone (0 – 13.6 m) was 7.9%, somewhat less than the 10.2% obtained in the extended hyporheic zone across the Upper Transect. The mean soil moisture content at all depths in pits outside the extended hyporheic zone was 0.4%; this is consistent with the mean soil moisture content of 0.6% (excluding the extended hyporheic zone and distal components of the extended hyporheic zone) recorded for the Upper Transect.

The different distribution and decreased soil moisture content of the extended hyporheic zone in the Lower Transect is likely to be a result of differences in climatic conditions at the time of sampling. Unlike samples taken across the Upper Transect, between 7 and 16 January 2005, samples from the Lower Transect were taken on 25 January 2005, by which time the extended hyporheic zone had frozen at the surface and was starting to noticeably dry out. Furthermore, flow in Goodspeed Stream ceased on 25 January, thus effectively disconnecting the recharge source of the hyporheic zone, while the increased presence of ice in the stream from 16 January onwards would have also

diminished the magnitude of exchange taking place between the stream and extended hyporheic zone.

5.2.3.2 Soil electrical conductivity

Soil electrical conductivity values in the Goodspeed Lower Transect ranged from 25 – 570 μS/cm, being considerably lower than electrical conductivity values recorded across the Upper Transect. The greatest concentration of salt was recorded at the surface of the pit at 12.1 m (Figure 5.22), within the extended hyporheic zone (0 – 13.6 m).

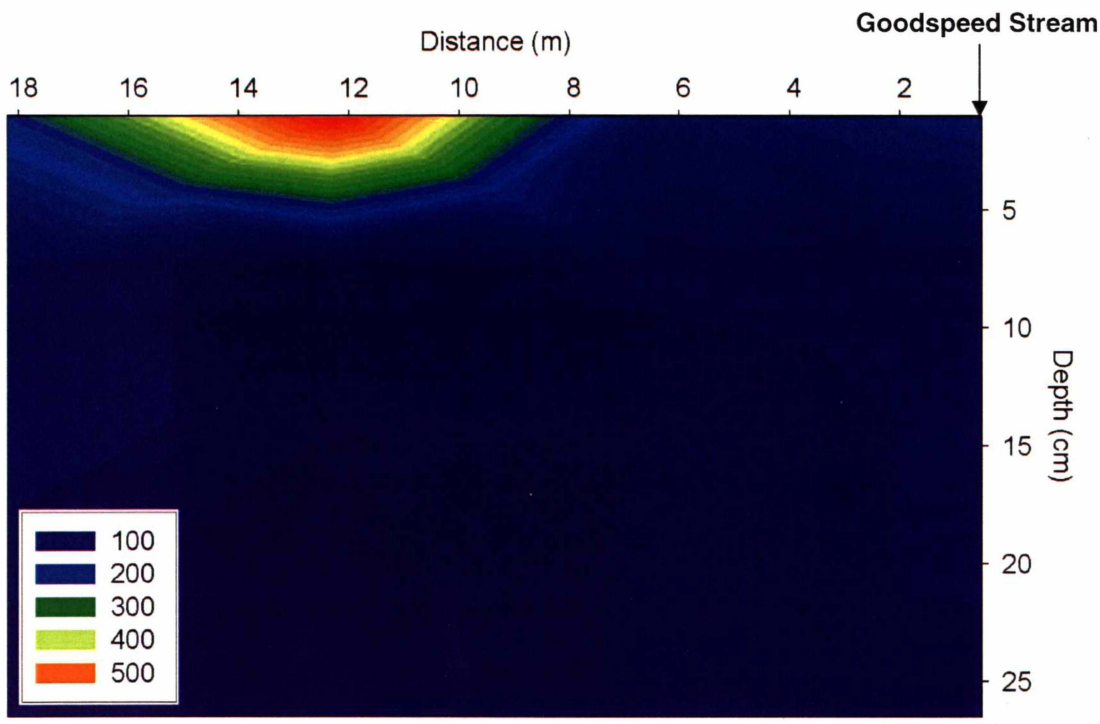

Figure 5.22. Soil electrical conductivity across the Goodspeed Lower Transect.

As observed for the Upper Transect, soil electrical conductivity was generally highest at the soil surface and decreased substantially below 5 cm depth. The precipitation of salts at or close to the soil surface indicates that the zone of maximum evaporation occurred between 0 and 5 cm depth, acting to concentrate salts within this zone. The decrease in electrical conductivity with depth again contrasts electrical conductivity data reported by Bockheim (1979, 1980, 1997).

The lower electrical conductivity values recorded across the Lower Transect may reflect a more frequent flushing of salts in soils at sites closer to Goodspeed Stream. The increased frequency of flushing may be explained by a frequency/magnitude relationship, whereby salts in soils at distances less than approximately 20 m from Goodspeed Stream, are flushed at more frequent intervals than those further out on the fan. Thus, salts in soils close to the stream may be flushed on an annual basis, giving rise to low electrical conductivity values, while soils of the outer fan may only be flushed every 100 years, enabling salts to accumulate over a greater time period.

5.2.3.3 Depth to ice cement

The depth to ice cement across the Goodspeed Lower Transect ranged from 3 – 38 cm, and generally increased with distance from the stream (Figure 5.23). Both maximum and minimum depths to ice cement occurred within the extended hyporheic zone (0 – 13.6 m). The shallow depth to ice cement reflects the climatic conditions when samples were taken. Air temperature was below 0 °C almost continually, and soil temperatures were decreasing, thus wetter soils froze solid near the soil surface.

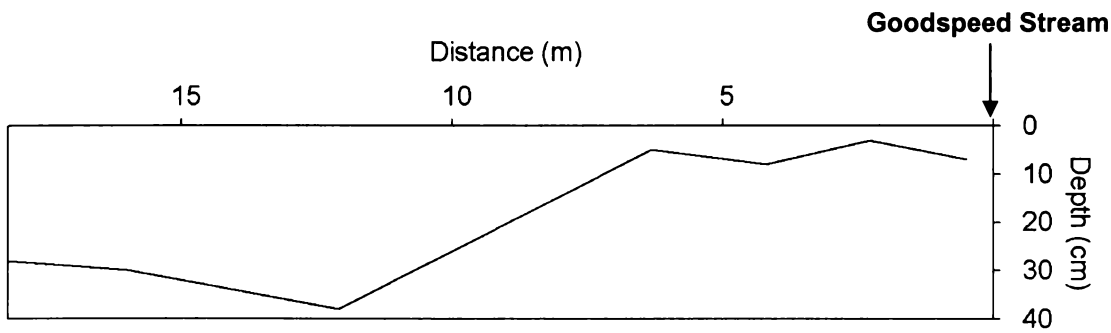

Figure 5.23. Depth to ice cement across the Goodspeed Lower Transect on 25 January 2005.

The mean soil gravimetric moisture content of all samples in each pit was correlated to depth to ice cement in the pit (Figure 5.24), and showed a similar degree of correlation to that observed for the Upper Transect. The correlation was not improved by segregating data into visibly moist and visibly dry categories. As

for the Upper Transect, the negative correlation indicated that lower soil moisture contents were related to greater depths to ice cement, and vice-versa.

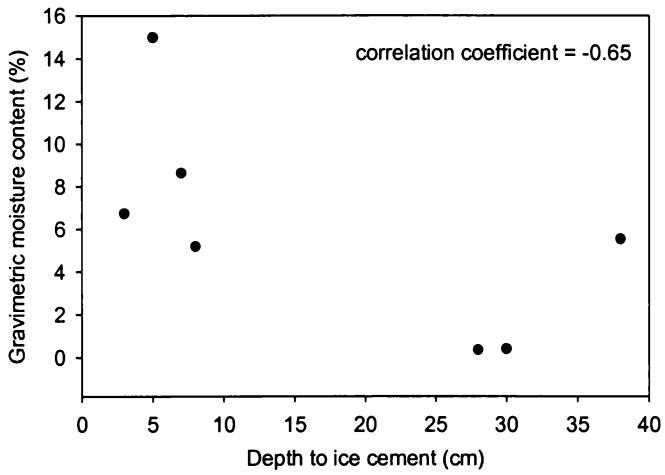

Figure 5.24. Correlation between mean soil gravimetric moisture content and depth to ice cement across the Goodspeed Lower Transect.

5.2.3.4 Relationship between soil moisture content and electrical conductivity

There was no correlation between soil gravimetric moisture content and soil electrical conductivity across the Goodspeed Lower Transect (Figure 5.25). Excluding data from outside the extended hyporheic zone increased the correlation slightly, though the fewer number of data points may reduce the validity of the correlation (Figure 5.26).

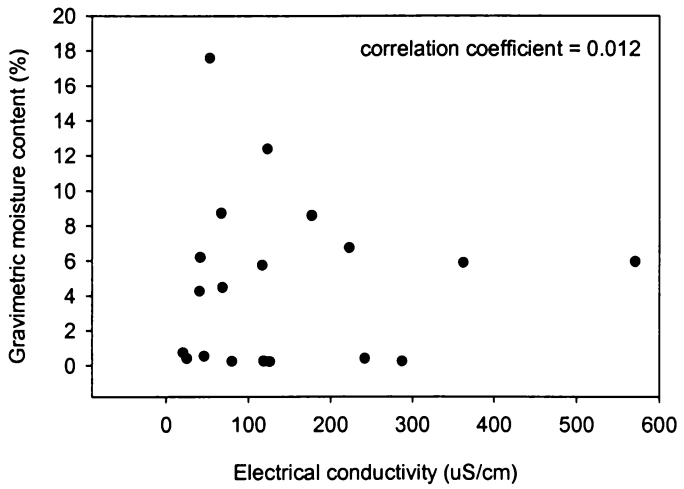

Figure 5.25. Correlation between soil gravimetric moisture content and soil electrical conductivity across the Goodspeed Lower Transect.

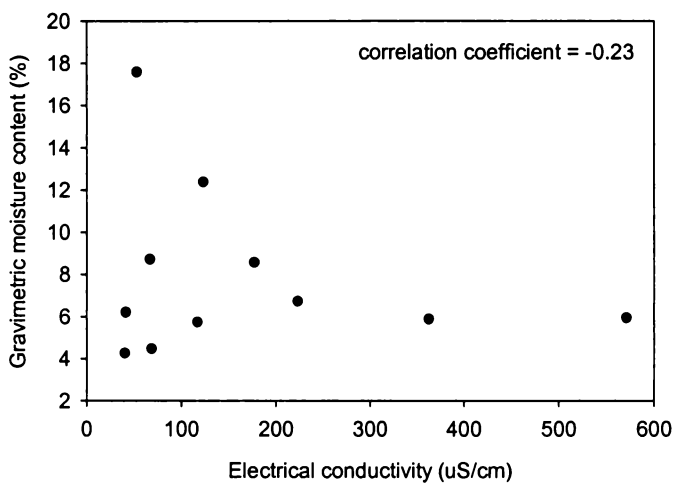

Figure 5.26. Correlation between soil gravimetric moisture content and soil electrical conductivity within the extended hyporheic zone (0 – 13.6 m) on the Goodspeed Lower Transect.

5.3 Goodspeed Stream hyporheic zone and adjacent banks

Samples from the Goodspeed Stream extended hyporheic zone and adjacent dry banks were taken from ten sites along Goodspeed Stream on 28 January 2005 (Section 3.2.4). The purpose of sampling the extended hyporheic zone and adjacent dry soils was to further investigate the relationship between soil moisture content and salt concentration, while also providing data relevant to characterisation of the Goodspeed Stream extended hyporheic zone.

5.3.1 Soil gravimetric moisture content and electrical conductivity

At sites along Goodspeed Stream, mean soil gravimetric moisture content ranged from 0.9 – 19.4% within the extended hyporheic zone, and from 0.2 – 0.5% on the dry stream banks immediately beyond the extended hyporheic zone (Table 5.3). The mean soil moisture content of the extended hyporheic zone was 9.5%, whereas the mean moisture content of the dry stream banks was 0.3%.

Soil electrical conductivity was generally higher on the dry stream banks, with the exceptions being sites GS 1 and GS 4 where electrical conductivity was greater in the extended hyporheic zone. Electrical conductivity tended to increase with distance from the terminal face of the Goodspeed Glacier. This may be indicative of salt translocation, with salts being mobilised from upstream sites, transported within the stream or hyporheic zone, and deposited at sites on the lower alluvial fan following evaporation of soil moisture.

Table 5.3. Mean soil moisture content and electrical conductivity at sites along Goodspeed Stream.

Site	Mean soil moisture content – ext. hypo. zone (%)	Mean soil moisture content – dry banks (%)	Mean soil electrical conductivity – ext. hypo. zone (µS/cm)	Mean soil electrical conductivity – dry banks (µS/cm)
GS 1*	3.1	0.2	742	235
GS 3*	5.1	0.3	478	558
GS 4*	0.9	0.2	1804	237
GS 5*	4.3	0.3	644	680
GS 6	19.4	0.2	130	169
GS 7	12.8	0.2	152	265
GS 8	14.2	0.2	148	335
GS 9	14.6	0.4	108	979
GS 10	8.4	0.2	103	254
GS 11	12.5	0.5	78	193
Mean	**9.5**	**0.3**	**439**	**391**

* denotes sites on the Goodspeed lower alluvial fan. All other sites are located upstream of the fan.

There was a weak correlation between soil gravimetric moisture content and soil electrical conductivity at sites along Goodspeed Stream (Figure 5.27). The correlation was substantially improved by excluding data from within the extended hyporheic zone (Figure 5.28).

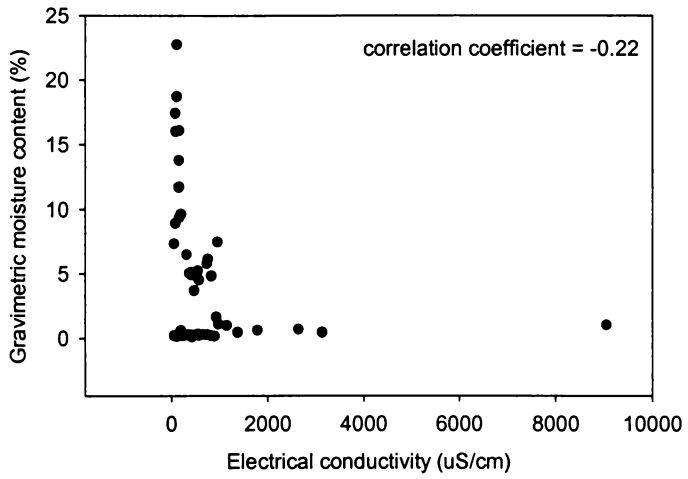

Figure 5.27. Correlation between soil gravimetric moisture content and soil electrical conductivity for sites along Goodspeed Stream.

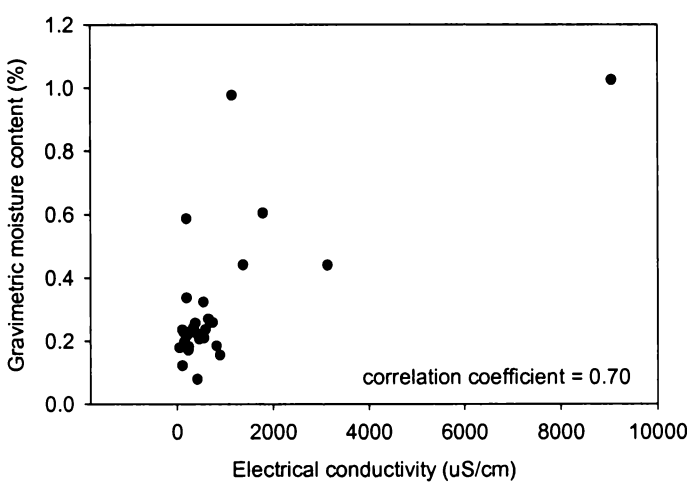

Figure 5.28. Correlation between soil gravimetric moisture content and soil electrical conductivity in visibly dry soils at sites along Goodspeed Stream.

The exclusion of data from the extended hyporheic zone resulted in a positive correlation, as observed for the Goodspeed Upper Transect. Furthermore, the negative correlation between moisture content and electrical conductivity in the extended hyporheic zone at sites along Goodspeed Stream (Figure 5.29) lends support to the suggestion that a threshold condition pertaining to soil moisture content exists.

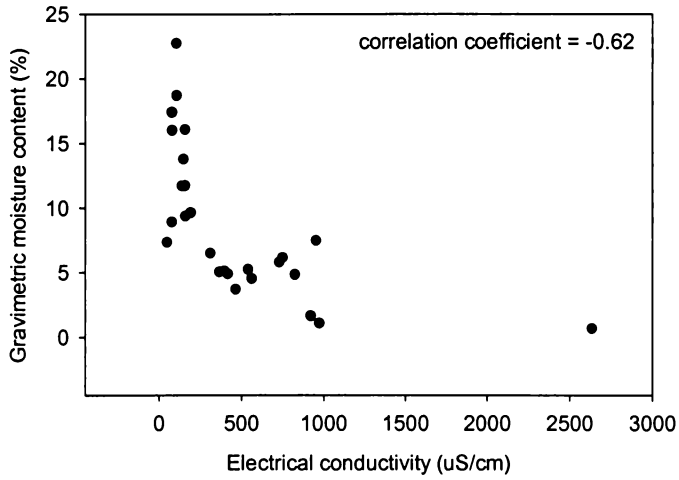

Figure 5.29. Correlation between soil gravimetric moisture content and soil electrical conductivity in soils of the extended hyporheic zone at sites along Goodspeed Stream.

5.4 Summary and conclusions

Soil gravimetric moisture content, soil electrical conductivity, particle size distribution, and depth to ice cement across the Goodspeed lower alluvial fan were measured. Data from sites upstream of the lower alluvial fan corroborated measurements of soil moisture content and electrical conductivity made within the lower alluvial fan. A pedotransfer function was used to estimate soil moisture potential across the fan; the likely fate of spills on the fan and in the extended hyporheic zone was considered based on the soil moisture potential and results from Claridge et al.'s (1997) spill migration experiment carried out on dry soils near Lake Vanda.

The following conclusions can be drawn from this chapter:

- Soil gravimetric moisture content on the Goodspeed lower alluvial fan was <1% in soils that were not supplied with moisture from Goodspeed Stream;

- In soils of the Goodspeed Stream extended hyporheic zone, gravimetric moisture contents were up to ~20%;

- Soil gravimetric moisture content generally decreased with distance from Goodspeed Stream, though subsurface moisture (θ_g up to 4%) was present 74 m from the stream within distal components of the hyporheic zone;

- Visibly moist soils probably had a minimum gravimetric moisture content of close to 2%;

- Soil electrical conductivity was highly variable, being dependent on the moisture and evaporation regime of individual sites, though generally being greatest at the soil surface;

- Soil gravimetric moisture content and electrical conductivity were positively correlated in visibly dry soils of the Upper Transect and at sites along Goodspeed Stream. The correlation was negative in soils of the extended hyporheic zone, thus suggesting there may be a threshold of soil moisture content above which salts are re-mobilised;

- Particle size distribution of the <2 mm fraction across the Goodspeed lower alluvial fan was dominated by medium sand (45%). Silt and clay comprised 2.3% of the <2 mm fraction;

- Depth to ice cement in early January ranged from 15 cm immediately adjacent to Goodspeed Stream, to 54 cm at the eastern-most extent of the Goodspeed lower alluvial fan;

- Small spills on the Goodspeed lower alluvial fan, outside the extended hyporheic zone, would be likely to be driven laterally, away from Goodspeed Stream, and to the soil surface due to gradients in soil moisture potential;

- Large spills would be likely to migrate downwards to the ice cement before progressing down-slope towards the Onyx River, which would transport contaminants to Lake Vanda;

- Contaminants spilled on the Goodspeed lower alluvial fan may be re-mobilised during periods of increased melt.

Chapter 6
Discussion and interpretation of stream vulnerability to human activities

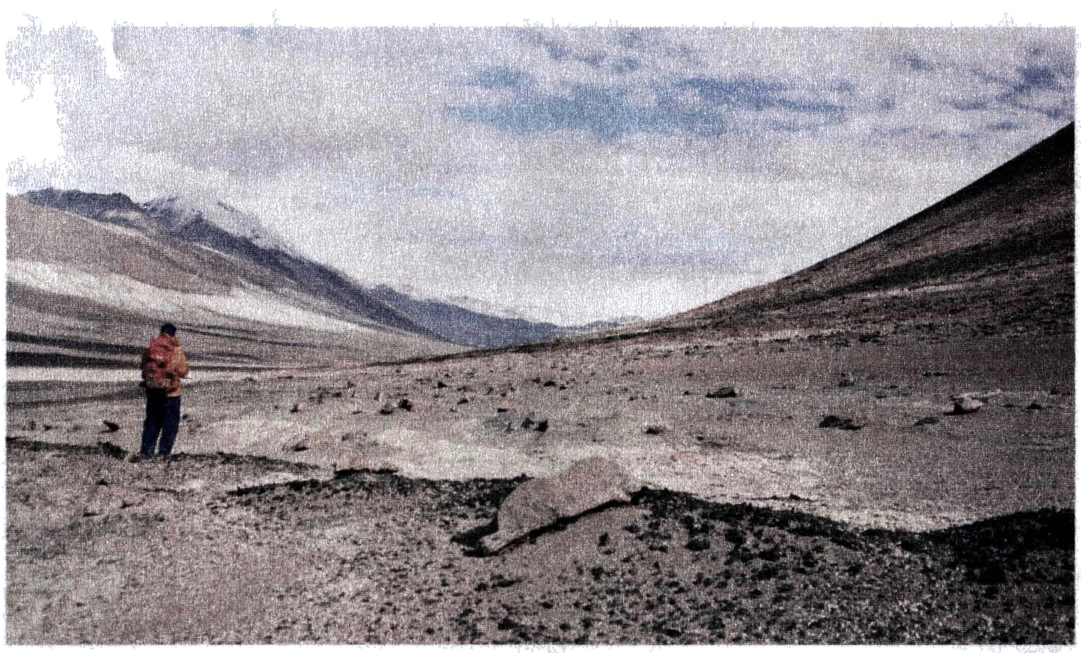

Chapter 6 Discussion and interpretation of stream vulnerability to human activities

6.1 Introduction

This chapter provides discussion of results presented in the previous two chapters. Particular emphasis is placed on the vulnerability of moistened areas to spills, though impacts of physical disturbance are also considered. Vulnerability zones, based on measurements and observations at the Goodspeed Stream site, are extrapolated to other ephemeral streams on alluvial fans in Wright Valley.

6.2 Vulnerability of areas adjacent to streams

Streams are vulnerable to spills that may occur in stream channels and hyporheic zones, as well as on the associated alluvial fans. The impacts of a spill within a stream channel or near-stream hyporheic zone are likely to be more immediate, whereas spills on alluvial fans may be perceived to have comparatively little likelihood of being incorporated into streams. This perception provides the premise for the delineation of vulnerability zones.

Lake Vanda is fed by summer meltwater from the alpine glaciers of lower Wright Valley, via the Onyx River (Turnbull et al., 1994; Isaac et al., 1996). Therefore, contaminants transported to the Onyx River are fed into Lake Vanda, which, having no outlet, means that contaminants not volatilised will remain in the lake, with few opportunities for self-remediation. Lake Vanda is an enclosed, thermo-haline, stratified lake in which bottom temperatures can be as high as 25.5 °C (Isaac et al., 1996).

An Environmental Code of Conduct has been developed for the McMurdo Dry Valleys; guidelines for behaviour within these areas are published in the

McMurdo Dry Valleys ASMA Manual (Antarctica New Zealand, 2004). This research builds on the existing guidelines, providing a scientific premise for further, more specific recommendations.

6.3 Vulnerability zones

Three vulnerability zones were identified for streams, hyporheic zones, and alluvial fans in Lower Wright Valley, based on data and observations from the Goodspeed lower alluvial fan. The vulnerability zones were derived primarily from consideration of the likelihood of contaminants spilled on these areas to be incorporated into streams within Wright Valley, though their vulnerability to physical disturbance was also considered.

The main human activities considered in defining the vulnerability zones were camping, unloading/re-loading helicopters, and walking. Camping presents a risk to the Dry Valleys environment through the re-fuelling of primuses and spilling of human wastes. The storage of fuels is an issue at larger field camps unable to rely solely on renewable energy sources. Camping also creates a higher intensity of soil disturbance than walking (Waterhouse, 2001), due to the repetition of activities within a small area. Unloading and re-loading of helicopters also presents a risk, again through spilling fuels and human wastes. The physical disturbances arising from walking to and from field sites has a more dispersed impact, with tracks often being distributed across large parts of the landscape.

While contamination from human wastes and fuel spills is likely to be a minor component of the overall impact of field activities (Waterhouse, 2001), the potential impacts on the broader environment, if a large spill did occur, would be considerable, particularly if the spill was in a zone where liquid water may flow.

6.3.1 Zone 1

Zone 1 includes stream channels and any other areas of surface water or areas where surface water is likely to be present at some stage during summer (Figure 6.1). Zone 1 includes the near-stream hyporheic zone, and is the most vulnerable to impacts from human activities. The risk of contamination to streams and surface waters is high, as anything spilled within streams or the near-stream hyporheic zone will rapidly be incorporated into the stream network, which ultimately flows into Lake Vanda.

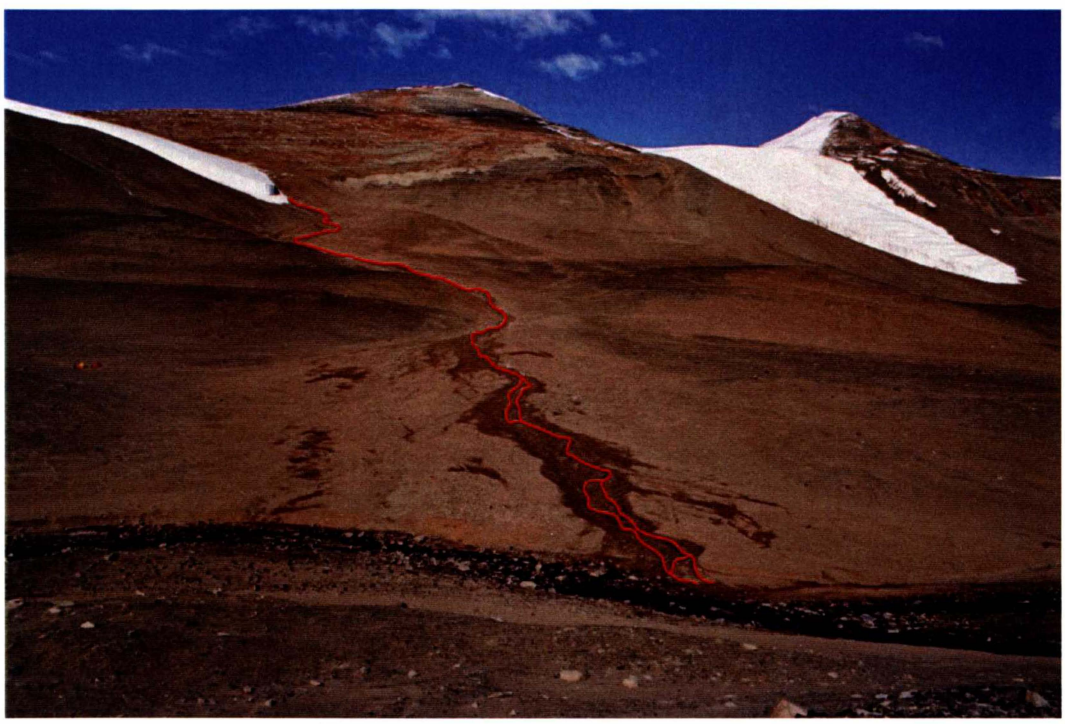

Figure 6.1. View of the Goodspeed lower alluvial fan, showing vulnerability Zone 1.

The short period (generally between 4 and 10 weeks annually) during which ephemeral streams flow means that there is limited time for disturbances to the stream bed or banks to be restored by natural fluvial processes. Fine sediments within the stream channels are particularly susceptible to boot imprints from walking. However, if the disturbance is only to the stream bed and not stream biota, it can be rapidly restored through the redistribution of fine material within the stream. Physical disturbance to the stream banks is likely to be more

permanent, as there are no active processes that can restore banks to their pre-disturbed state.

Antarctica New Zealand (2004) are aware of the impacts of physical disturbance on stream channels and banks, and advise that "stream crossings should be avoided, though if crossings are necessary, designated crossing points should be used." It is also advised to avoid walking in stream beds or close to stream sides so as to prevent disturbance to stream biota and stream banks (Antarctica New Zealand, 2004).

6.3.2 Zone 2

Zone 2 encompasses the extended hyporheic zone adjacent to streams (Figure 6.2). Zone 2 is moderately vulnerable to human activities, as water and solutes within the extended hyporheic zone are exchanged with the main stream channel (McKnight et al., 1999; Gooseff et al., 2003). Therefore, it is important to treat Zone 2 with the same care as Zone 1 due to the exchanges of water and solutes that take place.

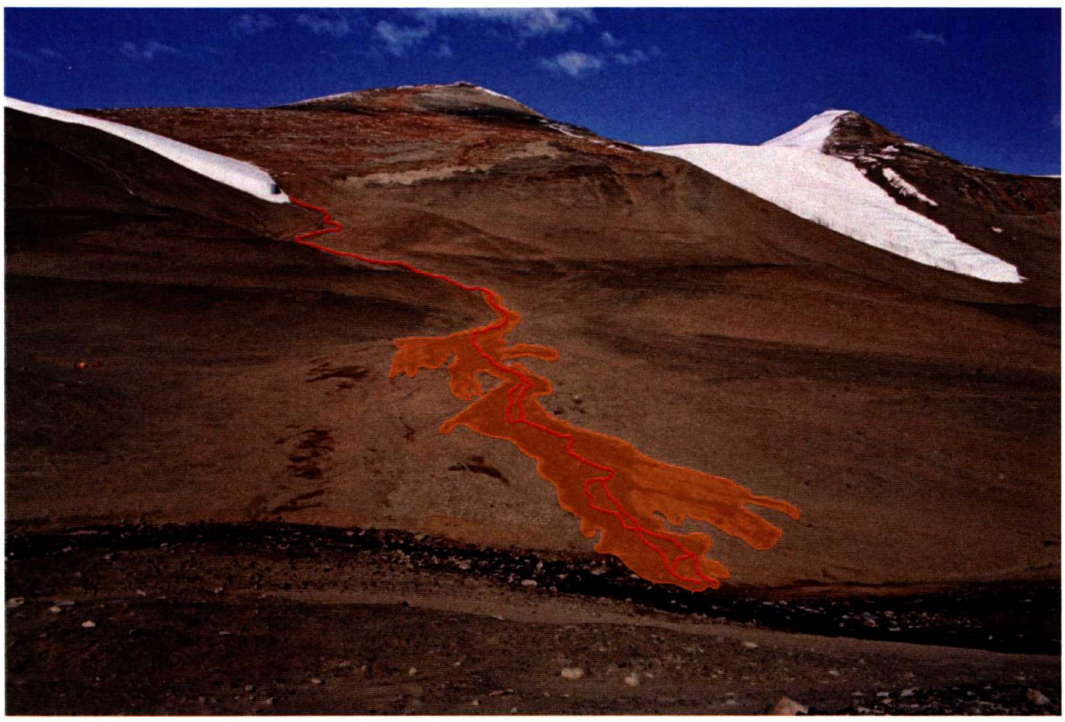

Figure 6.2. View of the Goodspeed lower alluvial fan, showing vulnerability Zones 1 (red) and 2 (orange).

Any spills within the extended hyporheic zone could potentially reach the stream through hyporheic exchange processes, and thus be transported to the Onyx River, and ultimately Lake Vanda. Furthermore, the presence of ice cement at depths between 15 and 40 cm below the soil surface within the extended hyporheic zone acts to reduce the depth of soil available for adsorption of spills.

While gradients in soil moisture potential and observations of salt precipitation at the edge of the extended hyporheic zone indicate that soil moisture is driven laterally, away from the stream, spills of large volumes (sufficient to cause saturated flow) are likely to move downwards to the ice cement before being translocated down-slope under gravity towards the Onyx River. The downwards movement of moisture is exacerbated by soil gravimetric moisture contents of up to 20% within the extended hyporheic zone.

Walking can cause disturbance to the extended hyporheic zone. As disturbances to the hyporheic zone are not readily repaired through fluvial action, the impacts of walking are likely to persist longer than those within the stream channel. Residual impacts of boot prints within extended hyporheic zones may be

exacerbated by freezing at the soil surface effectively preserving boot prints. However, freeze-thaw processes operating within the active layer may ameliorate surface disturbances early in the following summer season.

6.3.3 Zone 3

Zone 3 denotes soils of alluvial fans, and includes the distal components of the hyporheic zone (Figure 6.3). Alluvial fans are the least vulnerable of the three zones considered, as the presence of water is generally sparse. Mean soil gravimetric moisture content at all depths in soils of the Goodspeed lower alluvial fan (Upper Transect), excluding pits within the distal components of the hyporheic zone, was 0.6% in samples taken between 7 and 16 January 2005.

The relatively low soil moisture content dictates that, although ice cement was present at a depth of between 30 and 55 cm in January, small spills (where no saturated flow occurs) are unlikely to reach the ice cement, thus migration from the spill origin will be limited. The limited downwards migration of moisture is highlighted by gradients in soil moisture potential indicating that moisture will be drawn to the surface, with precipitation of salts at the soil surface providing a further reflection of this trend. Where larger spills (leading to saturated flow) occur, moisture will migrate downwards to the ice cement before flowing down-slope under gravity.

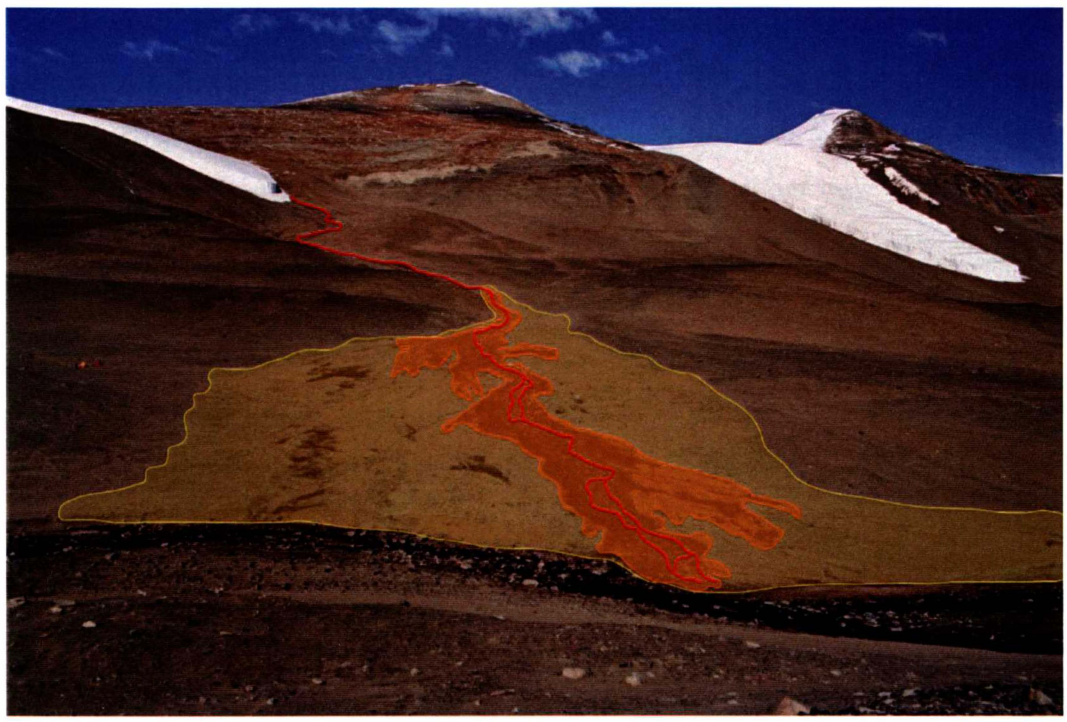

Figure 6.3. View of the Goodspeed lower alluvial fan, showing vulnerability Zones 1 (red), 2 (orange), and 3 (yellow).

Soil gravimetric moisture contents of up to 5% were recorded in the subsurface soil at a distance of 82 m across the Goodspeed Upper Transect (74 m from Goodspeed Stream); this was within a distal component of the hyporheic zone. Relatively high soil gravimetric moisture contents (≤ 7%) were also recorded in other distal hyporheic zones at 67 and 29 m across the Goodspeed Upper Transect. The relatively high moisture contents recorded in the distal hyporheic zones probably reflect subsurface flow paths beneath the fan. Consequently, the distal hyporheic zones have potential to develop into flowing channels during periods of increased melt, thus re-mobilising contaminants. Mobilisation of contaminants would again lead to their incorporation into the Onyx River, and ultimately Lake Vanda.

Even under climatic conditions similar to those recorded in January 2005, it would be possible for spills within distal components of the hyporheic zone to reach the Onyx River. Large spills (where saturated flow occurs) are likely to migrate downwards to the ice cement, before flowing down-slope towards the Onyx River. During periods of colder conditions, the depth to ice cement will be

smaller, thus further exacerbating the risk of down-slope transportation of contaminants along the surface of the ice cement. While meltwater production will generally be lesser during colder summers, contaminants will remain within the fan, thus being susceptible to transport in subsequent higher flow years.

The vulnerability of alluvial fans to physical disturbances such as walking is considered to be moderate. Tracks are readily formed in the soft fan surface, with wind being the primary agent of restoration. Freeze-thaw processes will not contribute to site remediation outside of the distal hyporheic zones due to the low soil moisture contents which are prevalent throughout the majority of alluvial fans in Wright Valley.

6.3.4 Permanence of the vulnerability zones

The nature of alluvial fans dictates that, at some stage, the active stream channel is likely to change its course, probably as a result of a high flow event. Consequently, the vulnerability zones defined will migrate across the fan accordingly. Therefore, in delineating the vulnerability zones for the Goodspeed lower alluvial fan (Figures 6.1, 6.2 and 6.3), it is important to note that the delineations are applicable to the current stream channel and hyporheic zones, as observed in January 2005.

6.4 Recommendations for risk mitigation in vulnerable zones

While some human activity is unavoidable in the identified vulnerable zones, the type(s) of activity, appropriate to the level of vulnerability, can be stipulated. Antarctica New Zealand (2004) advise that "campsites should be located as far away as practical from lakeshores, streambeds, ...to avoid damage or contamination. Do not camp in streambeds, even if they are dry."

For all three zones, this research indicates that camping should not be permitted, as camping presents a relatively high level of risk of spills and physical

disturbance. The main risks of spills associated with camping are the storage and pouring of fuels and waste liquids, and the unloading and re-loading of helicopters. The risks of spills can be readily mitigated through the use of a spill tray when pouring fuel, and by taking care when transferring waste liquids.

Walking is a secondary impact resulting from camping, though the long-term risk posed to the area is low. Alluvial fans are relatively dynamic parts of the Dry Valley landscape, and are therefore likely to recover relatively rapidly from disturbances created by walking. The impacts from walking can be minimised by "rock-hopping" across streams if they must be crossed, and using designated tracks through areas frequented by members of a field party (Antarctica New Zealand, 2004).

Within both Zones 1 and 2, no activities other than walking through the zones should occur. This includes no eating, drinking or transferral of liquids. Within Zone 3, eating and drinking is permissible, though care should be taken. Where possible, toileting should not take place within Zone 3.

6.5 Identification of vulnerable areas when stream flow not evident

For field parties arriving early or late in the season when there is no obvious stream flow, it is still important to recognise the vulnerable areas, as spills within any of the vulnerable zones will, ultimately, be mobilised by stream flow at some stage.

6.5.1 Stream channels (Zone 1)

Stream channels are generally obvious, with some incision common (Figure 6.4). Stream beds may also be armoured, having a layer of larger clasts lining the stream channel.

Figure 6.4. Incised stream channel, Lower Wright Valley.

6.5.2 Extended hyporheic zones (Zone 2)

Identification of extended hyporheic zones is simple if surface water is present, as extended hyporheic zones develop adjacent to stream channels and are evident as dark bands of moistened soil (Figure 6.5). Recognition of the lateral extent of extended hyporheic zones is commonly aided by the presence of a band of salts which have precipitated at the soil surface, either on a stream bank or just beyond (Figure 6.6). However, if there is no evidence of moistened soil or salt precipitation near the stream channel, the extended hyporheic zone should be considered to extend up to 15 m either side of the stream channel.

Figure 6.5. Moistened soil adjacent to a stream channel, indicative of an extended hyporheic zone. (Photo: M.R. Balks)

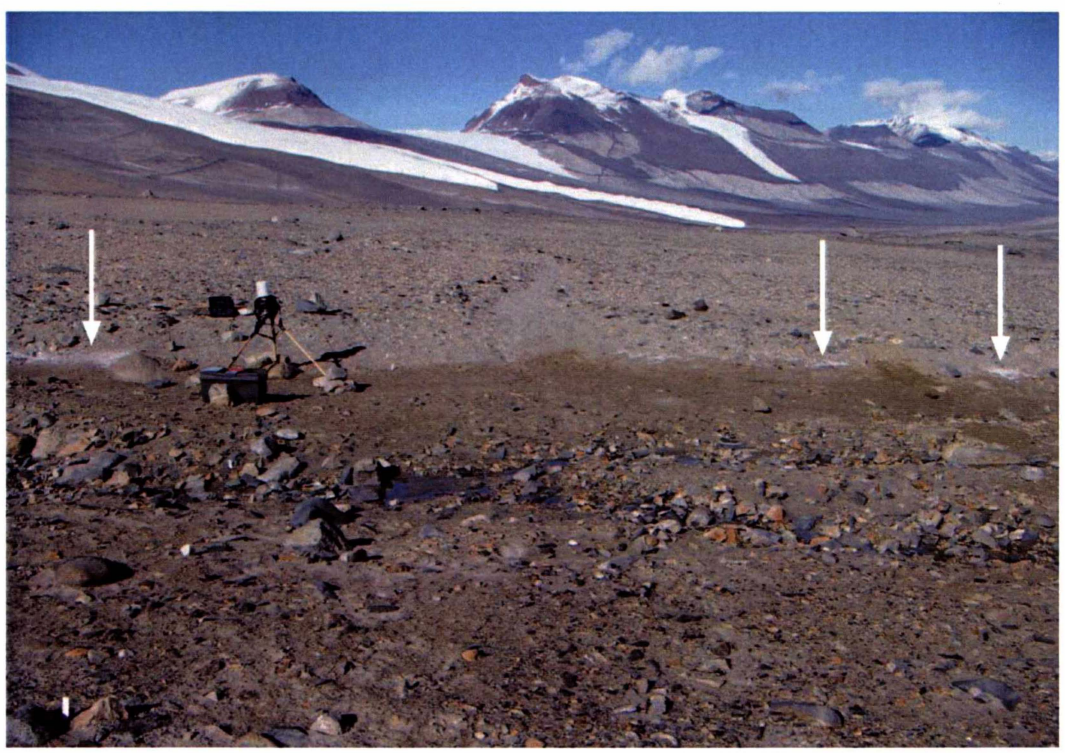

Figure 6.6. Salt precipitation at the edge of the Goodspeed Stream extended hyporheic zone.

6.5.3 Alluvial fans (Zone 3)

An alluvial fan is a fan-shaped sediment deposit (Figure 6.7). Alluvial fans are typically formed in areas where streams flow from faster flowing reaches out onto an area with a lower gradient. The decrease in stream power associated with the decrease in stream gradient causes the bed load to be deposited, forming a conical, fan-shaped deposit. Multiple stream channels occur on alluvial fans, and the "main" stream channel may migrate across the fan relatively frequently.

Figure 6.7. Alluvial fan on the lower slopes of the Olympus Range, Wright Valley.

6.6 Other streams – Lower Wright Valley

The vulnerability zones were developed as a result of the study of Goodspeed Stream, its hyporheic zones, and soils of the Goodspeed lower alluvial fan, and can be broadly applied to other ephemeral streams and alluvial fans in Lower Wright Valley. The vulnerability ratings (Zones 1, 2 and 3) were generalised in order to be transferable to streams sourced from other glaciers in Wright Valley.

6.6.1 Hart Glacier (Figure 6.8)

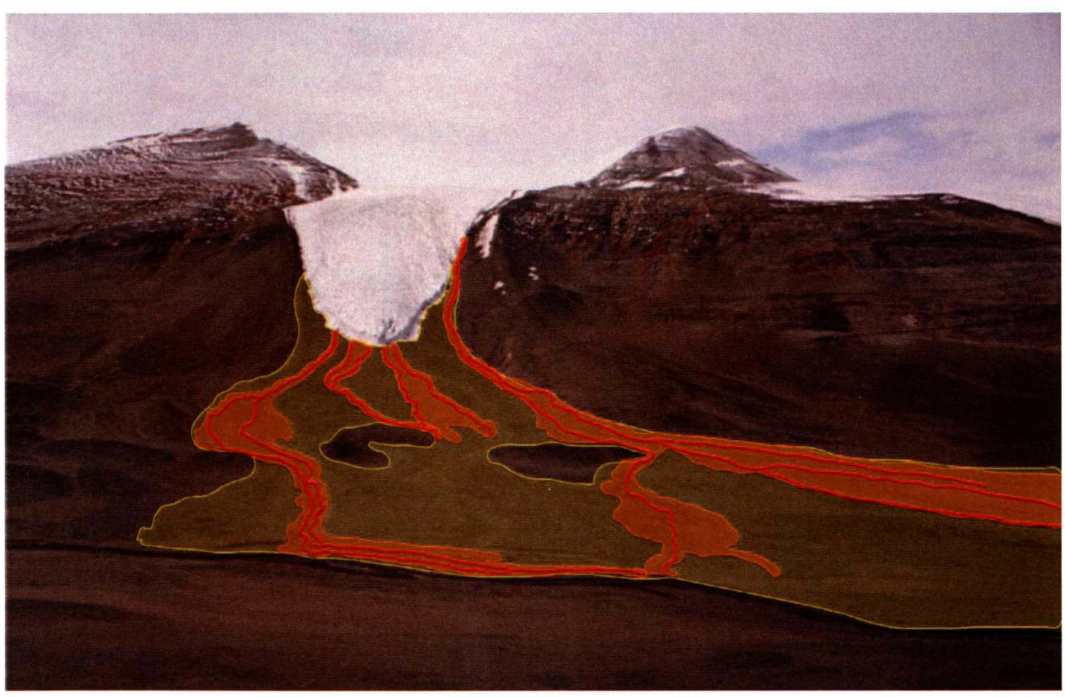

Figure 6.8. View of the Hart Glacier and alluvial fan, showing vulnerability Zones 1 (red), 2 (orange), and 3 (yellow). The non-shaded areas within the fan represent moraines or other raised surface features, and have minimal vulnerability to human impacts.

6.6.2 Merserve Glacier (Figure 6.9)

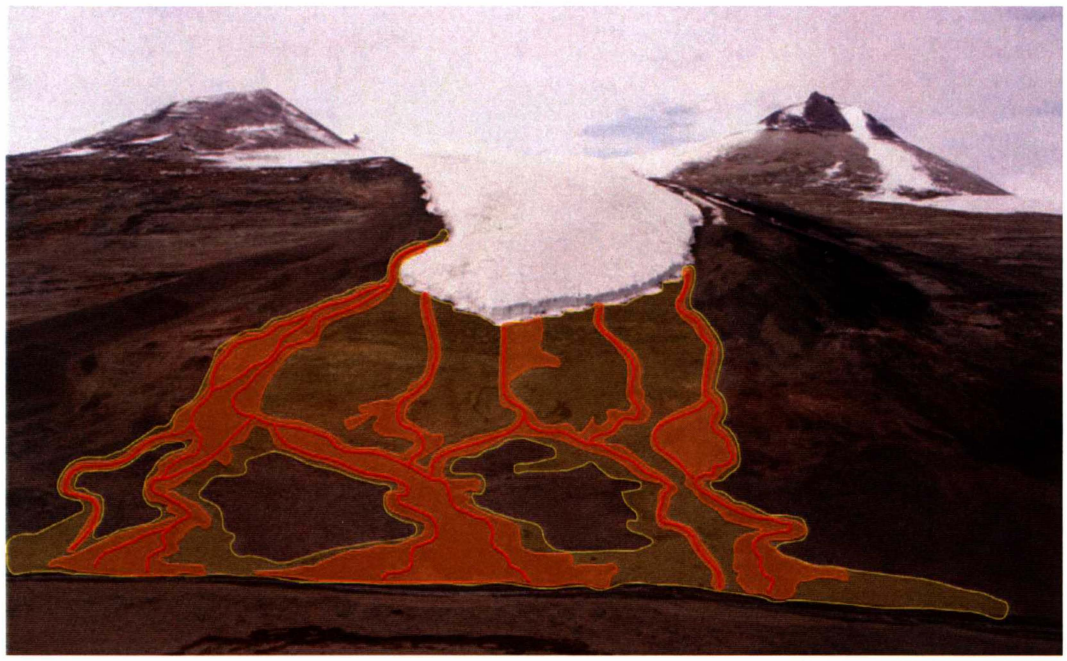

Figure 6.9. View of the Merserve Glacier and alluvial fan, showing vulnerability Zones 1 (red), 2 (orange), and 3 (yellow). The non-shaded areas within the fan represent moraines or other raised surface features, and have minimal vulnerability to human impacts.

6.6.3 Bartley Glacier (Figure 6.10)

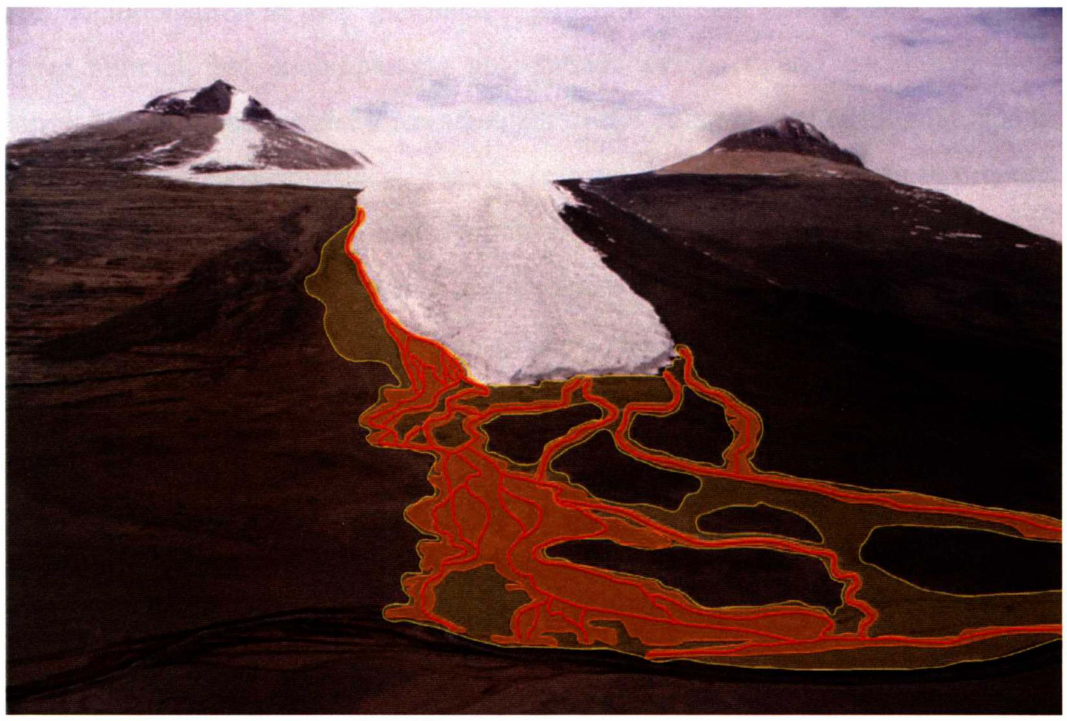

Figure 6.10. View of the Bartley Glacier and alluvial fan, showing vulnerability Zones 1 (red), 2 (orange), and 3 (yellow). The non-shaded areas within the fan represent moraines or other raised surface features, and have minimal vulnerability to human impacts.

6.7 Further research

The documentation of soil gravimetric moisture content across the Goodspeed lower alluvial fan, encompassing near-stream, extended and distal hyporheic zones, has provided a basis for assessment of the vulnerability of alluvial fans to spills and physical disturbance. Further research could be undertaken in order to characterise the time-scale over which exchanges occur between Goodspeed Stream and the distal components of the hyporheic zone, using an isotopic tracer technique similar to that used by Gooseff et al. (2003). This method could also be used to estimate the potential storage area in distal components of the hyporheic zone and in subsurface flow paths beneath the Goodspeed lower alluvial fan.

A similar study could be carried out in order to corroborate results from this study. Data could be obtained from a larger ephemeral stream with a broader lower alluvial fan, such as that associated with Bartley Stream. An assessment of the extent to which stream biota such as algae and mosses, observed within Bartley Stream, are found relative to soil moisture content could be made. Microbiological analyses could also be undertaken. Data could then be applied to both the Wright and Taylor Valleys, with a more comprehensive map of vulnerability to spills, physical disturbance, and biota being produced.

There is also an apparent paucity of information pertaining to the relationship between stream flow, air temperature and solar radiation. Radiation balance studies could be combined with regular, automated stream flow measurements and air mass balances in order to better relate climatic parameters such as solar radiation and air temperature to stream flow.

6.8 Summary and conclusions

The assessment of the vulnerability of streams, hyporheic zones and associated fans to impacts from human activities in Lower Wright Valley suggests that spills on alluvial fans have a relatively high risk of contaminating Lake Vanda. However, this study provides no indication of the time-scale over which contamination may occur; it is primarily an assessment of the possibility of contamination occurring.

The following are the main conclusions from this study:

- Stream flow in Goodspeed Stream ranged from 0 ℓ s^{-1} to approximately 2.5 ℓ s^{-1} during the period 4 – 24 January 2005. Stream flow in Goodspeed Stream ceased, probably for the season, on 24 January 2005;

- Decreases in solar radiation and air temperature appeared to cause the cessation of seasonal flow in Goodspeed Stream, though based on twice daily measurements of stream flow no strong relationships between air temperature, solar radiation and stream flow were obtained;

- The mean width of the Goodspeed Stream near-stream hyporheic zone at the Goodspeed Stream daily monitoring site was 0.44 m over the period 4 – 22 January 2005. The extended hyporheic zone had a mean width of 8 m (including Goodspeed Stream and the near-stream hyporheic zone) at the Goodspeed Stream daily monitoring site during the period 4 – 30 January 2005. The maximum lateral extent of the Goodspeed Stream extended hyporheic zone was 20.5 m at a site on the Goodspeed lower alluvial fan;

- Distal components of the Goodspeed Stream hyporheic zone were recorded 21, 59 and 74 m from the right branch of Goodspeed Stream (29, 67 and 82 m along the Goodspeed Upper Transect);

- Soil gravimetric moisture content within distal components of the Goodspeed Stream hyporheic zone was up to 7%. The moisture observed at these sites was likely to have been the result of moisture moving down the fan, beneath the ground surface;

- The gravimetric soil moisture content within the Goodspeed Stream extended hyporheic zone was up to 20%;

- Mean soil gravimetric moisture content at all depths within visibly dry soils of the Goodspeed lower alluvial fan was 0.6%;

- Ice cement was present beneath the Goodspeed lower alluvial fan at depths between 30 and 55 cm over the period 7 – 16 January 2005;

- Salts were concentrated on the western-most edge of the Goodspeed extended hyporheic zone and on raised bar features on the lower alluvial fan, reflecting the movement and evaporation of soil moisture. The correlation between soil gravimetric moisture content and electrical conductivity was positive for visibly dry soils and negative for soils within the extended hyporheic zone suggesting there may be a threshold of soil moisture content above which salts are re-mobilised;

- Small spills on alluvial fans are likely to be driven laterally, away from streams due to gradients in soil moisture potential. Large spills on alluvial fans have a relatively high risk of contamination to streams, as they would migrate downwards to the ice cement before being transported down-slope towards the Onyx River under gravity;

- Three vulnerability zones were developed based on data and observations from the Goodspeed lower alluvial fan, and have been extrapolated to streams sourced from three other glaciers in Wright Valley, based on geomorphic interpretation.

References

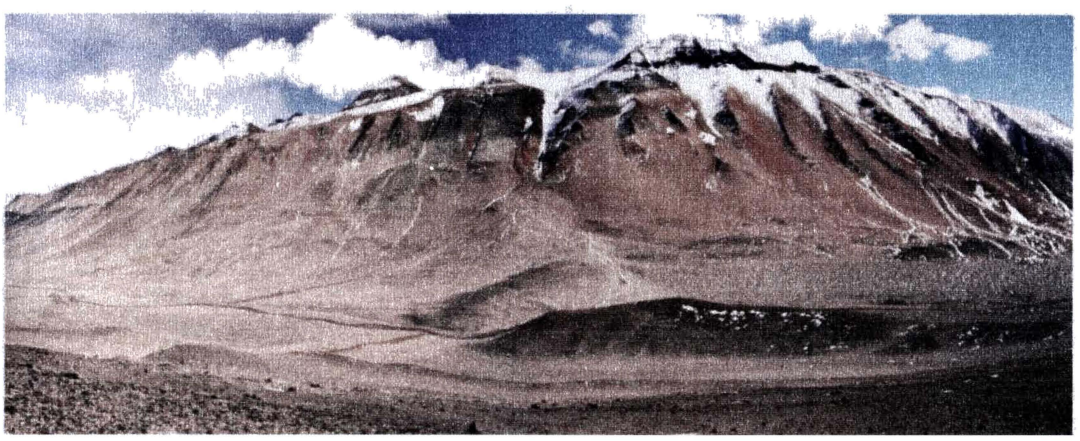

References

Anderton, P.W. and Fenwick, J.K., 1976. Dry Valleys, Antarctica 1973 - 74. Hydrological Research: Annual Report No. 37 (interim report), Ministry of Works and Development, Wellington 42 pp.

Antarctica New Zealand, 2004. McMurdo Dry Valleys ASMA Manual: 2004-2005. Antarctica New Zealand, Christchurch, NZ, 58 pp.

Balks, M.R., Paetzold, R.F., Kimble, J.M., Aislabie, J.M. and Campbell, I.B., 2002. Effects of hydrocarbon spills on the temperature and moisture regimes of Cryosols in the Ross Sea region. Antarctic Science, 14(4): 319-326.

Benninghoff, W.S., 1987. The Antarctic Ecosystem. Environment International, 13: 9-14.

Blakemore, L.C., Searle, P.L. and Daly, B.K., 1987. Methods for Chemical Analysis of Soils. NZ Soil Bureau Scientific Report 80. NZ Soil Bureau, Lower Hutt.

Bockheim, J.G., 1979. Relative age and origin of soils in eastern Wright Valley, Antarctica. Soil Science, 128(3): 142-152.

Bockheim, J.G., 1980. Properties and classification of some desert soils in coarse-textured glacial drift in the Arctic and Antarctic. Geoderma, 24: 45-69.

Bockheim, J.G., 1990. Soil development rates in the Transantarctic Mountains. Geoderma, 47: 59-77.

Bockheim, J.G., 1997a. Properties and classification of cold desert soils from Antarctica. Soil Science Society of America Journal, 61: 224-231.

Bockheim, J.G., 1997b. Properties and classification of cold desert soils from Antarctica. Soil Science Society of America Journal, 61(1): 224-231.

Bockheim, J.G., 2002. Landform and soil development in the McMurdo Dry Valleys, Antarctica: a regional synthesis. Arctic, Antarctic, and Alpine Research, 34(3): 308-317.

Bouma, J., 1989. Using soil survey data for quantitative land evaluation. Advances in Soil Science, 9: 177-213.

Bromley, A.M., 1985. Weather observations, Wright Valley, Antarctica. New Zealand Meteorological Service, Wellington, NZ, 37 pp.

Bull, C., 1966. Climatological observations in ice-free areas of Southern Victoria Land, Antarctica. In: M.J. Rubin (Editor), Studies in Antarctic meteorology. Antarctic Research Series Volume 9. American Geophysical Union, Washington, D.C., pp. 177-194.

Campbell, D.I., MacCulloch, R.J.L. and Campbell, I.B., 1997a. Thermal regimes of some soils in the McMurdo Sound region, Antarctica. In: W.B. Lyons, C. Howard-Williams and I. Hawes (Editors), Ecosystem Processes in Antarctic Ice-Free Landscapes. A.A. Balkema, Rotterdam, pp. 45-55.

Campbell, I.B., 2003. Soil characteristics at a long-term ecological research site in Taylor Valley, Antarctica. Australian Journal of Soil Research, 41: 351-364.

Campbell, I.B., Balks, M.R. and Claridge, G.G.C., 1993. A simple visual technique for estimating the impact of fieldwork on the terrestrial environment in ice-free areas of Antarctica. Polar Record, 29(171): 321-328.

Campbell, I.B. and Claridge, G.G.C., 1969. A classification of frigic soils - the zonal soils of the Antarctic continent. Soil Science, 107(2): 75-85.

Campbell, I.B. and Claridge, G.G.C., 1975. Morphology and age relationships of Antarctic Soils. In: R.P. Suggate and M.M. Cresswell (Editors), Quaternary Studies. The Royal Society of New Zealand, Wellington, pp. 83-88.

Campbell, I.B. and Claridge, G.G.C., 1982. The influence of moisture on the development of soils of the cold deserts of Antarctica. Geoderma, 28: 221-238.

Campbell, I.B. and Claridge, G.G.C., 1987. Antarctica: Soils, weathering, processes and environment. Developments in Soil Science 16. Elsevier Science Publishers, The Netherlands.

Campbell, I.B., Claridge, G.G.C. and Balks, M.R., 1998a. Short- and long-term impacts of human disturbances on snow-free surfaces in Antarctica. Polar Record, 34(188): 15-24.

Campbell, I.B., Claridge, G.G.C., Balks, M.R. and Campbell, D.I., 1997b. Moisture content in soils of the McMurdo Sound and Dry Valley region of Antarctica. In: W.B. Lyons, C. Howard-Williams and I. Hawes (Editors), Ecosystem Processes in Antarctic Ice-Free Landscapes. A.A. Balkema, Rotterdam, pp. 61-76.

Campbell, I.B., Claridge, G.G.C., Campbell, D.I. and Balks, M.R., 1998b. The soil environment of the McMurdo Dry Valleys, Antarctica. In: J.C. Priscu (Editor), Ecosystem Dynamics in a Polar Desert. Antarctic Research Series, Volume 72. American Geophysical Union, Washington, D.C., pp. 297-322.

Chinn, T.J., 1975. Hydrological Research Report, Dry Valleys, Antarctica 1974 - 75 (Draft Only), Ministry of Works and Development, Christchurch 53 pp.

Chinn, T.J., 1980. Hydrological Research Report, Dry Valleys, Antarctica 1970 - 71. (A revised reprint of Ross Dependency Research Committee Report

No. 639) WS 290 (interim report), Ministry of Works and Development, Christchurch 44 pp.

Chinn, T.J., 1981a. Hydrological Research Report, Dry Valleys, Antarctica 1975 - 76. Report No. WS 473, Ministry of Works and Development, Christchurch 74 pp.

Chinn, T.J., 1983. Hydrology and Glaciology, Dry Valleys, Antarctica. Annual Report for 1976 - 77 and 1977 - 78. Report No. WS 531, Ministry of Works and Development, Christchurch 49 pp.

Chinn, T.J. and Cumming, R.J., 1983. Hydrology and Glaciology, Dry Valleys, Antarctica. Annual Report for 1978 - 79. Report No. WS 810, Ministry of Works and Development, Christchurch 137 pp.

Chinn, T.J. and Dickson, R.J.H., 1986. Hydrology and Glaciology, Dry Valleys, Antarctica: Annual Report for 1982 - 83. Report No. WS 1188, Ministry of Works and Development, Christchurch 95 pp.

Chinn, T.J. and Maze, I., 1983. Hydrology and Glaciology, Dry Valleys, Antarctica. Annual Report for 1980 - 81. Report No. WS 900, Ministry of Works and Development, Christchurch 64 pp.

Chinn, T.J. and Oliver, A.K.C., 1983. Hydrology and Glaciology, Dry Valleys, Antarctica. Annual Report for 1979 - 80. Report No. WS 808, Ministry of Works and Development, Christchurch 49 pp.

Chinn, T.J.H., 1981b. Hydrology and climate in the Ross Sea area. Journal of the Royal Society of New Zealand, 11(4): 373-386.

Chinn, T.J.H. and Woods, A.D.H., 1984. Hydrology and Glaciology, Dry Valleys, Antarctica: Annual Report for 1981 - 82. Report No. WS 1017, Ministry of Works and Development, Christchurch 63 pp.

Claridge, G.G.C., 1965. The clay mineralogy and chemistry of some soils from the Ross Dependency, Antarctica. New Zealand Journal of Geology and Geophysics, 8: 186-220.

Claridge, G.G.C. and Campbell, I.B., 1977. The salts in Antarctic soils, their distribution and relationship to soil processes. Soil Science, 123(6): 377-384.

Claridge, G.G.C., Campbell, I.B. and Balks, M.R., 1997. Ionic migration in soils of the Dry Valley region. In: W.B. Lyons, C. Howard-Williams and I. Hawes (Editors), Ecosystem Processes in Antarctic Ice-Free Landscapes. A.A. Balkema, Rotterdam, pp. 137-143.

Clow, G.D., McKay, C.P., Simmons, G.M., (Jr.) and Wharton, R.A., (Jr.), 1988. Climatological observations and predicted sublimation rates at Lake Hoare, Antarctica. Journal of Climate, 1(7): 715-728.

Conovitz, P.A., McKnight, D.M., MacDonald, L.H., Fountain, A.G. and House, H.R., 1998. Hydrologic processes influencing streamflow variation in Fryxell Basin, Antarctica. In: J.C. Priscu (Editor), Ecosystem dynamics in a polar desert: The McMurdo Dry Valleys, Antarctica. Antarctic Research Series, Volume 72. American Geophysical Union, Washington, D.C., pp. 93-108.

Dana, G.L., Wharton, R.A., (Jr.) and Dubayah, R., 1998. Solar radiation in the McMurdo Dry Valleys, Antarctica. In: J.C. Priscu (Editor), Ecosystem dynamics in a polar desert: The McMurdo Dry Valleys, Antarctica. Antarctic Research Series, Volume 72. American Geophysical Union, Washington, D.C., pp. 39-64.

Denton, G.H., Sugden, D.E., Marchant, D.R., Hall, B.L. and Wilch, T.I., 1993. East Antarctic sensitivity to Pliocene climatic change from a Dry Valleys perspective. Geografiska Annaler, 75A(4): 155-204.

Doran, P.T., McKay, C.P., Clow, G.D., Dana, G.L., Fountain, A.G., Nylen, T. and Lyons, W.B., 2002. Valley floor climate observations from the McMurdo dry valleys, Antarctica, 1986-2000. Journal of Geophysical Research-Atmospheres, 107(D24).

Fenwick, J.K. and Anderton, P.W., 1975. Dry Valleys, Antarctica 1972 - 73. Hydrological Research: Annual Report No. 34 (interim report), Ministry of Works and Development, Wellington 37 pp.

Fountain, A.G., Dana, G.L., Lewis, K.J., Vaughn, B.H. and McKnight, D.M., 1998. Glaciers of the McMurdo Dry Valleys, Southern Victoria Land, Antarctica. In: J.C. Priscu (Editor), Ecosystem dynamics in a polar desert: The McMurdo Dry Valleys, Antarctica. Antarctic Research Series, Volume 72. American Geophysical Union, Washington, D.C., pp. 65-75.

Fountain, A.G., Lyons, W.B., Burkins, M.B., Dana, G.L., Doran, P.T., Lewis, K.J., McKnight, D.M., Moorhead, D.L., Parsons, A.N., Priscu, J.C., Wall, D.H., Wharton, R.A., (Jr.) and Virginia, R.A., 1999. Physical controls on the Taylor Valley ecosystem, Antarctica. BioScience, 49(12): 961-971.

Genthon, C., Krinner, G. and Deque, M., 1998. Intra-annual variability of Antarctic precipitation from weather forecasts and high-resolution climate models. Annals of Glaciology, 27: 488-494.

Gooseff, M.N., McKnight, D.M., Runkel, R.L. and Duff, J.H., 2004. Denitrification and hydrologic transient storage in a glacial meltwater stream, McMurdo Dry Valleys, Antarctica. Limnology and Oceanography, 49(5): 1884-1895.

Gooseff, M.N., McKnight, D.M., Runkel, R.L. and Vaughn, B.H., 2003. Determining long time-scale hyporheic zone flow paths in Antarctic streams. Hydrological Processes, 17(9): 1691-1710.

Guglielmin, M., Balks, M. and Paetzold, R., 2003. Towards an Antarctic active layer and permafrost monitoring network. In: Phillips, Springman and Arenson (Editors), Permafrost. Swets and Zeitlinger, Lisse, pp. 337-341.

Hall, B.L. and Denton, G.H., 2005. Surficial geology and geomorphology of eastern and central Wright Valley, Antarctica. Geomorphology, 64(1-2): 25-65.

Hall, B.L., Denton, G.H., Lux, D.R. and Bockheim, J.G., 1993. Late Tertiary Antarctic paleoclimate and ice-sheet dynamics inferred from surficial deposits in Wright Valley. Geografiska Annaler, 75 A(4): 239-267.

Hillel, D., 2004. Introduction to environmental soil physics. Elsevier Academic Press, San Diego, 494 pp.

House, H.R., McKnight, D.M. and von Guerard, P., 1995. The influence of stream channel characteristics on stream flow and annual water budgets for lakes in Taylor Valley. Antarctic Journal of the United States, 30: 284-287.

Isaac, M.J., Chinn, T.J., Edbrooke, S.W. and Forsyth, P.J., 1996. Geology of the Olympus Range area, southern Victoria Land, Antarctica, scale 1:50 000. Institute of Geological and Nuclear Sciences geological map 20. Institute of Geological and Nuclear Sciences Limited, Lower Hutt, New Zealand, 1 sheet + 60 pp.

Kennedy, A.D., 1993. Water as a limiting factor in the Antarctic terrestrial environment: A biogeographical synthesis. Arctic and Alpine Research, 25(4): 308-315.

Keys, J.R., 1980. Air temperature, wind, precipitation and atmospheric humidity in the McMurdo Region. Publication No. 17, (Antarctic Data Series No. 9). Geology Department, Victoria University of Wellington, Wellington, NZ, 57 pp.

Keys, J.R. and Williams, K., 1981. Origin of crystalline, cold desert salts in the McMurdo region, Antarctica. Geochimica Et Cosmochimica Acta, 45: 2299-2309.

Lewis, K.J., Fountain, A.G. and Dana, G.L., 1999. How important is terminus cliff melt?: A study of the Canada Glacier terminus, Taylor Valley, Antarctica. Global and Planetary Change, 22: 105-115.

Lyons, W.B., Bartek, L.R., Mayewski, P.A. and Doran, P.T., 1997a. Climate history of the McMurdo Dry Valleys since the last glacial maximum: A synthesis. In: W.B. Lyons, C. Howard-Williams and I. Hawes (Editors), Ecosystem Processes in Antarctic Ice-Free Landscapes. A.A. Balkema, Rotterdam, pp. 15-22.

Lyons, W.B., Welch, K.A., Nezat, C.A., Crick, K., Toxey, J.K., Mastrine, J.A. and McKnight, D.M., 1997b. Chemical weathering rates and reactions in the Lake Fryxell Basin, Taylor Valley: Comparison to temperate river basins. In: W.B. Lyons, C. Howard-Williams and I. Hawes (Editors), Ecosystem Processes in Antarctic Ice-Free Landscapes. A.A. Balkema, Rotterdam, pp. 147-154.

Marchant, D.R. and Denton, G.H., 1996. Miocene and Pliocene paleoclimate of the Dry Valleys region, Southern Victoria land: A geomorphological approach. Marine Micropaleontology, 27(1-4): 253-271.

Marchant, D.R., Denton, G.H., Sugden, D.E. and Swisher, C.C., III., 1993. Miocene glacial stratigraphy and landscape evolution of the western Asgard Range, Antarctica. Geografiska Annaler, 75A(4): 303-330.

McBratney, A.B., Minasny, B., Cattle, S.R. and Vervoort, R.W., 2002. From pedotransfer functions to soil inference systems. Geoderma, 109: 41-73.

McCraw, J.D., 1967. Soils of Taylor Dry Valley, Victoria Land, Antarctica, with notes on soils from other localities in Victoria Land. New Zealand Journal of Geology and Geophysics, 10(2): 498-539.

McKnight, D.M., House, H.R. and von Guerard, P., 1994. McMurdo LTER: Streamflow measurements in Taylor Valley. Antarctic Journal - Review: 230-232.

McKnight, D.M., Niyogi, D.K., Alger, A.S., Bomblies, A., Conovitz, P.A. and Tate, C.M., 1999. Dry valley streams in Antarctica: Ecosystems waiting for water. Bioscience, 49(12): 985-995.

Milne, J.D.G., Clayden, B., Singleton, P.L. and Wilson, A.D., 1995. Soil Description Handbook (Revised Edition). Manaaki Whenua Press, Lincoln, New Zealand.

Minasny, B., McBratney, A.B. and Bristow, K.L., 1999. Comparison of different approaches to the development of pedotransfer functions for water-retention curves. Geoderma, 93: 225-253.

Nichols, R.L., 1966. Geomorphology of Antarctica. In: J.C.F. Tedrow (Editor), Antarctic soils and soil forming processes. Antarctic Research Series Volume 8. American Geophysical Union, Washington, D.C., pp. 1-46.

Niyogi, D.K., Tate, C.M., McKnight, D.M., Duff, J.H. and Alger, A.S., 1997. Species composition and primary production of algal communities in Dry Valley streams in Antarctica: Examination of the functional role of biodiversity. In: W.B. Lyons, C. Howard-Williams and I. Hawes (Editors), Ecosystem processes in Antarctic ice-free landscapes. A.A. Balkema, Rotterdam, pp. 171-179.

Nylen, T.H., Fountain, A.G. and Doran, P.T., 2004. Climatology of katabatic winds in the McMurdo dry valleys, southern Victoria Land, Antarctica. Journal of Geophysical Research-Atmospheres, 109(D3).

Potton, C. and Green, B., 2003. Improbable Eden: The Dry Valleys of Antarctica. Craig Potton Publishing, Nelson, N.Z., 128 pp.

Prentice, M.L., Kleman, J. and Stroeven, A.P., 1998. The composite glacial erosional landscape of the northern McMurdo Dry Valleys: Implications for Antarctic Tertiary glacial history. In: J.C. Priscu (Editor), Ecosystem dynamics in a polar desert: The McMurdo Dry Valleys, Antarctica. Antarctic Research Series, Volume 72. American Geophysical Union, Washington, D.C., pp. 1-38.

Scanlon, B.R., Christman, M., Reedy, R.C., Porro, I., Simunek, J. and Flerchinger, G.N., 2002. Intercode comparisons for simulating water balance of surficial sediments in semiarid regions. Water Resources Research, 38(12): 1323, doi: 10.1029/2001WR001233.

Thompson, D.C., Bromley, A.M. and Craig, R.M.F., 1971a. Ground temperatures in an Antarctic Dry Valley. New Zealand Journal of Geology and Geophysics, 14(3): 477-483.

Thompson, D.C., Craig, R.M.F. and Bromley, A.M., 1971b. Climate and surface heat balance in an Antarctic Dry Valley. New Zealand Journal of Science, 14: 245-251.

Treonis, A.M., Wall, D.H. and Virginia, R.A., 1999. Invertebrate biodiversity in Antarctic dry valley soils and sediments. Ecosystems, 2(6): 482-492.

Turnbull, I.M., Allibone, A.H., Forsyth, P.J. and Heron, D.W., 1994. Geology of the Bull Pass - St Johns Range area, southern Victoria Land, Antarctica, scale 1:50 000. Institute of Geological and Nuclear Sciences geological map 14. Institute of Geological and Nuclear Sciences Limited, Lower Hutt, New Zealand, 1 sheet + 52 pp.

van Genuchten, M.T., 1980. A closed-form equation for predicting the hydraulic conductivity of unsaturated soils. Soil Science Society of America Journal, 44: 892-898.

Vincent, W.F., Howard-Williams, C. and Broady, P.A., 1993. Microbial communities and processes in Antarctic flowing waters. In: E.I. Friedmann (Editor), Antarctic Microbiology. Wiley-Liss, New York, pp. 543-569.

Wall, A.M., Balks, M.R., Campbell, D.I. and Paetzold, R.F., 2004. Soil moisture measurement in the Ross Sea Region of Antarctica using Hydra soil moisture probes. In: B. Singh (Editor), Supersoil 2004. 3rd Australian and New Zealand Soils Conference, University of Sydney, Australia, 5-9 December 2004. Published on CDROM. Website: www.regional.org.au/au/asssi/. pp. 1-9.

Waterhouse, E.J. (Editor), 2001. Ross Sea Region 2001: A state of the environment report for the Ross Sea region of Antarctica. New Zealand Antarctic Institute, Christchurch, NZ.

Wynn-Williams, D.D., 1990. Ecological aspects of Antarctic microbiology. In: K.C. Marshall (Editor), Advances in Microbial Ecology, Volume 11. Plenum Press, New York, pp. 71-146.

Appendices

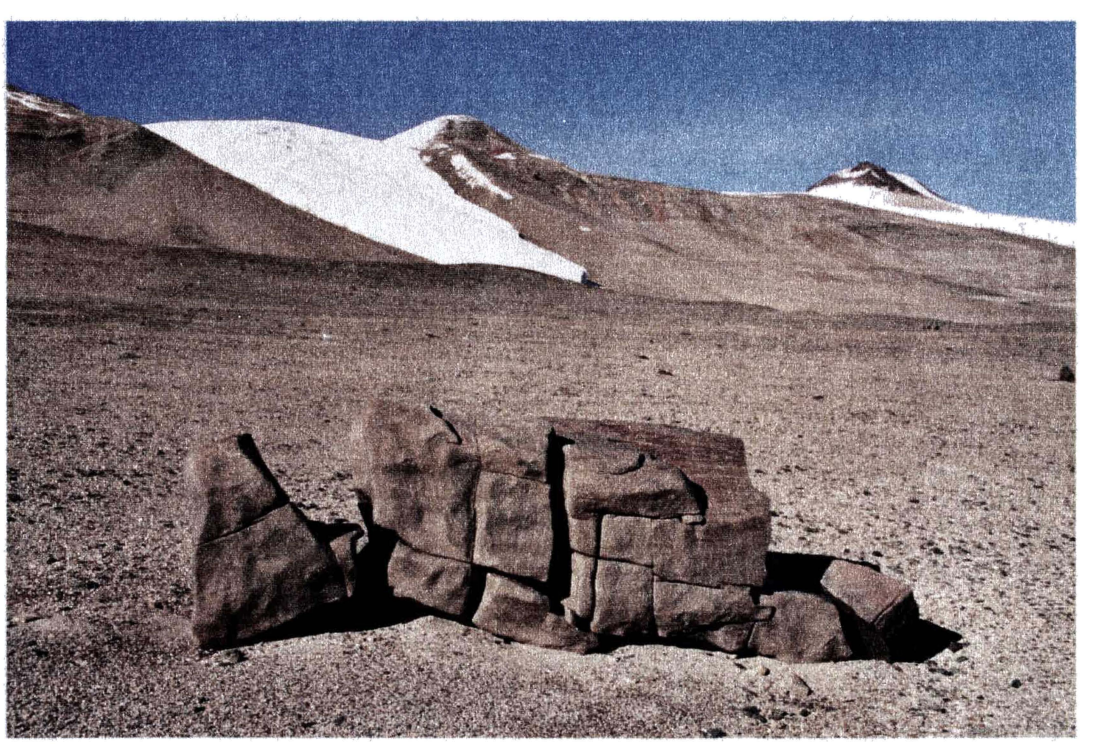

Appendix I. Soil profile descriptions.

Profile description for soils of the Goodspeed lower alluvial fan.

Described by:	Fiona Shanhun
Date:	6 January 2005
Location:	77° 29' 14.1" S 162° 21' 26.2" E 10 m west of Goodspeed Stream; 230 m upstream from the confluence of Goodspeed Stream with the Onyx River
Elevation:	249 m
Slope:	5°
Aspect:	North
Parent material:	Colluvium over till over sand
Landform:	Alluvial fan over Onyx drift
Patterned ground:	Strongly developed low centre polygons – tend to be square shaped
Soil moisture status:	Dry throughout profile
Permafrost:	Dry permafrost at <40 cm. Ice cemented below 75 cm.
USDA classification:	Mixed Sandy-skeletal Typic Anhyorthel

D	0 – 3 cm	yellowish gray (2.5Y 5/1) extremely gravelly sand; loose; weakly weathered; subangular to angular clasts; quartz rich granites are iron stained; clear smooth boundary. Salt stage I – coatings on the underside of stones.
B_{w1}	3 – 15 cm	greyish yellow (2.5Y 6/2) extremely gravelly sand; loose; apedal single grain; moderately weathered; angular clasts; quartz rich granites are iron stained; indistinct smooth boundary. Salt stage 0.
B_{w2}	15 – 40 cm	yellowish brown (2.5Y 5/4) stony cobbly gravelly sand; loose; apedal single grain; moderately weathered with occasional clatsts showing evidence of surface weathering – carbonate coatings on the underside of clasts; subangular with some angular and subrounded clasts; quartz rich granites are iron stained; diffuse smooth boundary. Salt stage I.

b2B_w 40 – 60 cm	yellowish brown (2.5Y 5/4) stony cobbly gravelly loamy sand; loose; apedal single grain; weakly weathered; angular clasts; quartz rich granites are iron stained; sharp smooth boundary. Salt stage 0.
b3C 60 – 75 cm	yellowish gray (2.5Y 6/1) sand; loose; apedal single grain; nil weathering; sharp smooth boundary. Salt stage 0.

Profile description for soils on outer edges of the Goodspeed lower alluvial fan.

Described by:	Fiona Shanhun
Date:	18 January 2005
Location:	77° 29' 10.5" S 162° 21' 42.8" E 151.5 m across the Goodspeed Upper Transect
Elevation:	233 m
Slope:	2° to the west
Aspect:	North
Parent material:	Onyx drift
Landform:	Footslope of Loop Moraine (site is west of moraine crest)
Patterned ground:	Incomplete polygons with partially low centre. No continuous boundary. Weakly developed.
Soil moisture status:	Dry throughout profile
Permafrost:	Dry permafrost at <40 cm. Ice cemented below 54 cm.
USDA classification:	Mixed Sandy-skeletal Typic Anhyorthel

D	0 – 2 cm	yellowish gray (2.5Y 6/1) very gravelly sand; loose; apedal single grain; weakly weathered; subangular to angular clasts; quartz rich granites are iron stained; abrupt smooth boundary. Salt stage I – coatings on the underside of stones.
BC	2 – 7 cm	dull yellow (2.5Y 6/3) medium sand; loose; apedal single grain; weakly weathered; subangular to angular clasts; some iron stains on granites; 2 – 3 cm distinct wavy boundary. Salt stage 0.
$b2Bw_1$	7 – 35 cm	dull yellow (2.5Y 6/4) cobbly gravelly sand; very weak; massive breaking to single grain; slightly cemented; weakly weathered; angular clasts; few faint iron stains on granites; clear irregular boundary. Salt stage 0.
$b2Bw_2$	35 – 54cm	yellowish brown (2.5Y 5/4) very stony cobbly gravelly sand; very weak; massive breaking to single grain; slightly cemented; weakly weathered; subangular to angular clasts; quartz rich granites are iron stained; sharp smooth boundary. Salt stage 0.

Appendix II. Data obtained from sites across the Goodspeed Upper Transect (site GS Trans).

Sample ID	Site	Date	Dist. across transect (m)	Depth - top (cm)	Depth - bottom (cm)	>2 mm θ_g (%)	<2 mm θ_g (%)	EC (µs/cm)	pH
1	GS Trans	7/1/05	0	0	2	0.1	0.2	761	7.9
2	GS Trans	7/1/05	0	2	5	0.2	0.4	2270	7.8
3	GS Trans	7/1/05	0	5	15	0.2	0.9	10520	7.6
5	GS Trans	7/1/05	0	15	30	0.3	0.7	3885	7.8
6	GS Trans	7/1/05	0.3	20	30	0.0	0.5	n/d	n/d
7	GS Trans	7/1/05	0.3	30	40	0.5	1.4	n/d	n/d
8	GS Trans	7/1/05	1.0	0	2	0.2	0.3	2020	8.0
9	GS Trans	7/1/05	1.0	2	5	0.2	0.6	3135	8.0
10	GS Trans	7/1/05	1.0	5	15	0.3	0.7	2195	7.9
11	GS Trans	7/1/05	1.0	15	25	0.2	1.7	170	8.3
12	GS Trans	7/1/05	1.8	0	2	n/d	0.3	n/d	n/d
13	GS Trans	7/1/05	1.8	2	5	n/d	0.5	n/d	n/d
14	GS Trans	7/1/05	1.8	5	15	n/d	0.5	n/d	n/d
15	GS Trans	7/1/05	1.8	15	25	n/d	1.7	n/d	n/d
16	GS Trans	7/1/05	2.1	0	2	0.6	1.7	9660	9.1
17	GS Trans	7/1/05	2.1	2	5	1.2	3.4	428	9.0
18	GS Trans	7/1/05	2.1	5	15	2.1	4.3	104	8.8
19	GS Trans	7/1/05	2.1	15	25	8.5	8.7	75	8.6
20	GS Trans	7/1/05	2.5	0	2	n/d	4.1	n/d	n/d
21	GS Trans	7/1/05	2.5	2	5	n/d	9.0	n/d	n/d
22	GS Trans	9/1/05	2.5	5	15	n/d	12.9	n/d	n/d
23	GS Trans	9/1/05	2.5	15	25	n/d	12.8	n/d	n/d
24	GS Trans	7/1/05	2.9	0	2	n/d	5.6	3775	8.8
25	GS Trans	7/1/05	2.9	2	5	n/d	12.6	566	8.4
26	GS Trans	7/1/05	2.9	5	15	n/d	6.6	138	8.6
27	GS Trans	7/1/05	2.9	15	30	n/d	12.5	102	8.4
28	GS Trans	7/1/05	3.3	0	10	n/d	15.9	n/d	n/d
29	GS Trans	7/1/05	3.3	10	20	n/d	16.5	n/d	n/d
30	GS Trans	9/1/05	3.3	0	2	n/d	8.6	n/d	n/d
31	GS Trans	9/1/05	3.3	2	5	n/d	14.8	n/d	n/d
32	GS Trans	9/1/05	3.3	5	10	n/d	17.4	n/d	n/d
33	GS Trans	7/1/05	3.6	0	2	n/d	21.7	176	8.4
34	GS Trans	7/1/05	3.6	2	5	n/d	17.0	70	8.5
35	GS Trans	9/1/05	3.6	5	15	n/d	15.7	56	8.6
36	GS Trans	9/1/05	4.5	0	2	n/d	10.4	n/d	n/d
37	GS Trans	9/1/05	4.5	2	5	n/d	11.6	n/d	n/d
38	GS Trans	9/1/05	4.5	5	15	n/d	6.5	n/d	n/d
39	GS Trans	9/1/05	4.5	15	30	n/d	12.0	n/d	n/d
40	GS Trans	9/1/05	6.8	0	2	n/d	10.1	235	8.3
41	GS Trans	9/1/05	6.8	2	5	n/d	9.0	60	8.6
42	GS Trans	9/1/05	6.8	5	15	n/d	14.4	58	8.5
43	GS Trans	9/1/05	6.8	15	30	n/d	13.0	46	8.5
44	GS Trans	9/1/05	8.8	0	2	n/d	14.7	n/d	n/d
45	GS Trans	9/1/05	8.8	2	5	n/d	18.5	n/d	n/d
46	GS Trans	9/1/05	8.8	5	15	n/d	18.7	n/d	n/d
47	GS Trans	9/1/05	8.8	15	30	n/d	9.6	n/d	n/d
48	GS Trans	9/1/05	9.8	0	2	n/d	4.5	1024	9.0
49	GS Trans	9/1/05	9.8	2	5	n/d	4.0	512	8.7
50	GS Trans	9/1/05	9.8	5	15	n/d	7.1	50	8.3
51	GS Trans	9/1/05	9.8	15	35	n/d	5.4	43	8.2
52	GS Trans	9/1/05	13.2	0	2	n/d	2.3	n/d	n/d
53	GS Trans	9/1/05	13.2	2	5	n/d	3.3	n/d	n/d
54	GS Trans	9/1/05	13.2	5	15	n/d	2.7	n/d	n/d
55	GS Trans	9/1/05	13.2	15	40	n/d	8.0	n/d	n/d
56	GS Trans	9/1/05	15.8	0	2	n/d	0.2	273	8.8
57	GS Trans	9/1/05	15.8	2	5	n/d	0.2	85	8.4
58	GS Trans	9/1/05	20.4	0	2	n/d	0.3	n/d	n/d

Sample ID	Site	Date	Dist. across transect (m)	Depth - top (cm)	Depth - bottom (cm)	>2 mm θ_g (%)	<2 mm θ_g (%)	EC (µs/cm)	pH
59	GS Trans	9/1/05	20.4	2	5	n/d	0.4	n/d	n/d
60	GS Trans	9/1/05	20.4	5	15	n/d	0.2	n/d	n/d
61	GS Trans	9/1/05	20.4	15	35	n/d	1.5	n/d	n/d
62	GS Trans	10/1/05	25.5	0	2	0.2	0.2	201	8.8
63	GS Trans	10/1/05	25.5	2	5	0.2	0.3	114	8.7
64	GS Trans	10/1/05	25.5	5	10	0.3	0.5	61	8.5
65	GS Trans	10/1/05	25.5	10	30	1.0	1.9	37	8.6
66	GS Trans	10/1/05	29.0	0	2	n/d	3.1	n/d	n/d
67	GS Trans	10/1/05	29.0	2	5	n/d	7.5	n/d	n/d
68	GS Trans	10/1/05	29.0	5	15	n/d	4.3	n/d	n/d
69	GS Trans	10/1/05	29.0	15	32	n/d	6.3	n/d	n/d
70	GS Trans	10/1/05	43.2	0	2	n/d	0.2	179	8.9
71	GS Trans	10/1/05	43.2	2	5	n/d	0.2	137	8.6
72	GS Trans	10/1/05	43.2	5	12	n/d	0.2	44	8.8
73	GS Trans	10/1/05	43.2	12	30	n/d	1.8	34	8.4
74	GS Trans	10/1/05	56.2	0	2	n/d	0.2	n/d	n/d
75	GS Trans	10/1/05	56.2	2	5	n/d	0.5	n/d	n/d
76	GS Trans	10/1/05	56.2	5	15	n/d	1.1	n/d	n/d
77	GS Trans	10/1/05	56.2	15	30	n/d	2.9	n/d	n/d
78	GS Trans	10/1/05	66.6	0	2	n/d	0.9	5375	n/d
79	GS Trans	10/1/05	66.6	2	5	n/d	1.7	4175	n/d
80	GS Trans	10/1/05	66.6	5	15	n/d	2.8	1540	7.7
81	GS Trans	10/1/05	66.6	15	30	n/d	2.3	313	7.9
82	GS Trans	10/1/05	66.6	30	42	n/d	2.8	181	8.1
83	GS Trans	10/1/05	72.0	0	2	n/d	0.2	n/d	n/d
84	GS Trans	10/1/05	72.0	2	5	n/d	0.3	n/d	n/d
85	GS Trans	10/1/05	72.0	5	15	n/d	0.4	n/d	n/d
86	GS Trans	10/1/05	72.0	15	30	n/d	0.6	n/d	n/d
87	GS Trans	10/1/05	72.0	30	52	n/d	0.5	n/d	n/d
88	GS Trans	11/1/05	82.4	0	2	0.6	2.2	7800	n/d
89	GS Trans	11/1/05	82.4	2	5	0.6	1.0	285	8.2
90	GS Trans	11/1/05	82.4	5	15	0.7	1.5	116	8.4
91	GS Trans	11/1/05	82.4	15	30	2.5	5.1	186	8.2
92	GS Trans	11/1/05	82.4	30	42	2.5	3.5	210	8.3
93	GS Trans	11/1/05	88.0	0	2	n/d	0.2	n/d	n/d
94	GS Trans	11/1/05	88.0	2	5	n/d	0.3	n/d	n/d
95	GS Trans	11/1/05	88.0	5	15	n/d	0.6	n/d	n/d
96	GS Trans	11/1/05	88.0	15	35	n/d	0.5	n/d	n/d
97	GS Trans	11/1/05	88.0	35	46	n/d	0.4	n/d	n/d
98	GS Trans	16/1/05	104.0	0	2	n/d	0.2	85	8.4
99	GS Trans	16/1/05	104.0	2	5	n/d	0.2	127	8.4
100	GS Trans	16/1/05	104.0	5	20	n/d	0.3	416	8.1
101	GS Trans	16/1/05	104.0	20	36	n/d	0.3	286	8.2
102	GS Trans	16/1/05	123.9	0	2	n/d	0.2	n/d	n/d
103	GS Trans	16/1/05	123.9	2	5	n/d	0.4	n/d	n/d
104	GS Trans	16/1/05	123.9	5	15	n/d	0.6	n/d	n/d
105	GS Trans	16/1/05	123.9	15	30	n/d	0.6	n/d	n/d
106	GS Trans	16/1/05	123.9	30	43	n/d	1.0	n/d	n/d
107	GS Trans	25/1/05	151.5	0	2	n/d	0.1	56	8.3
108	GS Trans	25/1/05	151.5	2	7	n/d	0.3	319	8.2
109	GS Trans	25/1/05	151.5	7	35	n/d	0.5	514	7.7
110	GS Trans	25/1/05	151.5	35	54	n/d	0.5	116	8.3

Appendix III. Data obtained from re-sampling of the upper two increments at sites across the Goodspeed Upper Transect.

Sample ID	Site	Date	Dist. across transect (m)	Depth -top (cm)	Depth -bottom (cm)	<2 mm θ_g (%)
130	GS Trans Re-S	27/1/05	0	0	2	0.2
131	GS Trans Re-S	27/1/05	0	2	5	0.5
132	GS Trans Re-S	27/1/05	2.2	0	2	0.6
133	GS Trans Re-S	27/1/05	2.2	2	5	3.2
134	GS Trans Re-S	27/1/05	3.3	0	2	16.3
135	GS Trans Re-S	27/1/05	3.3	2	4	15.6
136	GS Trans Re-S	27/1/05	4.5	0	2	7.4
137	GS Trans Re-S	27/1/05	4.5	2	5	6.2
138	GS Trans Re-S	27/1/05	6.8	0	2	1.7
139	GS Trans Re-S	27/1/05	6.8	2	5	8.2
140	GS Trans Re-S	27/1/05	8.8	0	2	4.9
141	GS Trans Re-S	27/1/05	9.8	0	2	4.9
142	GS Trans Re-S	27/1/05	9.8	2	5	7.2
143	GS Trans Re-S	27/1/05	13.2	0	2	2.2
144	GS Trans Re-S	27/1/05	13.2	2	5	4.3
145	GS Trans Re-S	27/1/05	15.8	0	2	0.3
146	GS Trans Re-S	27/1/05	15.8	2	5	1.6
147	GS Trans Re-S	27/1/05	20.4	0	2	0.2
148	GS Trans Re-S	27/1/05	20.4	2	5	0.2
149	GS Trans Re-S	27/1/05	25.5	0	2	6.0
150	GS Trans Re-S	27/1/05	25.5	2	5	6.0
151	GS Trans Re-S	27/1/05	29.0	0	2	3.4
152	GS Trans Re-S	27/1/05	29.0	2	5	4.8
153	GS Trans Re-S	27/1/05	43.2	0	2	0.1
154	GS Trans Re-S	27/1/05	43.2	2	5	0.2
155	GS Trans Re-S	27/1/05	56.2	0	2	0.1
156	GS Trans Re-S	27/1/05	56.2	2	5	0.8
157	GS Trans Re-S	27/1/05	66.6	0	2	1.1
158	GS Trans Re-S	27/1/05	66.6	2	5	1.4
159	GS Trans Re-S	27/1/05	72.0	0	2	0.1
160	GS Trans Re-S	27/1/05	72.0	2	5	0.3
161	GS Trans Re-S	27/1/05	82.4	0	2	0.8
162	GS Trans Re-S	27/1/05	82.4	2	5	0.8
163	GS Trans Re-S	27/1/05	88.0	0	2	0.2
164	GS Trans Re-S	27/1/05	88.0	2	5	0.2
165	GS Trans Re-S	27/1/05	104.0	0	2	0.1
166	GS Trans Re-S	27/1/05	104.0	2	5	0.2
167	GS Trans Re-S	27/1/05	123.9	0	2	0.2
168	GS Trans Re-S	27/1/05	123.9	2	5	0.3
169	GS Trans Re-S	27/1/05	151.5	0	2	0.2
170	GS Trans Re-S	27/1/05	151.5	2	5	0.5

Appendix IV. Data obtained from sites across the Goodspeed Lower Transect (site GS T 2).

Sample ID	Site	Date	Dist. across transect (m)	Depth -top (cm)	Depth -bottom (cm)	<2 mm θ_g (%)	EC (µs/cm)
111	GS T 2	25/1/05	0.5	0	2	8.6	177
112	GS T 2	25/1/05	0.5	2	7	8.7	67
113	GS T 2	25/1/05	2.3	0	3	6.7	223
114	GS T 2	25/1/05	4.2	0	2	5.9	363
115	GS T 2	25/1/05	4.2	2	8	4.5	69
116	GS T 2	25/1/05	6.3	0	2	12.4	123
117	GS T 2	25/1/05	6.3	2	5	17.6	53
118	GS T 2	25/1/05	12.1	0	2	5.9	571
119	GS T 2	25/1/05	12.1	2	5	5.7	117
120	GS T 2	25/1/05	12.1	5	15	4.3	41
121	GS T 2	25/1/05	12.1	15	38	6.2	42
122	GS T 2	25/1/05	16.0	0	2	0.2	126
123	GS T 2	25/1/05	16.0	2	5	0.2	119
124	GS T 2	25/1/05	16.0	5	15	0.4	25
125	GS T 2	25/1/05	16.0	15	30	0.7	21
126	GS T 2	25/1/05	18.2	0	2	0.4	242
127	GS T 2	25/1/05	18.2	2	5	0.2	288
128	GS T 2	25/1/05	18.2	5	15	0.2	80
129	GS T 2	25/1/05	18.2	15	28	0.5	46

Appendix V. Data obtained from sites along Goodspeed Stream. All samples are surface samples (0-2 cm).

Sample ID	Site	Date	Description	<2 mm θ_g (%)	EC (µs/cm)
171	GS11	28/1/05	LB dry	0.3	194
172	GS11	28/1/05	LB hypo	8.9	77
173	GS11	28/1/05	RB dry	0.6	193
174	GS11	28/1/05	RB hypo	16.0	79
175	GS 10	28/1/05	LB dry	0.2	49
176	GS 10	28/1/05	LB hypo	9.4	158
177	GS 10	28/1/05	RB dry	0.2	459
178	GS 10	28/1/05	RB hypo	7.3	47
179	GS 9	28/1/05	LB dry	0.6	1784
180	GS 9	28/1/05	LB hypo	11.7	139
181	GS 9	28/1/05	RB dry	0.2	175
182	GS 9	28/1/05	RB hypo	17.4	77
183	GS 8	28/1/05	LB dry	0.2	561
184	GS 8	28/1/05	LB hypo	9.6	191
185	GS 8	28/1/05	RB dry	0.1	110
186	GS 8	28/1/05	RB hypo	18.7	106
187	GS 7	28/1/05	LB dry	0.2	108
188	GS 7	28/1/05	LB hypo	13.8	147
189	GS 7	28/1/05	RB dry	0.1	422
190	GS 7	28/1/05	RB hypo	11.7	157
191	GS 6	28/1/05	LB dry	0.2	206
192	GS 6	28/1/05	LB hypo	16.1	157
193	GS 6	28/1/05	RB dry	0.2	132
194	GS 6	28/1/05	RB hypo	22.7	104
195	GS 3	28/1/05	LB dry	0.3	739
196	GS 3	28/1/05	LB hypo	4.9	416
197	GS 3	28/1/05	RB dry	0.3	377
198	GS 3	28/1/05	RB hypo	5.2	541
199	GS 4	28/1/05	LB dry	0.2	330
200	GS 4	28/1/05	LB hypo	0.7	2635
201	GS 4	28/1/05	RB dry	0.2	145
202	GS 4	28/1/05	RB hypo	1.1	973
203	GS 1	28/1/05	LB dry	0.2	238
204	GS 1	28/1/05	LB hypo	1.6	922
205	GS 1	28/1/05	RB dry	0.2	232
206	GS 1	28/1/05	RB hypo	4.5	563
207	GS 5	28/1/05	LB dry	0.2	818
208	GS 5	28/1/05	LB hypo	3.7	465
209	GS 5	28/1/05	RB dry	0.3	543
210	GS 5	28/1/05	RB hypo	4.8	824

Appendix VI. Data used in calculating the soil moisture potential at sites across the Goodspeed Upper Transect.

θ_r	θ_s	n	α	ρ (kg m^{-3})	g (m s^{-2})
0.0014	0.3	1.77	0.1	1000	9.8

Dist. across trans. (m)	Depth (m)	θ_g (%)	θ_v (%)	Ψ_m (kPa)	Ψ_g (kPa)	Ψ_t (kPa)
0	-0.01	0.2	0.4	-15.4	-0.1	-15.5
0	-0.04	0.4	0.7	-7.6	-0.3	-7.9
0	-0.10	0.9	1.5	-2.7	-1.0	-3.7
0	-0.10	1.0	1.7	-2.3	-1.0	-3.3
0	-0.23	0.7	1.2	-3.5	-2.2	-5.7
0.3	-0.25	0.5	0.8	-6.5	-2.5	-8.9
0.3	-0.35	1.4	2.3	-1.5	-3.4	-5.0
1.0	-0.01	0.3	0.5	-11.7	-0.1	-11.8
1.0	-0.04	0.6	0.9	-5.1	-0.3	-5.5
1.0	-0.10	0.7	1.2	-3.7	-1.0	-4.7
1.0	-0.20	1.7	2.8	-1.2	-2.0	-3.2
1.8	-0.01	0.3	0.5	-12.6	-0.1	-12.7
1.8	-0.04	0.5	0.8	-6.6	-0.3	-7.0
1.8	-0.10	0.5	0.8	-6.3	-1.0	-7.3
1.8	-0.20	1.7	2.8	-1.2	-2.0	-3.2
2.1	-0.01	1.7	2.9	-1.2	-0.1	-1.3
2.1	-0.04	3.4	5.5	-0.5	-0.3	-0.8
2.1	-0.10	4.3	7.0	-0.4	-1.0	-1.3
2.1	-0.20	8.7	14.4	-0.1	-2.0	-2.1
2.5	-0.01	4.1	6.8	-0.4	-0.1	-0.5
2.5	-0.04	9.0	14.9	-0.1	-0.3	-0.5
2.5	-0.10	12.9	21.3	-0.1	-1.0	-1.1
2.5	-0.20	12.8	21.1	-0.1	-2.0	-2.0
2.9	-0.01	5.6	9.3	-0.3	-0.1	-0.4
2.9	-0.04	12.6	20.7	-0.1	-0.3	-0.4
2.9	-0.10	6.6	10.8	-0.2	-1.0	-1.2
2.9	-0.23	12.5	20.6	-0.1	-2.2	-2.3
3.3	-0.05	15.9	26.2	-0.1	-0.5	-0.6
3.3	-0.15	16.5	27.2	-0.1	-1.5	-1.5
3.3	-0.01	8.6	14.3	-0.1	-0.1	-0.2
3.3	-0.04	14.8	24.4	-0.1	-0.3	-0.4
3.3	-0.08	17.4	28.8	-0.1	-0.7	-0.8
3.6	-0.01	21.7	35.8	0.0	-0.1	-0.1
3.6	-0.04	17.0	28.0	-0.1	-0.3	-0.4
3.6	-0.10	15.7	25.9	-0.1	-1.0	-1.0
4.5	-0.01	10.4	17.1	-0.1	-0.1	-0.2
4.5	-0.04	11.6	19.1	-0.1	-0.3	-0.4
4.5	-0.10	6.5	10.8	-0.2	-1.0	-1.2
4.5	-0.23	12.0	19.8	-0.1	-2.2	-2.3
6.8	-0.01	10.1	16.7	-0.1	-0.1	-0.2
6.8	-0.04	9.0	14.9	-0.1	-0.3	-0.5
6.8	-0.10	14.4	23.8	-0.1	-1.0	-1.1
6.8	-0.23	13.0	21.5	-0.1	-2.2	-2.3
8.8	-0.01	14.7	24.3	-0.1	-0.1	-0.2
8.8	-0.04	18.5	30.5	-0.1	-0.3	-0.4
8.8	-0.10	18.7	30.9	-0.1	-1.0	-1.0
8.8	-0.23	9.6	15.8	-0.1	-2.2	-2.3
9.8	-0.01	4.5	7.5	-0.3	-0.1	-0.4
9.8	-0.04	4.0	6.7	-0.4	-0.3	-0.7
9.8	-0.10	7.1	11.8	-0.2	-1.0	-1.2
9.8	-0.25	5.4	9.0	-0.3	-2.5	-2.7
13.2	-0.01	2.3	3.9	-0.8	-0.1	-0.9
13.2	-0.04	3.3	5.5	-0.5	-0.3	-0.8
13.2	-0.10	2.7	4.5	-0.7	-1.0	-1.6

Dist. across trans. (m)	Depth (m)	θ_g (%)	θ_v (%)	Ψ_m (kPa)	Ψ_g (kPa)	Ψ_t (kPa)
13.2	-0.28	8.0	13.3	-0.2	-2.7	-2.9
15.8	-0.01	0.2	0.4	-15.0	-0.1	-15.1
15.8	-0.04	0.2	0.3	-21.1	-0.3	-21.5
20.4	-0.01	0.3	0.5	-12.8	-0.1	-12.9
20.4	-0.04	0.4	0.7	-6.9	-0.3	-7.2
20.4	-0.10	0.2	0.4	-14.5	-1.0	-15.5
20.4	-0.25	1.5	2.5	-1.4	-2.5	-3.9
25.5	-0.01	0.2	0.4	-15.3	-0.1	-15.4
25.5	-0.04	0.3	0.5	-11.1	-0.3	-11.5
25.5	-0.08	0.5	0.9	-5.5	-0.7	-6.2
25.5	-0.20	1.9	3.1	-1.1	-2.0	-3.0
29.0	-0.01	3.1	5.1	-0.6	-0.1	-0.7
29.0	-0.04	7.5	12.3	-0.2	-0.3	-0.5
29.0	-0.10	4.3	7.0	-0.4	-1.0	-1.3
29.0	-0.24	6.3	10.4	-0.2	-2.3	-2.5
43.2	-0.01	0.2	0.3	-19.6	-0.1	-19.7
43.2	-0.04	0.2	0.3	-21.1	-0.3	-21.4
43.2	-0.09	0.2	0.3	-19.2	-0.8	-20.0
43.2	-0.21	1.8	3.0	-1.1	-2.1	-3.2
56.2	-0.01	0.2	0.4	-16.5	-0.1	-16.6
56.2	-0.04	0.5	0.7	-6.7	-0.3	-7.0
56.2	-0.10	1.1	1.8	-2.1	-1.0	-3.1
56.2	-0.23	2.9	4.8	-0.6	-2.2	-2.8
66.6	-0.01	0.9	1.4	-2.9	-0.1	-3.0
66.6	-0.04	1.7	2.7	-1.2	-0.3	-1.6
66.6	-0.10	2.8	4.6	-0.6	-1.0	-1.6
66.6	-0.23	2.3	3.8	-0.8	-2.2	-3.0
66.6	-0.36	2.8	4.6	-0.6	-3.5	-4.2
72.0	-0.01	0.2	0.3	-23.5	-0.1	-23.6
72.0	-0.04	0.3	0.4	-13.8	-0.3	-14.1
72.0	-0.10	0.4	0.7	-7.7	-1.0	-8.6
72.0	-0.23	0.6	1.0	-4.8	-2.2	-7.0
72.0	-0.41	0.5	0.7	-6.6	-4.0	-10.7
82.4	-0.01	2.2	3.6	-0.9	-0.1	-1.0
82.4	-0.04	1.0	1.7	-2.3	-0.3	-2.6
82.4	-0.10	1.5	2.5	-1.4	-1.0	-2.4
82.4	-0.23	5.1	8.4	-0.3	-2.2	-2.5
82.4	-0.36	3.5	5.8	-0.5	-3.5	-4.0
88.0	-0.01	0.2	0.3	-23.4	-0.1	-23.5
88.0	-0.04	0.3	0.5	-12.4	-0.3	-12.8
88.0	-0.10	0.6	1.0	-4.9	-1.0	-5.9
88.0	-0.25	0.5	0.9	-5.2	-2.5	-7.7
88.0	-0.41	0.4	0.7	-7.4	-4.0	-11.4
104.0	-0.01	0.2	0.3	-25.2	-0.1	-25.3
104.0	-0.04	0.2	0.4	-15.0	-0.3	-15.3
104.0	-0.13	0.3	0.5	-10.0	-1.2	-11.2
104.0	-0.28	0.3	0.5	-12.5	-2.7	-15.3
123.9	-0.01	0.2	0.3	-22.2	-0.1	-22.3
123.9	-0.04	0.4	0.6	-9.1	-0.3	-9.5
123.9	-0.10	0.6	0.9	-4.9	-1.0	-5.9
123.9	-0.23	0.6	1.1	-4.2	-2.2	-6.4
123.9	-0.37	1.0	1.7	-2.3	-3.6	-5.9
151.5	-0.01	0.1	0.2	-28.0	-0.1	-28.1
151.5	-0.05	0.3	0.5	-11.4	-0.4	-11.8
151.5	-0.21	0.5	0.7	-6.7	-2.1	-8.8
151.5	-0.45	0.5	0.8	-5.9	-4.4	-10.2